



THE HONG KONG  
POLYTECHNIC UNIVERSITY

香港理工大學

Pao Yue-kong Library

包玉剛圖書館

---

## Copyright Undertaking

This thesis is protected by copyright, with all rights reserved.

**By reading and using the thesis, the reader understands and agrees to the following terms:**

1. The reader will abide by the rules and legal ordinances governing copyright regarding the use of the thesis.
2. The reader will use the thesis for the purpose of research or private study only and not for distribution or further reproduction or any other purpose.
3. The reader agrees to indemnify and hold the University harmless from and against any loss, damage, cost, liability or expenses arising from copyright infringement or unauthorized usage.

### IMPORTANT

If you have reasons to believe that any materials in this thesis are deemed not suitable to be distributed in this form, or a copyright owner having difficulty with the material being included in our database, please contact [lbsys@polyu.edu.hk](mailto:lbsys@polyu.edu.hk) providing details. The Library will look into your claim and consider taking remedial action upon receipt of the written requests.

**ECONOMIC OPERATION AND  
TRANSACTIONAL ENERGY MANAGEMENT  
FOR MICROGRIDS WITH DISTRIBUTED  
ENERGY RESOURCES**

**LYU CHENG**

**PhD**

**The Hong Kong Polytechnic University**

**2022**

The Hong Kong Polytechnic University

Department of Electrical Engineering

**Economic Operation and Transactive  
Energy Management for Microgrids  
with Distributed Energy Resources**

**LYU Cheng**

A thesis submitted in partial fulfilment of the requirements for the  
degree of Doctor of Philosophy

July, 2022

# Certificate of Originality

I hereby declare that this thesis is my own work and that, to the best of my knowledge and belief, it reproduces no material previously published or written, nor material that has been accepted for the award of any other degree or diploma, except where due acknowledgement has been made in the text.

\_\_\_\_\_(Signed)

LYU Cheng \_\_\_\_\_ (Name of student)

For Mama and Papa

# Abstract

Over the last decade, the increasing penetration of distributed energy resources (DERs) provides a clean and efficient solution to combat the climate change and reduce the dependence on fossil fuel. The trending adoption of microgrids as the new operation paradigm brings about many economic and environmental benefits as well as the flexibility of self-organized system operation. Recently, plenty of research works have been carried out on the operation and management of microgrids. However, some limitations are noted in these works with respect to e.g. the economic operation of microgrids, especially considering the complexities of components, e.g., battery degradation and renewable forecasting errors. This thesis aims to address aforementioned challenges by developing advanced methods and solutions that can enhance both the economic operation and transactive energy management within a single microgrid and among multiple microgrids.

Due to the high penetration of DERs, the economic operation of a microgrid is confronted with several challenges. First of all, since it is difficult to accurately forecast the production output of renewables well beforehand, the short-term economic dispatch is essentially an uncertainty-embedded decision-making problem. In addition, it is hard to characterize the degradation process of battery storage systems, and therefore it is challenging to formulate the battery degradation cost function. In this regard, a novel real-time degradation model is specially developed for lithium-ion battery energy storage systems to resemble the battery material degradation as much as possible.

Microgrids located within the same geographical areas can be interconnected

when making energy scheduling decisions. Cooperative management can be beneficial and economic for microgrids to complement each other in terms of matching the power supply with the demand at the minimum cost. However, challenges lie in the mechanism design for proactive participations into the cooperation. To enable transactive energy trading within multiple microgrids, a comprehensive peer-to-peer(P2P) energy sharing framework is proposed. In this framework, the social welfare of microgrids is maximized, and both the power flow loss and shadow price are involved.

To enable the transactive management in alignment with existing electricity market timeline, a hierarchical P2P market with different timescales is proposed for microgrids to further explore their flexibilities. In the proposed tri-level P2P transaction market, the day-ahead market provides preliminary energy schedule decisions; the intra-day market is introduced to generate corrective actions to complement day-ahead decisions; the real-time regulation market can further guarantee the short-term balance of power supply-and-demand. Furthermore, the possible communication failures in the cyber network are innovatively taken into account and a communication failure-robust algorithm is accordingly designed.

To summarize, the high penetration of DERs virtually imposes various challenges to the operation and management of microgrids from technical, economic and security perspectives. Throughout this thesis, new energy management and operation strategies with different advantages are developed for microgrids with DERs to address these challenges accordingly. With the achievements in this thesis, future works including the further enhancement and validations of the developed strategies through real-world implementations can be carried out.

# Publications Arising from the Thesis

## Journal Publications:

- [1] **Cheng Lyu**, Youwei Jia, and Zhao Xu, “A Novel Communication-less Approach to Economic Dispatch for Microgrids,” *IEEE Transactions on Smart Grid*, vol. 12(2021), no. 1, pp. 901-904.
- [2] **Cheng Lyu**, Youwei Jia, and Zhao Xu, “Fully decentralized peer-to-peer energy sharing framework for smart buildings with local battery system and aggregated electric vehicles,” *Applied Energy*, vol. 299(2021), pp. 117243.
- [3] **Cheng Lyu**, Youwei Jia, and Zhao Xu, “DRO-MPC-based data-driven approach to real-time economic dispatch for islanded microgrids,” *IET Generation, Transmission & Distribution*, vol. 24(2020), no. 14, pp. 5704-5711.
- [4] **Cheng Lyu**, Youwei Jia, and Zhao Xu, “Hierarchical Peer-to-Peer Energy Trading Framework of Multi-Microgrids with High Operational Uncertainty,” prepared to submit.
- [5] Mengge Shi, Han Wang, **Cheng Lyu**, Peng Xie, Zhao Xu and Youwei Jia, “A hybrid model of energy scheduling for integrated multi-energy microgrid with hydrogen and heat storage system,” *Energy Reports*, vol. 7(2021), pp. 357-368.
- [6] Peng Xie, Youwei Jia, **Cheng Lyu**, Han Wang, Mengge Shi and Hongkun Chen, “Optimal Sizing of Renewables and Battery Systems for Hybrid AC/DC Microgrids Based on Variability Management,” *Applied Energy*, vol. 321(2022), pp. 119250.

## Conference Publications:

- [1] **Cheng Lyu**, Youwei Jia, Zhao Xu and Mengge Shi, “Real-Time Operation Optimization of Islanded Microgrid with Battery Energy Storage System,” *2020 IEEE PES General Meeting (PESGM)*(Online), August 2020, pp. 1-5. **(Best Conference Paper)**
- [2] **Cheng Lyu**, Youwei Jia and Zhao Xu, “Peer-to-Peer Energy Cooperation in Building Community over A Lossy Network,” *2021 IEEE PES General Meeting (PESGM)*(Online), July 2021, pp. 1-5. **(Best Conference Paper)**
- [3] **Cheng Lyu**, Youwei Jia and Zhao Xu, “Co-operative P2P Trading and Voltage Regulation Service in Unbalanced Distribution Networks,” *2022 IEEE PES General Meeting (PESGM)*(Online), July 2022. Accepted.
- [4] **Cheng Lyu**, Youwei Jia and Zhao Xu, “Tube-based Model Predictive Control Approach for Real-time Operation of Energy Storage System,” *2020 International Conference on Smart Grids and Energy Systems (SGES)*(Online), November 2020, pp. 493-497.
- [5] **Cheng Lyu**, Youwei Jia, Zhao Xu and Mengge Shi, “Integrating Peer-to-Peer Energy Trading of Microgrids into Deregulated Electricity Market by Cascaded Model Predictive Control,” *5th IEEE Conference on Energy Internet and Energy System Integration(EI2)*(Online), October, 2021, pp. 114-118.
- [6] Mengge Shi, **Cheng Lyu**, Han Wang, Peng Xie and Youwei Jia, “Two-stage Energy Management Strategy for Hydrogen Energy Storage System Embedded Microgrids,” *The 10th Renewable Power Generation Conference (RPG)*(Online), October, 2021, pp. 311-317.

# Acknowledgements

I would like to give my warmest thanks to my chief supervisor, Professor Zhao Xu, for his endless guidance and support through my study in PolyU. I learnt a lot from him and got many aspirations for my future life. I would like to thank Dr. Youwei Jia for providing me with valuable help on my research, especially during my visit to Southern University of Science and Technology. You were always positive that I could make breakthroughs.

I would like to express sincere gratitude to my friends and peers for their encouragement and accompany. Thanks to Dong Wang and Jiemei Luo for offering me support; to Huayi Wu for our cooperation in Teaching Assistant courses; to Peng Xie, Mengge Shi, Zixu Zhou, and Xingzhao Yang for their help during my visit to SUSTech; to all the PolyU smart microgrid group members, Yi He, Yufei He, Xu Xu for sharing their pains and joys in the PhD life.

In addition, I would also like to express special appreciations to my dear parents for their unconditional care and love. I would like to say thanks to my elder sister, Fen Lyu, for her constant support during my outbound study. I also give deep loves to my wife, Xinyue Fei, for accompanying me and offering me encouragements.

Lastly, I appreciate the financial support from Hong Kong PhD Fellowship from RGC.

# Contents

<b>Abstract</b>	<b>ii</b>
<b>Publications arising from the thesis</b>	<b>iv</b>
<b>Acknowledgements</b>	<b>vi</b>
<b>List of Figures</b>	<b>xi</b>
<b>List of Tables</b>	<b>xiv</b>
<b>1 Introduction</b>	<b>1</b>
1.1 Background . . . . .	1
1.2 Literature Review . . . . .	5
1.3 Objectives and Primary Contributions . . . . .	11
1.4 Thesis Organization . . . . .	13
<b>2 Short-term Economic Operation of Microgrids with BESSs</b>	<b>15</b>
2.1 Introduction . . . . .	15
2.2 Battery and Microgrid Model . . . . .	18
2.2.1 Battery Operation Model . . . . .	19
2.2.2 Battery Marginal Degradation Model . . . . .	20
2.3 Problem Formulation and Methodology . . . . .	24
2.3.1 Cost Function . . . . .	24

2.3.2	Operation Constraints . . . . .	25
2.3.3	Weighted MPC Approach . . . . .	27
2.4	Case Study . . . . .	28
2.4.1	Case Configuration . . . . .	28
2.4.2	Simulation and Analysis . . . . .	30
2.5	Summary for the Chapter . . . . .	36
<b>3</b>	<b>Peer-to-Peer Energy Sharing of Smart Building Microgrids</b>	<b>37</b>
3.1	Introduction . . . . .	37
3.2	Smart Building Microgrid Model . . . . .	41
3.2.1	HVAC Units in Building Microgrids . . . . .	43
3.2.2	Electric Vehicle . . . . .	44
3.2.3	Model of Battery Energy Storage System . . . . .	47
3.2.4	Operation Cost of Building Without Energy Sharing . . . . .	48
3.3	Energy Sharing Problem Formulation . . . . .	50
3.3.1	Operation Model of Energy Sharing . . . . .	50
3.3.2	Energy Sharing Pricing . . . . .	52
3.3.3	Problem Decomposition . . . . .	54
3.4	Proposed Decentralized Algorithm . . . . .	56
3.4.1	Algorithm Design . . . . .	56
3.4.2	Features of the Framework . . . . .	61
3.5	Numerical Simulations . . . . .	63
3.5.1	Case Configuration . . . . .	63
3.5.2	Results and Discussion . . . . .	66
3.6	Summary for the Chapter . . . . .	76
<b>4</b>	<b>Hierarchical Transactive Market based on Distributed MPC</b>	<b>77</b>

4.1	Introduction . . . . .	77
4.2	Overview of the Local Transactive Market Design . . . . .	80
4.2.1	DM: Pre-schedule Problem . . . . .	82
4.2.2	IM: Adjustment Problem . . . . .	83
4.2.3	RM: Real-time Problem . . . . .	84
4.2.4	Settlement Issue . . . . .	84
4.3	Microgrid Operation Model . . . . .	85
4.3.1	System Description . . . . .	85
4.3.2	Cost Function . . . . .	86
4.3.3	Constraints . . . . .	87
4.4	Multi-stage Market Problem Formulation . . . . .	89
4.4.1	Cooperative DM Operation Problem . . . . .	90
4.4.2	Cooperative IM Operation Problem . . . . .	91
4.4.3	RM Operation Problem . . . . .	92
4.4.4	Unified Market Optimization Problem . . . . .	94
4.5	Distributed Algorithm Design . . . . .	94
4.5.1	Problem Decomposition . . . . .	95
4.5.2	Communication-Loss-Robust Distributed Algorithm . . . . .	96
4.5.3	Algorithm Implementation and Scalability . . . . .	98
4.6	Case Study . . . . .	99
4.6.1	Simulation Setup . . . . .	99
4.6.2	Results and Discussion . . . . .	100
4.7	Summary for the Chapter . . . . .	108
<b>5</b>	<b>Network Constrained P2P Energy Trading in Unbalanced DNs</b>	<b>110</b>
5.1	Introduction . . . . .	110
5.2	Multi-phase Distribution Network Model . . . . .	113

5.3	Co-operative Optimization Problem Formulation . . . . .	116
5.3.1	Objective Function . . . . .	116
5.3.2	Prosumer Cost in P2P Market . . . . .	117
5.3.3	Voltage Regulation Cost . . . . .	118
5.4	Case Study . . . . .	121
5.4.1	Simulation Setup . . . . .	121
5.4.2	Results and Discussion . . . . .	122
5.5	Summary for the Chapter . . . . .	126
<b>6</b>	<b>Conclusion and Future Work</b>	<b>127</b>
6.1	Conclusion . . . . .	127
6.2	Directions for Future Work . . . . .	129
	<b>Bibliography</b>	<b>131</b>

# List of Figures

1.1	Thesis organization and structure. . . . .	14
2.1	The life cycle degradation curve against the charging-discharging depth. . . . .	21
2.2	Illustration of battery segmental marginal cost in empirical use. . .	22
2.3	Illustration of model prediction control. . . . .	27
2.4	One-year power data: solar energy data and load consumption. . .	29
2.5	Marginal cost of the battery energy system. . . . .	30
2.6	Battery SoC curve: from $C^S$ battery model. . . . .	32
2.7	Battery SoC curve: from $C^A$ battery model. . . . .	32
2.8	Energy optimization results (23rd day): from $C^S$ battery model. . .	33
2.9	Energy optimization results (23rd day): from $C^A$ battery model. . .	33
2.10	The operation cost increase amount (23rd day): from $C^A$ battery model, discount rate $r = 0.9$ . . . . .	34
2.11	The operation cost increase amount (one-day): from $C^A$ battery model, discount rate $r = 0.9$ . . . . .	35
2.12	The operation cost increase amount (one-day): from $C^A$ battery model, discount rate $r = 0.6$ . . . . .	35
3.1	The structure of smart buildings community. . . . .	43
3.2	Problem decomposition of energy sharing. . . . .	63

3.3	Algorithm flowchart of the decentralized algorithm implementation. . . . .	64
3.4	Basic uncontrollable load in buildings. . . . .	65
3.5	Time-of-use electricity price. . . . .	65
3.6	EV instantaneous charging demand. . . . .	66
3.7	Hourly data of buildings: renewable energy and load. . . . .	66
3.8	Energy management profiles: Building 1 before energy sharing. . .	67
3.9	Energy management profiles: Building 3 before energy sharing. . .	68
3.10	Grid power trading profiles in smart buildings: without and with energy sharing. . . . .	69
3.11	Energy management profiles of building 1 and 2: after energy sharing. . . . .	70
3.12	Energy management profiles of building 3 and 4: after energy sharing. . . . .	71
3.13	Energy level of battery energy systems. . . . .	72
3.14	Charging power profile and energy level of electric vehicle aggregators. . . . .	73
3.15	Energy sharing profiles between peers. . . . .	74
3.16	Consensus energy sharing price. . . . .	75
3.17	Convergence of the energy sharing price in each building. . . . .	75
4.1	Illustration of the hierarchical framework of the proposed P2P local transactive market. . . . .	82
4.2	Peer-to-peer market structure of multi-microgrids. . . . .	86
4.3	Illustration of the communication failure on the lossy P2P network. . . . .	97
4.4	Forecasting generation of base solar PV energy and wind energy in DM and updates in IM sessions. . . . .	100

4.5	Purchasing energy plan. . . . .	101
4.6	P2P trading profiles and optimal P2P price consensus. . . . .	103
4.7	SoC profiles of battery energy storage systems. . . . .	104
4.8	Energy profiles of microgrids in RM. . . . .	105
4.9	Flexible load profiles in RM. . . . .	106
4.10	Performance of proposed algorithm. . . . .	107
4.11	Operation status of ESS in MG4 when maintenance plan is scheduled at the opening of IM6. . . . .	108
4.12	Comparison of P2P imported energy of MG4 from neighboring peers without and with maintenance plan scheduled at the opening of IM6. . . . .	109
5.1	Comparison of sequential methods and the proposed framework. . . . .	120
5.2	Modified IEEE 37-bus distribution system. . . . .	122
5.3	Three-phase bus voltage profile after the proposed model. . . . .	123
5.4	Three-phase P2P energy trading profiles after proposed co-operative optimization. . . . .	124
5.5	Three-phase bus voltage magnitude comparison: initial case (Initial), sequential model (Seq.) and proposed joint model. . . . .	126

# List of Tables

2.1	Generator Data . . . . .	28
2.2	BESS Data . . . . .	29
2.3	Total Energy Output and Cost on Day 23 . . . . .	34
3.1	Nomenclature . . . . .	42
3.2	Cost Comparison with and without Energy Sharing (\$) . . . . .	76
4.1	Nomenclature of Chapter 4 . . . . .	80
4.2	Day-ahead Market and Intra-day Market Sessions . . . . .	81
4.3	Microgrid Data Setup of Simulations . . . . .	100
5.1	Active(kW) and Reactive Power(kVar) of Load Agents . . . . .	123
5.2	Cost Comparison Between Different Models (\$) . . . . .	125

# Chapter 1

## Introduction

### 1.1 Background

Over the last decades, the world has witnessed the amazingly rapid deployment of renewable energy resources. According to the report [1], the global installation of renewables increased by more than 260 GW in 2020, surpassing the previous record by nearly 30%, in which solar photovoltaic (PV) energy and wind energy share 127 GW and 111 GW, respectively. By far, most renewables are still integrated into the electric power grid either in a centralized or distributed manner. Large-scale renewable energy farms are integrated through high voltage transmission networks at certain locations, while small-scale renewable energies are connected with medium and low voltage distribution networks dispersedly.

Distributed energy resource (DER) refers to small-scale electric power generations that are directly connected to medium-voltage or low-voltage distribution networks (DN) [2]. DERs can provide an alternative to the traditional electric power grid by deploying distributed green energy such as PV, wind, hydrogen and storage. In this regard, an essential distinction of DERs is that the energy they produce is close to where the energy is consumed. Typically, the scale of

---

DER varies from 1kW to 10MW, which is much smaller than conventional power generations. During the last years, end-use customers have played a crucial role in adopting the DERs thanks to the dropping installation cost and customer-friendly policies [3]. For example, the Solar Energy Industries Association (SEIA) reported that residential solar installations exceeded 1 GW in a single quarter (e.g., 2021 Q4) and one out of every 600 US homeowners is now installing solar each quarter [4]. In China, distributed solar PV is growing remarkably faster than utility-scale PV installations, from 13% in 2016 to 31% in 2019 of the total solar PV cumulative capacity [5]. Similar growth can also be observed in countries like Australia, Canada and Germany that adopt favorable subsidy schemes to attract more renewable-DER customers [6].

With the rapid growth of DER installed capacity, the requirement for grid integration has significantly increased. Meanwhile, the number of DER stakeholders in the electric power grid has continuously expanded. In addition, the randomness and volatility of distributed generations greatly harm the system stability and complicate the distribution network operation and scheduling. In this context, microgrids came into being as a promising solution: Microgrid is a local distribution system that can accommodate DERs on a small or micro scale [7]. The goals of microgrids are to attain reliability especially with the high penetration of renewables. From the perspective of the power grid, microgrids take small agents into a group, and they act as a controllable and autonomous part of the whole distribution system [8]. That is, within the microgrid, when the power generation is more than the consumption, the microgrid can be treated as a source; otherwise, the microgrid can be seen as a load within the power system. The specific structure of microgrids can minimize or even eliminate the

---

transmission losses throughout the power generation to load demand. Microgrids have several main advantages. To begin with, microgrids integrate various power generations and storage close to the load, and can provide full control on these components so that microgrids can satisfy around 80% to 100% of local power demand therein [9]. In addition, microgrids can provide two operation modes: the grid-connected mode (on-grid mode) and the islanded mode (stand-alone mode) [10]. Specifically, the islanded mode signifies that the microgrid operates independently by controlling the power generation and managing the load demand [11]. In this way, microgrids show advantages over expensive grid integration, particularly in remote areas due to environmental or architectural limits. Last but not least, microgrids include distributed storage systems and advanced management techniques such as monitoring, control and automation to improve the energy efficiency in a sustainable grid. The equipped energy storage system (ESS) contributes to the integration of renewables into the microgrid by flattening the fluctuations, improving the power quality and offering frequency and other ancillary services [12, 13].

Thanks to the aforementioned advantages, microgrids have witnessed a significant increasing deployment worldwide. Among others, the US has taken a leading position in deploying microgrids [14]. Moreover, according to the market revenue analysis in [15], Asia Pacific is expected to be the dominant region with 41.3% of total microgrid revenue; North America is expected to account for 32.5% of the global market share. Despite these trending promotions and outstanding advantages, microgrids require careful designing and specific considerations in the financial, technical, economic and regulatory domains to improve their efficiency [16, 17]. In order to economically utilize the various distributed resources, the energy management of microgrids has become a popular research topic [18, 19].

---

Energy management of microgrids solves the optimization problem that satisfies the supply-demand balance and minimizes the operation costs, subject to various constraints [20]. Owing to the above-mentioned new features of microgrids, the traditional dispatch methods are no longer fit for microgrids. On the one hand, the rapid development and popularization of flexible end-use consumers, e.g., electric vehicles, battery storage, controllable loads, heating ventilation and air conditioning system (HVAC), has imposed significant challenges to the model of microgrids [6]. On the other hand, the intermittence of renewable energy sources (e.g. PV, wind) is considerable. Therefore, the optimal dispatch strategies of microgrids deserve special investigation and careful design.

Recently, to further reinforce the reliability of microgrids, microgrids located in the same geographical area can be interconnected when making energy scheduling decisions [21]. Cooperative scheduling can be beneficial for multiple microgrids to complement each other despite the individual performances. Through the interactions between the distribution network and microgrids, a superior status can be achieved by the coordinated operation of multiple microgrids [22, 23]. For instance, interconnected microgrids can jointly optimize their energy dispatching and trading by exploiting the diversity of supply and demand patterns in different microgrids. Specifically, one microgrid may have excessive local renewable generation, while the other microgrid is in need of energy supplies to serve its local demands [24].

The distribution system is facing the proliferation of DERs, and these small-scale, flexible assets can participate in the energy market via aggregators. Generally, customer behaviors will inevitably impact the operation of distribution networks. On the one hand, the nodal power injection or consumption patterns will change the power flow that may cause power congestion; on the other hand,

it may bring voltage violations that should be carefully addressed. In addition, the distribution system operator can exploit flexibility locally provided by available assets, e.g., elastic loads and reactive power resources for the enhancement of system security. Furthermore, in recent years, peer-to-peer transactive energy trading has been suggested as an extension of local transaction markets at the distribution system level [25]. In all, it is of significance to investigate a holistic framework of the energy trading market and network operation considering different timescale of hierarchical P2P transactions.

## 1.2 Literature Review

The economic operation plays a crucial role in the energy management of microgrids. By far, much attention has been paid to microgrid operation in the last decades [26]. Compared with the traditional power grids, the operation optimization and scheduling of microgrids are much more complicated due to the integration of renewables. It is mainly embodied in the uncertainty of wind energy output and solar PV output, as well as the prediction errors of various loads. As such, the operation models of the microgrid scheduling problem are complex and the objective functions are diverse [27]. For a microgrid system, the purpose of economic operation is to determine the production instructions to individual production units, based on available forecasting data (e.g., load demand, renewable energy output, electric vehicle, energy prices). Other available information can also be considered, such as customer comforts, operation constraints, and external factors (e.g., component states) [28]. During the operation, the production instructions are adjusted in real-time according to actual accessible data, and finally, microgrids can achieve safe, economic operation and optimal scheduling [29, 30].

The economic operation of microgrids is mathematically a multi-scenario, multi-objective and nonlinear optimization problem [31, 32]. Proper methods and algorithms should be studied and selected in specific research context. In [33], economic dispatch models for microgrids both in grid-connected and stand-alone modes are explored and a double-layer (i.e., schedule layer and dispatch layer) energy management approach is proposed. In [34], a bi-level scheduling framework is proposed to co-optimize the microgrid scheduling and battery swapping station operation which are two independent stakeholders with inherently conflicting objectives. Considering that controllable load and energy storage are typical flexible elements in microgrids, the scheduling of microgrids should therefore involve advanced techniques instructing the flexible load and energy storage [35, 36].

The uncertainty of renewable output and load consumption has been widely explored in the economic operation of microgrids in the last decades. Stochastic programming is one of the most popular methods for optimization problems under uncertainty. Firstly, a large number of scenarios are generated by sampling based on the probabilistic distribution; and then, each scenario is formulated as a convex optimization problem; finally, the decision-making solutions under corresponding scenarios are weighted, which is usually the welfare maximized or cost minimized expected value in the objective function [37]. In this context, multiple scenarios are considered in [38], and the stochastic programming problem is formulated considering the probabilistic distribution of renewable output based on historical data in a microgrid. Likewise, in [39], the two-stage stochastic programming is applied to the energy management of a multi-energy data center microgrid embedded with renewables and waste heat. Both the long-term and short-term uncertainty of renewables and energy storage systems (ESSs), are considered in

---

the multi-stage stochastic programming model [40]. Robust optimization is also a suitable tool for dealing with optimization problems under uncertainty. In robust optimization, it is assumed that the probabilistic distribution of random parameters can be unknown, and the decision-maker selects optimal solutions according to the worst realization of random variables [41]. That is, the worst-case scenario is considered. Essentially, robust optimization approaches create deterministic equivalents of an uncertain optimization problem [42]. In this context, robust optimization problems are less difficult to solve than stochastic programming, because they do not require the prior knowledge of the probabilistic distribution of random variables, nor do they need operate across multiple scenarios. Robust optimization model of microgrids is established in [43], considering the upper bound and lower bound of the forecast output of renewables. As such, the robust optimization model can be transferred to a convex programming problem and can be solved naturally by convex optimization techniques [44]. In [45], the demand response of thermal load is integrated into the energy management, and a robust decision-making strategy is proposed for the optimal energy management of a grid-connected multi-energy microgrid.

The stochastic programming relies on the probabilistic distribution of random variables, while the robust optimization results in conservative solutions to some extent. For a single microgrid with small-scale renewables, it is extremely difficult to accurately monitor and forecast the uncertainty [46]. In these cases, there is a lack of reliable available data sources as the input of the optimization model. The cumulative forecast errors can exert adverse impacts on the cycle life of ESS, and the operation economy of microgrids [47]. In this regard, online scheduling schemes have gained much attention in recent works [48]. Online

---

scheduling refers to making decisions in a near real-time manner without the accessible forecast data of generation or consumption [49]. In [48], an online optimal energy control method is presented accounting for the renewables. In addition, the safety operation condition of ESSs should be specially treated in microgrid operation optimization. Particularly, lithium-ion batteries is admirable and popular because of the lifespan advantages [50]. Due to the frequent charging and discharging patterns, it becomes a thorny issue to accurately sense and calculate the degradation of battery energy storage systems (BESSs) in small-scale microgrids. Despite no forecast energy data, an ideal real-time battery scheduling strategy can achieve the optimal usage of BESSs [51]. This is also confirmed in [49], in which the proposed fitted rolling horizon strategy can provide the optimal policy for the deterministic microgrid scheduling even with missing data, and can perform efficiently in the uncertain case study. The work in [52] formulates the online energy management model as an optimization problem and proposes a Lyapunov-based online scheme. The online energy management schemes are validated on an experimental test case and the strategies are evaluated in [53]. In [54] and [55], a retroactive approach is proposed for the microgrid real-time scheduling based on the unit commitment chance cost of generators.

As a closed-loop control strategy, model predictive control (MPC) can be well integrated with prediction models and optimization functions [56]. Increasingly more application fields have adopted this idea, and it has become an efficient way to solve the microgrid optimal scheduling problems containing random energy resources [57]. In order to increase the accuracy of the scheduling results, the model needs to make full use of the continuously updated forecast information of renewables such as PV and wind power [58]. The rolling optimization strategy, also known as receding horizon method, is mathematically based on MPC and

---

can effectively meet the operating requirements of the system [59]. MPC can be applied to manage the energy flows in microgrids with hybrid energy storage systems [60]. In [61], MPC-based hybrid electric vehicle management framework is presented by combining the rolling optimization with prediction feedback correction. As for an MPC-based building energy management system, the heating ventilation air-conditioning system is controlled according to the surroundings, and coordinates with the multi-energy resources to maintain the occupants' comforts [62, 63]. Thanks to the stability, MPC is suitable for individual and interconnected microgrids on both the converter-level and grid-level, which is a competitive alternative to conventional control and optimization methods [64]. Based on the feedback mechanism, the MPC algorithm can continuously update the optimal control strategy according to the update of the model input, and can effectively deal with the expected objective function and large-scale sequential constraints, so it has attracted more and more researchers' attention [65, 66].

Recent research on interconnected microgrids has shown that peer-to-peer (P2P) energy trading is a promising solution to smart microgrid energy management [67]. P2P is the concept emerging from network communication [68]. In energy management field, it is defined as direct energy trading between energy prosumers such as campus, hospital, offices and business center, among which excessive energy is transmitted and traded [69]. A hierarchical P2P microgrid trading and architecture is proposed for microgrid energy management [69]. Each microgrid in the distribution network can be regarded as an individual agent and decentralized P2P communication is investigated for the economic dispatch of microgrids in [70]. Some relevant research works include the energy sharing mechanism design based on a multi-agent simulation network [71], energy sharing through community battery control [72] and P2P energy sharing

---

among smart homes [73]. Most of the recent research presents centralized or decentralized structures for the P2P energy trading realization [25]. In centralized P2P trading models, the market operator coordinates the transactive market, where other energy participants can proactively sell or buy energy either to/from the utility grid or other peers [74, 75]. In the second category, decentralized models remove the need of central market operators, while frequent neighboring information exchange is necessary for global optimization of total social welfare maximization [76]. Participants in the P2P market are involved to earn profits or save costs by importing or exporting energy with peers instead of the utility grid [24]. The agent bidding strategies of sellers and buyers in the P2P market are modeled in [77]. In [78], a P2P market design is presented using cooperative coalition and blockchain. In [79], a smart building community can conduct P2P energy trading under the proposed framework, making full use of local flexible resources, such as battery storage systems and electric vehicles. In general, the decentralized P2P market models are reasonable for the applications on a large scale, in terms of independence, self-interest and privacy protection. Profit allocation is one of the most challenging issues in the design of P2P energy trading market. In [80], a privacy-preserving scheme is proposed for peers to allocate the total cost savings based on Nash bargaining theory that can obtain the Pareto-efficient solution. Likewise, market power is adopted as a metric to fairly allocate the cost savings [81]. A two-stage framework is put forward to sequentially determine the payment and the energy trading strategy [82]. The bilateral double auction scheme is formulated in [83] to determine the P2P trading price in a stable Stackelberg game. It should be noted that most of the above methods require solving the energy trading subproblem and the payment subproblem separately, which naturally leads to less fair and semi-optimal solutions.

### 1.3 Objectives and Primary Contributions

As reviewed in previous sections, the energy management of microgrids with DERs has gained much attention from researchers. However, the existing work is far away from the real-world implementation. In addition, some challenges come into being with the emerging unexpected conditions that the traditional approaches are unable to deal with, such as battery degradation and energy trading. Moreover, P2P energy transactions deserve an elegant mechanism design and market framework. In addition, the energy management of microgrids under uncertainty should take various constraints and operation conditions of distribution networks into consideration.

To fill in the research gaps, this thesis will develop active energy management and operation strategies for the single and multiple microgrids with DERs. The main contributions of the thesis are listed as four aspects:

1. The short-term economic operation framework is proposed in Chapter 2 for microgrids with battery storage energy systems (BESSs) and uncertain renewable productions. First of all, the impact of battery charging and discharging behavior on the life cycle degradation is analyzed. In addition, a novel real-time degradation model is specially developed for lithium-ion BESSs to resemble the battery material degradation as much as possible. Considering the short-term forecasting errors of renewable output, the microgrid operation optimization is formulated into a weighted MPC problem. Compared to existing works, the proposed MPC framework can reduce the operation cost, improve the battery storage performance, and meanwhile can well resolve the short-term uncertainty-embedded decision-making problems.

- 
2. Microgrids located within the same geographical areas can be interconnected when making energy scheduling decisions. Cooperative management can be beneficial and economic for microgrids to complement each other in terms of matching the power supply with the demand at the minimum cost. Chapter 3 develops an energy sharing framework for building microgrids, which is formulated as a cooperative welfare maximization problem. The flexible end-use equipments in buildings are modeled, such as HVAC, electric vehicles and batteries. The P2P trading amount and optimal price are both negotiated between trading peers in a private manner. The optimization problem is solved by a fully decentralized algorithm based on a modified version of ADMM. The case study shows that P2P energy sharing of smart buildings can improve the social welfare and can facilitate the realistic plug-and-play implementation.
  3. To enable the transactive management in alignment with existing electricity market timeline, a hierarchical P2P market with different timescales is proposed for microgrids to further explore their flexibilities in Chapter 4. In the proposed tri-level P2P transaction market, the day-ahead market provides preliminary energy schedule decisions; the intra-day market is introduced to generate corrective actions to complement day-ahead decisions; the real-time regulation market can further guarantee the short-term balance of power supply-and-demand. A decomposition strategy based on dual-consensus ADMM (DC-ADMM) is proposed to solve the P2P trading settlement in a fully distributed manner, in which the zero-sum payment term is explicitly determined. Furthermore, the possible communication failures in the cyber network are innovatively taken into account and a communication failure-robust algorithm is accordingly designed. Numerical

tests demonstrate the effectiveness of the proposed framework in motivating P2P energy transactions within the existing hierarchical electricity market environment, where the energy trading is settled with different timescales.

4. Considering the distribution system operation constraints, a two-stage network-constrained P2P transaction framework is proposed in Chapter 5. In the first stage, distribution network power flow is incorporated with P2P transactions which can preliminarily determine the energy trading amount based on forecasting information. In the second stage, the network operation constraints are respected by fully utilizing local flexible resources. A co-operative optimization model is formulated to solve the two-stage operation problem. In this regard, the implementation concerns can be well addressed for the P2P energy transactions at the distribution network level. In addition, the social welfare can be improved for the system operator since the P2P energy transaction and local flexibility resources are jointly optimized. Simulations on modified 37-bus cases verify that the proposed co-operative optimization framework can enhance both the economic cost performance and nodal voltage profiles.

## 1.4 Thesis Organization

This thesis is organized as in Fig. 1.1: In Chapter 2, a short-term economic operation model is developed for battery embedded microgrid. In Chapter 3, a P2P energy sharing framework is presented for building microgrids in consideration of dynamic elements including HVAC, battery energy storage systems, and electric vehicles. Chapter 4 presents a tri-level P2P trading framework for the microgrid cooperation based on distributed model predictive control method. In Chapter

5, a cooperative optimization model is developed for the two-stage network constrained P2P energy trading in a distribution grid, meanwhile considering the unbalanced power flows. In Chapter 6, this thesis is concluded and some directions are given for future works.

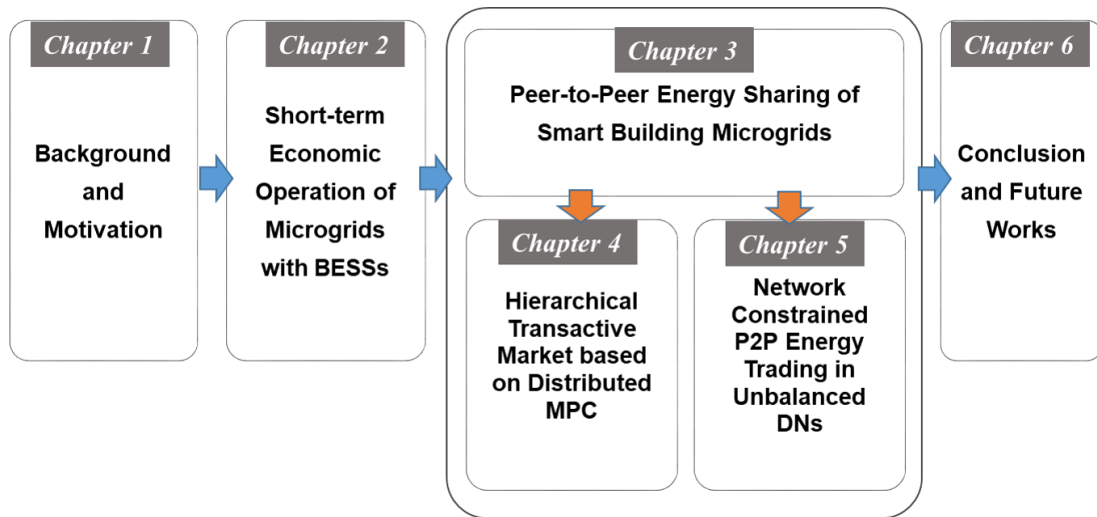


**Figure 1.1:** Thesis organization and structure.

## Chapter 2

# Short-term Economic Operation of Microgrids with BESSs

### 2.1 Introduction

In the last decades, microgrids have been a popular paradigm to integrate renewables, including wind energy and solar PV energy. In this way, human beings can reduce the dependence on fossil fuel energy, as well as cut down the polluting gas emissions. In general, there are several key elements in a microgrid: micro generators, wind turbines, solar panels, and storage systems [8]. There are typically two operation modes: grid-connected mode and isolated mode. In the grid-connected mode, microgrids can exchange energy with the utility grid to balance the local demands, while in the isolated mode, microgrids use local storage or generators to supply demands [84]. As mentioned in the previous chapter, microgrid energy management has gained more attention in recent years, with respect to operation model, economic dispatch, and DER uncertainty.

Economic operation seeks optimal operation instructions for the generators in the power system. For microgrids, the economic operation results ensure the

economic energy combinations between energy suppliers and flexible loads while minimizing the operation costs. Traditionally, this is achieved by day-ahead and intra-day instructions for the energy production amount based on different timescales of forecasting information. However, this is not the case for small-scale microgrids with intermittent DERs. The exact energy forecasting information for small-scale DERs becomes challenging in these microgrids because the uncertainty of renewables is relatively large. In this sense, making reliable plans in ahead is a difficult and tough issue for implementation. Thus, it is of importance to develop advanced methods to deal with the challenges posed by the intermittence of DERs. In this context, a few research works have proposed methods for the real-time operation of microgrids under uncertainty. Stochastic programming is a scenario-based approach to deal with optimization problem with random variables. Specifically, the probabilistic distribution function of random variables is supposed known and some typical scenarios are generated accordingly [85]. In [86], the renewable energy output is regarded a source of uncertainty, and a two-stage stochastic model is formulated for the microgrid operation problem. The power output of generators is determined in the first stage according to the system operator, while the utility energy trading is utilized in the second stage to complement the energy deficit or surplus. As mentioned in Chapter 1, one of the drawbacks of stochastic programming is that it requires to know the distribution function of random variables, and it suffers from computation burden to solve each scenario. On the other hand, robust optimization is adopted in [87] to address the random output of renewables. Instead of constructing scenarios, robust optimization considers the power range of renewables, i.e. lower bound and upper bound. The worst case in the range is selected as an optimization problem. For example, when the system operator seeks solutions to minimize the total cost,

the maximal cost in the renewable range is considered and then minimized. In this regard, robust optimization solves a min-max problem, and provides a robust solution. Due to the worst case is considered, the resultant solution is tractable but conservative. In most cases, that is, a larger total cost is generated for microgrid economic dispatch. In [88, 89], an online heuristic algorithm is proposed for the microgrid dispatch problem, which adopts a retroactive approach without the need of any forecasting information.

In addition, the battery energy storage system (BESS) degradation is not negligible in the operation cost calculation for microgrids [50]. In order to formulate a total operation cost minimization problem for all elements, it is vital to model the operation constraints of BESS and calculate the degradation cost of batteries, according to the sensible parameters, e.g., energy capacity, charging and discharging power, state of charge (SoC), temperatures and etc [90]. In this context, quite a few works focus on BESS operation model. For lithium-ion battery storage system, the degradation cost is not a fixed value because of the calendar aging and cycle aging [90]. In [91], it is pointed out that calendar aging is resulted from the material degradation in the battery over time, while the cycle aging of batteries refers to life fade caused by charging and discharging of batteries. In [51], an offline battery degradation cycle counting method is proposed, and the effectiveness is validated in experiments. Nevertheless, it is also pointed out that calculating the battery degradation cost in a real-time manner is challenging.

This chapter focuses on the short-term economic operation model of a single microgrid. Specifically, this chapter analyzes the lithium-ion BESS operation characteristic in detail. The charging and discharging life cycle constraints are modeled in the microgrid operation cost optimization. In addition, this chapter

presents an online degradation cost model for BESS based on the online auction theory. Furthermore, accounting for the forecast errors of renewables and loads, a modified version of MPC approach is designed to solve the short-term optimization problem. The main contributions of this chapter are summarized as follows.

- The lithium-ion BESS operation with respect to life cycle degradation is analyzed in detail. The charging and discharging life cycle constraints are modeled in the microgrid operation cost optimization problem. In addition, this chapter presents an online degradation cost model for BESSs based on the online auction theory.
- To account for the forecast errors of renewables and loads, a modified version of MPC approach is designed to solve the short-term optimization problem. Detailed simulations based on real-world data are carried out to test the proposed model and approach.

The rest of this chapter is organized as follows: Section 2.2 presents the operation model for battery energy storage system. The problem formulation and the MPC methodology are displayed in Section 2.3. Section 2.4 describes the case study and discusses the simulation results. Section 2.5 draws a summary of this chapter.

## 2.2 Battery and Microgrid Model

In general, there are three main basic elements in a microgrid, 1) micro generators such as diesel engine nits (DE), 2) micro turbines (MT), 3) renewable sources such as solar panel and wind turbines (WT) and 4) battery energy storage system. In this chapter, the battery operation model is first displayed and

then the microgrid real-time operation model is formulated into a modified MPC framework. In particular, the objective function and constraints are given in the following sections in detail.

### 2.2.1 Battery Operation Model

Energy storage system can supply the load by discharging and store the excessive energy by charging. In this regard, the charging and discharging processes should be modeled in a mathematical form. State of charge (SoC) is a state variable widely used in battery control problem to record the energy evolution of batteries:

$$\text{SoC}_t = \text{SoC}_{t-1} + \frac{P_t^{\text{ch}} \eta^{\text{ch}}}{B} \tau - \frac{P_t^{\text{dis}}}{\eta^{\text{dis}} B} \tau \quad (2.1)$$

where  $P_t^{\text{ch}}$  represents the charging power,  $P_t^{\text{dis}}$  represents the discharging power;  $\eta^{\text{ch}}$  indicates the charging efficiency, while  $\eta^{\text{dis}}$  indicates the discharging efficiency;  $B$  represents the energy capacity of battery storage;  $\tau$  represents the time interval, respectively. The daily operation of BESS should follow the security requirement including the battery SoC level constraints, charging power bound and discharging bound. That is,

$$\text{SoC}_{\min} \leq \text{SoC}_t \leq \text{SoC}_{\max} \quad (2.2a)$$

$$0 \leq P_t^{\text{ch}} \leq P_{\max}^{\text{ch}} \quad (2.2b)$$

$$0 \leq P_t^{\text{dis}} \leq P_{\max}^{\text{dis}} \quad (2.2c)$$

$$P_{\max}^{\text{ch}} \cdot P_{\max}^{\text{dis}} = 0 \quad (2.2d)$$

It should be noted that (2.2d) is added to guarantee that the battery storage is either charging or discharging in a single time slot. Even though this constraint

is nonlinear, it can be relaxed because the objective function formulated in section 2.3.1 can avoid simultaneous charging and discharging. That is to say, this constraint may be negligible in some works. For clarity, this chapter displays it explicitly.

## 2.2.2 Battery Marginal Degradation Model

The previous section gives some basic operation constraints as in most research works. However, the degradation cost is not considered in these constraints. In fact, the degradation cost is a necessary part for compared to the total operation cost. Hence, it should be covered in real-time optimization problem.

As explained above, degradation of battery material results mainly from cycle aging. The empirical degradation curve of a battery is shown in Fig. 2.1, which explains the life loss (assuming total life = 1) to cycle depth (discharging level/capacity). For example, a cycle depth of 0.3 results in a cycle life loss by 0.00004, while a cycle depth of 0.8 leads to a life loss by 0.00032. That is, the marginal degradation cost is not simply linear with the charging depth. Instead, the marginal cost increases with the cycle depth.

Let  $\psi$  denote the cycle life loss and  $\delta_t$  denote the discharging depth, the relationship between them can be summarized as below accordingly:

$$\psi(\delta_t) = \alpha \delta_t^{1+\beta} \quad \delta_t \in [0, 1] \quad (2.3)$$

where a polynomial function is deployed here to model the empirical stress curve. In (2.3),  $\alpha, \beta \geq 0$  are parameters to represent the curve shape. In real-time operation, the cycle depth  $\delta_t$  is unknown, but it relative to the discharging power  $P_t^{\text{dis}}$  that is observable. In this way, the marginal degradation can be attained by

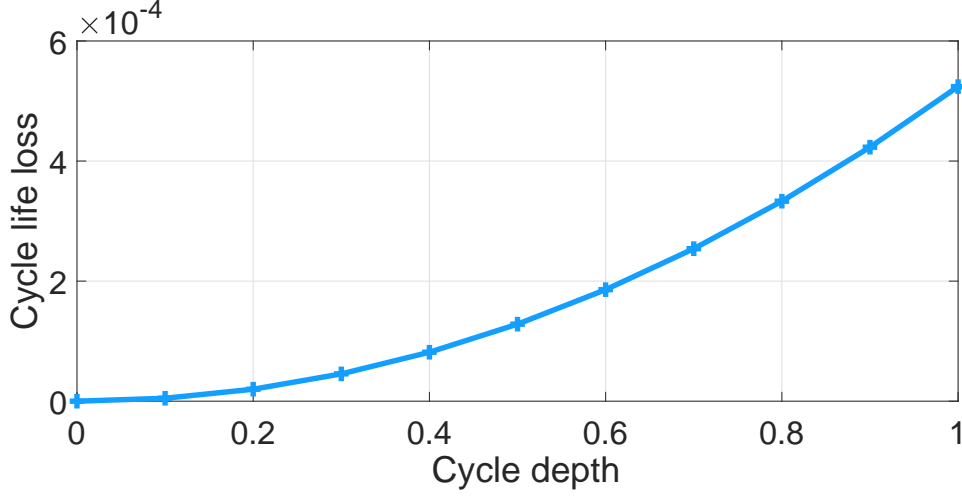


**Figure 2.1:** The life cycle degradation curve against the charging-discharging depth.

simply taking the derivative of (2.3) of discharging power:

$$\frac{\partial \psi(\delta_t)}{\partial P_t^{\text{dis}}} = \frac{d\psi(\delta_t)}{d\delta_t} \frac{\partial \delta_t}{\partial P_t^{\text{dis}}} = \frac{d\psi(\delta_t)}{d\delta_t} \frac{1}{\eta^{\text{dis}} B} \quad (2.4)$$

in which the first equation is the chain rule of derivative, and the second equality is the relationship of cycle depth with the charging power. Inspired by the recent work in counting the cycle depth that proved mathematically as accurate as empirical curves counted by offline rain-flow cycle counting algorithm [51], this chapter proposes a novel segmental method to approximate the real-time degradation cost. That is, an  $N$ -segment piece-wise linear function is designed to calculate the marginal degradation cost in (2.5):

$$C^S(\delta_t) = \frac{R}{\eta^{\text{dis}} B} \frac{\psi(\frac{i}{N}) - \psi(\frac{i-1}{N})}{1/N} \quad \delta_t \in \left[ \frac{i-1}{N}, \frac{i}{N} \right) \quad (2.5)$$

where  $C^S$  represents the proposed segmental marginal degradation cost,  $R$  represents the investment cost of a battery energy storage, the indexes  $i = 1, 2, \dots, N$  mean that the total capacity of the battery is divided into  $N$  segments, and each

segment shares  $1/N$  of the total energy capacity.

For instance, as in Fig. 2.2, the total capacity of the battery is divided into  $N = 5$  segments, namely segment  $i = 1, 2, 3, 4, 5$  from the bottom to top. We assume that the bottom segment is first-in-first-out, that is, the bottom segments has the lower price than top segments. It is the same idea from the marginal cost increase in Fig. 2.3. Then, the segment color becomes blank indicating that its stored energy is used, and the empirical SoC curve represents the total energy use strategy. As if the bottom segment is cheaper, they are prior to be utilized in the discharging and charging.

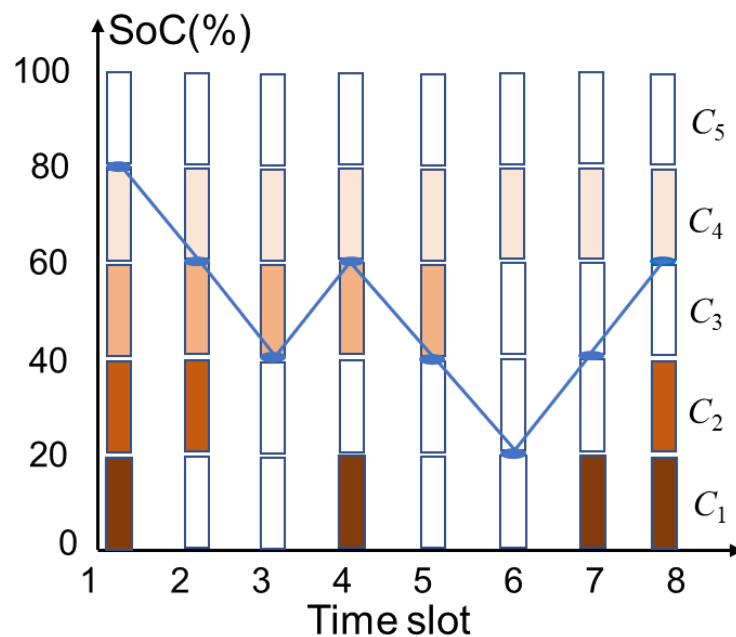


**Figure 2.2:** Illustration of battery segmental marginal cost in empirical use.

For the microgrid real-time operation, the marginal cost of battery is compared with the generator cost in an online fashion. That is, the system operator chooses cheaper energy when supplying local demands. However, there still remains one issue that the final cycle depth is unknown in the current time period.

What is known in real-time is the discharging power and real-time discharging cycle. The marginal cost is small for a low cycle depth while it is large at a deep cycle depth. In this regard, to avoid discharging continuously, the battery system should predict the final cycle depth based on the current cycle depth, and set the marginal battery price accordingly. From the microgrid system's perspective, a proper real-time pricing for the battery has two main purposes, i.e., 1) the real-time marginal price should be larger than the actual degradation cost as in fig. 2.1 and 2) the battery storage should be properly utilized with some remains as a reserve for emergence cases. Pricing scheme has been investigated in many works and one of the approaches satisfying the above two goals is online auction method in [92]. In light of this, this chapter designs an online degradation cost based on the online auction method.

- Observing the current discharging depth, the system operator anticipates the terminal cycle depth to be  $\gamma(\gamma > 1)$  times larger if the terminal cycle depth is smaller than the allowed one  $\delta_{\max}$ , normally 0.9 of the capacity.
- When the estimated cycle depth is larger than the allowed one  $\delta_{\max}$ , which means that the battery energy should no longer be utilized as before, the operator prefers local generators and increasing the marginal degradation price exponentially.

By these steps, the proposed real-time online auction-based degradation cost model for the battery energy storage system is summarized as below:

$$C^A(\delta_t) = \begin{cases} C^S(\gamma\delta_t) & \text{if } \delta_t \leq \frac{\delta_{\max}}{\gamma}, \\ C^S(\delta_{\max})e^{\theta(\delta_t - \frac{\delta_{\max}}{\gamma})} & \text{otherwise} \end{cases} \quad (2.6)$$

where  $C^A(\delta_t)$  is proposed online auction-based degradation cost for each segment

as (2.5), which is a function with the current cycle depth  $\delta_t$  at time  $t$ ;  $C^A(\delta_t)$  is defined with a modification of function  $C^S$  in (2.5);  $\gamma > 1$  and  $\theta$  are parameters defined by the shape function of the cycle depth curve [92]

$$\gamma = \max \{2, (1 + \beta)^{1/\beta}\} \quad (2.7)$$

$$\theta = \max \left\{ \frac{\gamma\beta}{\delta_{\max}}, \frac{\gamma}{\delta_{\max}(\gamma-1)} \ln\left(\frac{C_{\max}^M}{\alpha(1+\beta)\delta_{\max}}\right) \right\} \quad (2.8)$$

where  $\alpha$  and  $\beta$  are parameters in cycle life loss function (2.3);  $C_{\max}^M$  is a given value denoting the largest marginal cost of local generators in the microgrid. It should be mentioned that, the online auction-based degradation cost function  $C^A$  is defined based on the segmental cost model  $C^S$  but makes an improvement on the corresponding segmental model: it divides the total capacity of the battery into  $N'$  segments instead of  $N$  segments. Normally,  $N' > N$ . Essentially, this is the property of online auction mechanism, and the value of  $N'$  is given by  $\gamma$  and  $N$ . The energy stored in a segment has the marginal cost or price in  $C^A$ . In other words, when determining dispatching energy from the battery, the battery energy price is dependent on the segment it belongs to. In the next section, this feature will be simulated and discussed in detail in a real-world BESS.

## 2.3 Problem Formulation and Methodology

### 2.3.1 Cost Function

In islanded microgrids, the operation optimization aims to minimize the total cost while satisfying the local energy demands. Two parts are included in the total costs, the local generator cost and battery degradation cost. The local generator cost is modeled as a quadratic function with the power generation, and

the battery degradation cost is formulated as in the previous section. The total cost function is summarized as below:

$$F_t = \sum_{j=1}^M u_{j,t} (a_j (P_{j,t}^{\text{gen}})^2 + b_j P_{j,t}^{\text{gen}} + c_j) + \sum_{i=1}^{N'} C^A (P_{i,t}^{\text{dis}} + \epsilon P_{i,t}^{\text{ch}}) \quad (2.9)$$

where  $M$  represent the number of local generators with indexes  $j = 1, 2, \dots, M$ ;  $N'$  represents the number of segments of a BESS, with indexes  $i = 1, 2, \dots, N'$ . The parameters  $a_j, b_j, c_j$  are given to define the generator cost function;  $\epsilon$  is a small value to guide the charging in cheap segments.  $P_{j,t}^{\text{gen}}$  represents the generator  $j$  power output at time  $t$ ; the binary variable  $u_{j,t}$  represents the start-down state of the generator  $j$  at time  $t$ .

### 2.3.2 Operation Constraints

The previous section has given some basic operation constraints for the battery system, as listed in (2.1) and (2.2). Due to the proposed segmental battery degradation model, the total capacity of a battery is divided into  $N'$  segments. For each segment, (2.10)-(2.12) describes the relationship between each segment and the total capacity in terms of SoC, charging power and discharging power.

$$\text{SoC}_t = \sum_{i=1}^{N'} \text{soc}_{i,t} \quad (2.10)$$

$$P_t^{\text{ch}} = \sum_{i=1}^{N'} p_{i,t}^{\text{ch}} \quad (2.11)$$

$$P_t^{\text{dis}} = \sum_{i=1}^{N'} p_{i,t}^{\text{dis}} \quad (2.12)$$

where  $\text{soc}_{i,t}$ ,  $p_{i,t}^{\text{ch}}$  and  $p_{i,t}^{\text{dis}}$  are introduced as new decision variables to represent the SoC, charging power and discharging power of the  $i$ -th segment of the battery energy, respectively.

In addition, the generator operation should follow the power output limit constraint, ramping power constraint, and the minimal on/off duration constraint:

$$u_{j,t}P_{j,\min}^{\text{gen}} \leq P_{j,t}^{\text{gen}} \leq u_{j,t}P_{j,\max}^{\text{gen}} \quad (2.13)$$

$$P_{j,t}^{\text{gen}} - P_{j,t-1}^{\text{gen}} \leq P_j^{\text{RU}}, \quad P_{j,t-1}^{\text{gen}} - P_{j,t}^{\text{gen}} \leq P_j^{\text{RD}} \quad (2.14)$$

$$u_{j,t} - u_{j,t-1} \leq u_{j,t'}, \quad u_{j,t-1} - u_{j,t} \leq 1 - u_{j,t'} \quad (2.15)$$

where  $P_{j,\min}^{\text{gen}}$  and  $P_{j,\max}^{\text{gen}}$  represent the power output range of the generator,  $P_j^{\text{RU}}$  and  $P_j^{\text{RD}}$  represent the ramping up and down limit of the generator. The constraint (2.15) describes the minimal on and off duration requirement of the generator, where  $t' = t + 1, \dots, \min(t + T_j^{\text{on(off)}} - 1, H)$ ,  $T_j^{\text{on(off)}}$  represents the minimal on and off duration of the generator  $j$ ,  $H$  is the horizon window.

Lastly, the real-time power supply and demand balance is summarized as below.

$$\sum_{j=1}^M u_{j,t}P_{j,t}^{\text{gen}} + P_t^{\text{dis}} - P_t^{\text{ch}} \geq P_t^{\text{Lnet}} \quad (2.16)$$

The net load  $P_t^{\text{Lnet}}$  in (2.16) is defined by subtracting the local power demands by real-time power output of renewables. Here, we relax the exact equality into a inequality, aiming at to make the nonlinear optimization problem tractable for cutting-edge solvers. Note that the solutions will not change under this relaxations.

### 2.3.3 Weighted MPC Approach

This section formulated the microgrid operation problem into a rolling horizon framework based on a modified version MPC.

First of all, the MPC solves the optimization problem in a predefined multi-time horizon  $H$  based on the near future forecast information, as in Fig. 2.3. Doing so avoids myopic results which focus solely on the single time slot. Then, the solution of the first time slot is implemented. After updating the forecast information, the horizon window is then rolling forward while keeping the window length unchanged.

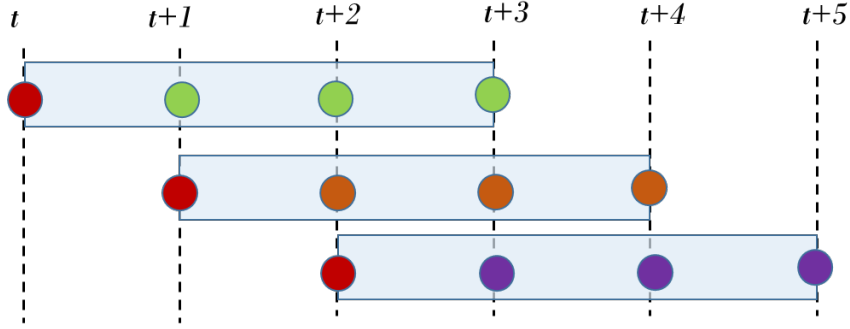


**Figure 2.3:** Illustration of model prediction control.

Because of the feedback mechanism, MPC enjoys the advantage of stability, and can potentially compensate for the forecast error in the optimization. In addition, this chapter considers that the forecast error in the horizon window, this chapter proposes a wighted MPC model in (2.17), which introduces discount rate  $r$  for the costs in each time slot.

$$\min \sum_{t'=t}^{t+H-1} r^{t'-t} F_{t'} \quad (2.17a)$$

$$\text{s.t. (2.1), (2.2), (2.10) – (2.15)} \quad (2.17b)$$

## 2.4 Case Study

This section conducts a case study to test the proposed model and approach in a islanded microgrid. The simulation platform is MATLAB 2019b and personal computer with Intel(R) Xeon(R) CPU E5-2650 two processors. The optimization problem is solved by the cutting-edge solver 'scip'.

### 2.4.1 Case Configuration

There are two generators in the microgrids, i.e.,  $M = 2$ . The parameters for the generators are given in Table 2.1 based on the data from [93]. In addition, the time interval for the operation is  $\tau = 15$  minutes,  $\epsilon = 0.001$  the generator minimal on and off duration is set as  $T^{\text{on}} = T^{\text{off}} = 1\text{h}$ . To simplify the problem solving procedure, the generator G1 is set on for all the time, while generator G2 is pending dispatching.

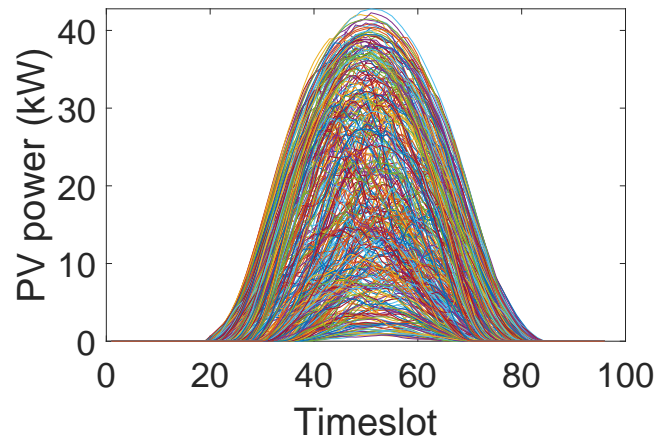
**Table 2.1:** Generator Data

Gen	$a(\$/(\text{kW})^2\text{h})$	$b(\$/\text{kWh})$	$c(\$)$
G1	0.0013	0.062	1.34
G2	0.0010	0.057	1.14
Gen	$P^{\text{RU(RD)}}(\text{kW})$	$P_{\text{max}}(\text{kW})$	$P_{\text{min}}(\text{kW})$
G1	240	50	6
G2	280	92	16.4

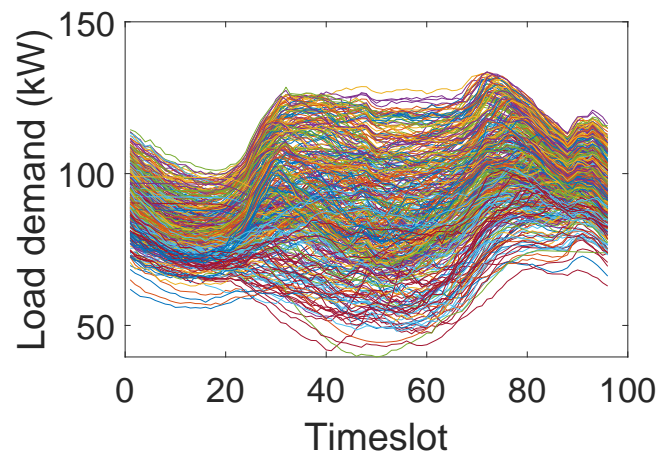
Moreover, the solar panel capacity is set as 45kW and the battery storage system data is displayed in Table 2.2. Note that the charging efficiency and discharging efficiency are set the same. Regarding the cycle loss curve shape, the parameters are derived from the empirical curve  $\alpha = 5.24 \times 10^{-4}$ ,  $\beta = 1.03$  [50]. In the formulated weighted MPC problem (2.17), the defaulted optimization window horizon is  $H = 4$ , the defaulted discount rate is set as  $r = 0.9$ , respectively.

**Table 2.2:** BESS Data

$B(\text{kWh})$	$R(\$)$	$\text{SoC}_{\min}$	$\text{SoC}_{\max}$	$P_{\max}(\text{kW})$	$\eta$
600	120000	20%	90%	120	0.95



(a) PV power output



(b) Load demand

**Figure 2.4:** One-year power data: solar energy data and load consumption.

In Fig. 2.4, the solar power generation and load demand profiles are illustrated for 365 days in year 2014-2015, which is scaled down from a real-world data in Belgium grid [55]. It is also noted that the net load value is always positive in all cases.

## 2.4.2 Simulation and Analysis

**Results of the battery degradation model** Firstly, the degradation cost model of the battery system is validated: both the segmental cost model  $C^S$  and the proposed online auction-based model  $C^A$  are illustrated in Fig. 2.5. In the online auction model,  $\gamma = 2$  in (2.6). The segment number in  $C^S$  is taken as  $N = 10$ , and the allowed largest cycle depth is set as  $\delta_{\max} = 0.8$ .

Regarding the blue curve  $C^S$ , the total capacity of a battery is divided into  $N = 10$  segments, with  $i = 1, 2, \dots, 10$ , each of which had 60 kWh capacity. The price of segment energy is in the horizontal axis. Meanwhile, the online auction model  $C^A$  is defined in the basis of  $C^S$ , and divides the total capacity into  $N' = 20$  segments, according to the definition equation (2.6). It is observed that the  $C^S$  curve is linear while the  $C^A$  curve is quasi-linear. It should be mentioned that, this is because that the cycle loss function is almost a quadratic function and its derivative is almost a linear function.

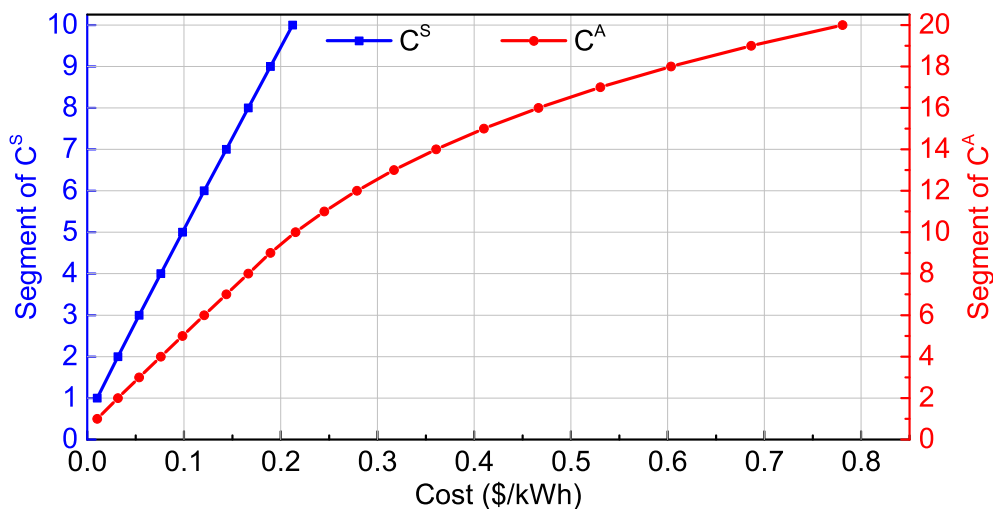


**Figure 2.5:** Marginal cost of the battery energy system.

Nevertheless, it is obviously seen that, the  $C^A$  cost curve (red curve) lies at

the right-hand side of the  $C^S$  cost curve (blue curve). This observation suggests that, for a segment with the same index in two model, the marginal cost is larger in the online auction model  $C^A$ . Meanwhile, it is seen that the number of segments in auction mode has been improved to  $N' = 20$ , i.e.  $\gamma N$ . Since there are twice more segments in the  $C^A$  model, the sub capacity of each segment becomes half in the  $C^S$  model. Recall the definition of  $C^A$  model in (2.6), the first 8 ( $= N\delta_{\max}$ ) segments have the same price as the first 8 segments in  $C^S$  model. But for the remaining 12 segments ( $i = 9, 10, \dots, 20$ ), the marginal price will increase exponentially. In this regard, there exists an incremental cost gap between two curves, which can not only guarantee covering the actual degradation cost but also provide a reserve for emergency conditions.

**Results of real-time operation optimization** One-year data is used to verify the proposed model, and the battery SoC profiles of the battery storage system are illustrated in Fig. 2.6 and Fig. 2.7. Note that the initial SoC = 60%, and the lower bound SoC = 20%. Fig.2.6 shows that with  $C^S$  model, BESS discharges at a fast rate and ends with SoC = 20%. It can be seen that the battery actively participates the optimal operation of the microgrid. Because the marginal cost is cheap compared to the generator cost, the battery energy is used very quickly. When the battery energy is almost used up, and the SoC reaches almost the lower bound  $SoC = 20\%$  in Fig.2.6, the SoC lower-bound constraint guarantee that the storage energy cannot be further used any more.

However, Fig.2.7 shows the battery eenergy SoC profiles from the proposed  $C^A$  model. A different result can be observed compared to the results above. That is, in most case, the battery storage is discharging in a slower rate, and the terminal SoC lies between 22% and 40%. This feature suggests that the battery

storage energy is not fully utilized at the beginning. Instead, there are some remainings as a spinning reserve, which shows advantages of the proposed model, especially for islanded microgrids in some emergency cases.

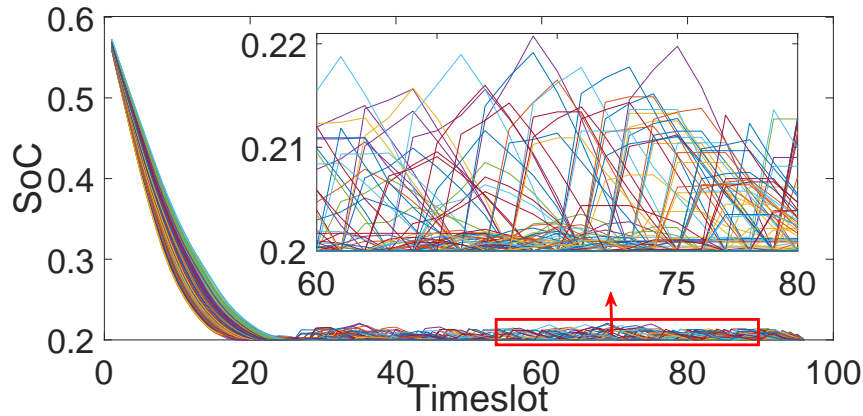


**Figure 2.6:** Battery SoC curve: from  $C^S$  battery model.

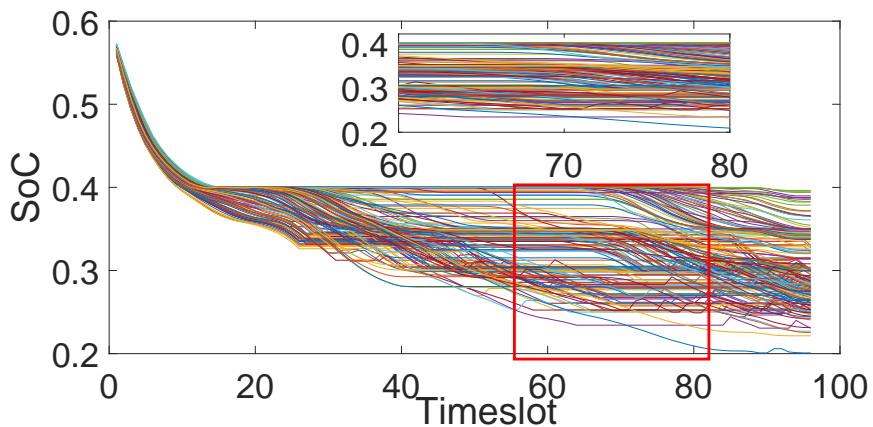


**Figure 2.7:** Battery SoC curve: from  $C^A$  battery model.

In the real-time operation, the generation profiles of the two local generations and battery storage are illustrated in Fig. 2.8 and 2.9. Note that the 23th day is taken as an example, as on that day the total net demand is the largest in one year. It is seen that, generator G2 has similar generation profiles in two model cases. This may be explained by that G2 has larger capacity than G1 and takes a large share to supply the net load. Meanwhile, it is observed in the  $C^S$  case that, the generator G2 starts up at  $t = 27$ , when the SoC of the battery storage system

almost reaches the minimal limit  $SoC_{\min} = 20\%$  in Fig. 2.8. However, for the  $C^A$  model case in Fig. 2.9, when the generator G1 starts up, the SoC of the battery storage system is  $SoC = 34.75\%$ . That is, the microgrid can make use of local generator earlier before using up the battery storage system in the  $C^A$  model case. This again reflect the advantage of the online auction-based degradation cost model.

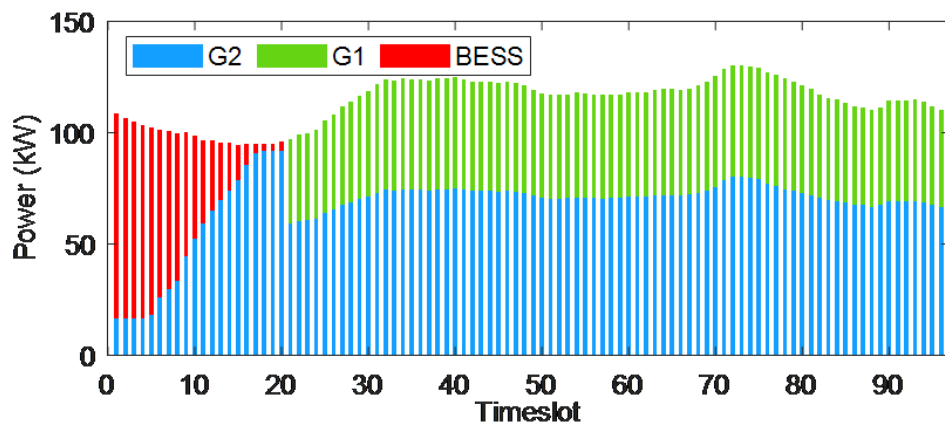


Figure 2.8: Energy optimization results (23rd day): from  $C^S$  battery model.

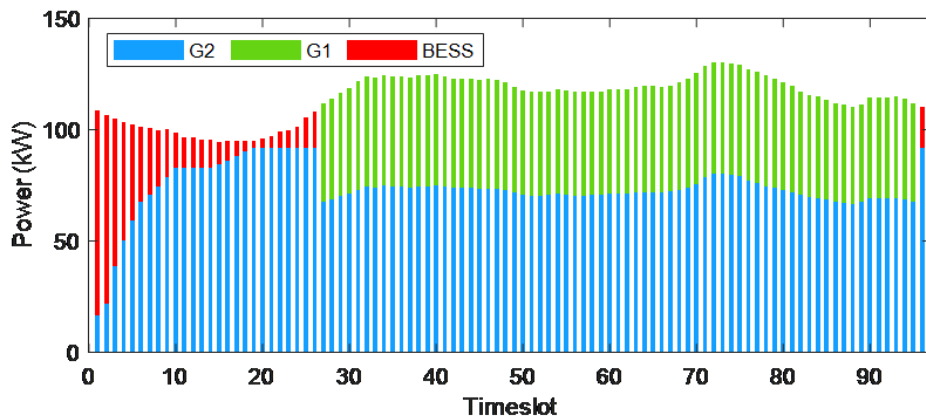


Figure 2.9: Energy optimization results (23rd day): from  $C^A$  battery model.

Regarding the total operation cost incurred by the generators and battery storage system, the energy output and costs on day 23 are compared in Table 2.3. It is seen that, as the energy from generator G2 is cheaper, it is scheduled to

output more energy in the  $C^A$  model. The results reveal that, despite that the battery price in  $C^A$  model is higher than that in  $C^S$  model, the resulting operation cost increases only by 0.85% (from 233.1\$ to 235.09\$). In addition, another benefit is that the final SoC of the battery storage system can increase by 50%. For the one-year simulations, the total cost in  $C^A$  model increases less than 3.1% compared to  $C^S$  model, in Fig. 2.10. This increase is reasonable because of the property of auction method which schedules more energy from generators instead of battery storage systems.

**Table 2.3:** Total Energy Output and Cost on Day 23

Cost Model	G1(kWh)	G2(kWh)	BESS(kWh)	Cost(\$)
$C^S$	697.43	1620.81	233.96	233.10
$C^A$	573.40	1799.28	171.32	235.09

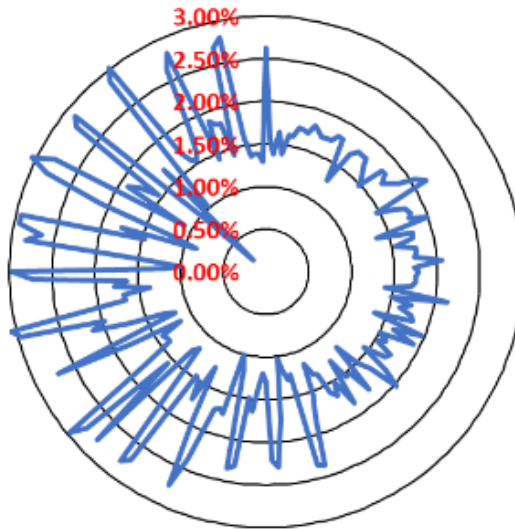


**Figure 2.10:** The operation cost increase amount (23rd day): from  $C^A$  battery model, discount rate  $r = 0.9$ .

**Sensitivity of weighted MPC parameters** In the proposed weighted MPC approaches, two defaulted value are selected: the horizon window length  $H$  and the discount rate  $r$ . At the end of this chapter, the sensitivity of these two

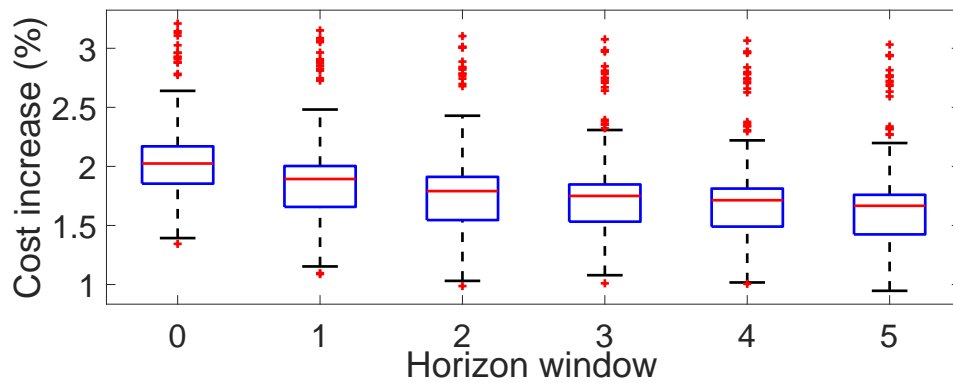


**Figure 2.11:** The operation cost increase amount (one-day): from  $C^A$  battery model, discount rate  $r = 0.9$ .

parameters are evaluated. It is seen from Fig. 2.11 and Fig. 2.12 that, the total cost increase percentage by the proposed  $C^A$  model compared to  $C^S$  is plotted by the Monte Carlo simulations on one year data with  $r = 0.9$  and  $r = 0.6$ .

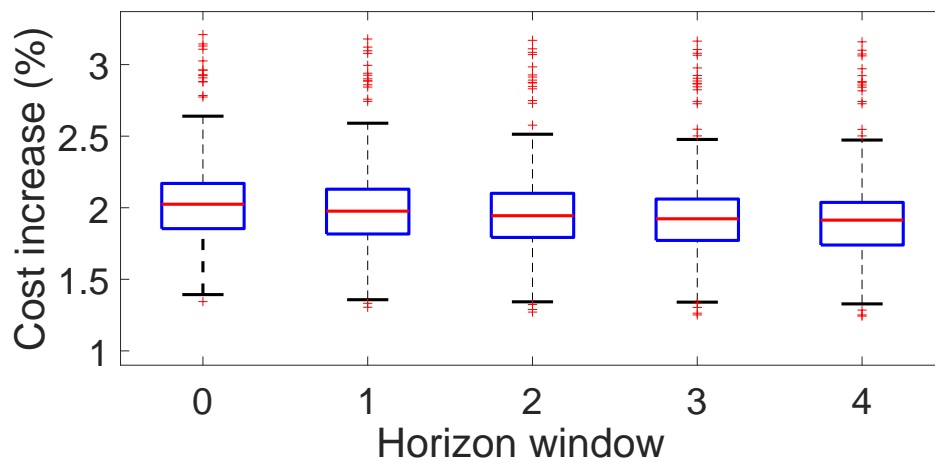


**Figure 2.12:** The operation cost increase amount (one-day): from  $C^A$  battery model, discount rate  $r = 0.6$ .

From the box-plots, one can see that the cost increase percentage ranges between 1% and 3.5%, with the average increase value ranging from 2% to 1.5% when the horizon window length varying from 0 to 5. In addition, even when

$H = 0$ , suggesting no forecast information is used in the optimization, the proposed weighted MPC approach can still get satisfying real-time instructions. Furthermore, when comparing two figures, one can find that, a small discount rate value can bring about a slow decreasing rate of the percentage value. This is because the small weights of future cost functions in the considered horizon window in (2.17a). It can be learned from this result that proper adjustment of the discount rate  $r$  can result in admirable dispatch results in specific microgrids according to the prediction performance. In particular, a large  $r$  is favorable in microgrids with accurate prediction. This equipment can help fully exploit the metrics of weighted MPC approach. On the other hand, for the microgrids with large forecast errors, a small  $r$  is preferable in these cases.

## 2.5 Summary for the Chapter

In this chapter, the short-term economic operation framework is proposed for microgrids with BESSs and uncertain renewable productions. First of all, the impact of battery charging and discharging behavior on the life cycle degradation is analyzed. A novel real-time degradation model is specially developed for lithium-ion BESSs to resemble the battery material degradation as much as possible. In addition, the proposed MPC framework can well address the challenges by the short-term forecasting errors in microgrid economic operation. The case study based on real-world data validates that the proposed model and approach can gain significant improvement in total operation cost reduction and has a significant potential to deal with inaccurate forecast information in real-world implementation.

## Chapter 3

# Peer-to-Peer Energy Sharing of Smart Building Microgrids

### 3.1 Introduction

The recent years have witnessed an amazing development of the building construction techniques and communication networks [94]. Thanks to the implementation of these advanced technology, the conventional end-use equipment in buildings becomes intelligent and automatic in control and management. For example, the lighting system, heating, ventilation, air conditioning (HVAC), storage system, and other ancillary control systems in the building are all becoming connected into the smart control system. In addition, more and more DERs are installed in buildings, which makes buildings become a typical representation of microgrids. In this regard, the traditional buildings become smart building microgrids in the modern world. The advantages brought by the smart buildings include 1) the performance of these electric appliances can be greatly improved, 2) the energy consumption of electric appliances can be reduced by intelligent control, and 3) importantly, the occupant comfort is assured by adaptive adjustment [95].

According to the report released by United Nations Environment Program<sup>1</sup>, buildings consume more than 40% of the annual energy use and carbon emission in the world. As for Hong Kong, Electrical and Mechanical Services Department (EMSD) reported that the building sector accounts for amazing over 93% of total annual electricity use in Hong Kong<sup>2</sup>. Therefore, putting forward advanced energy management schemes for smart building microgrids, can bring economic and environmental benefits in the urban low-carbon transition process.

Many research works have investigated the low-carbon transition for smart building microgrids. Some of the advanced methods for HVAC are summarized in [96], and the authors recommend to retrofit low-cost appliances in smart buildings. In [97], most popular management techniques for HVAC are reviewed, where the model predictive control (MPC) is regarded as a cutting-edge one to control HVAC system. Essentially, HVAC system adjusts the indoor temperature according to the outdoor temperature by consuming the electric power energy. In this context, battery storage systems can provide flexibility for the building microgrid aiming at saving costs and improving benefits [98]. Notably, building microgrids are close to each other in urban areas, e.g. business center, hospital, hostels. With respect to neighboring smart buildings, recent works present novel solutions of cooperative optimization operation, e.g., peer-to-peer (P2P) energy sharing [67, 99]. P2P energy sharing, also known as P2P energy trading, refers to bilateral energy trading that is negotiated by two energy production or consumption entities, or namely agents [100]. In the power systems, P2P energy sharing are introduced to the areas including battery storage system [72] and smart homes

---

<sup>1</sup>International Energy Agency for the Global Alliance for Buildings and Construction. “Global Status Report 2017-Towards a zero-emission, efficient, and resilient buildings and construction sector,” <https://www.worldgbc.org/sites>.

<sup>2</sup>Electrical and Mechanical Services Department. “Hong Kong Energy End-use Data 2019,” <https://www.emsd.gov.hk>.

[101]. Nevertheless, the implementation of P2P energy sharing still faces several challenges, including 1) the privacy of P2P sharing peers should be protected, and the information exchanged with others should be as less as possible; 2) a fair settlement strategy should be negotiated including the trading quantity and trading fees.

Recently, many researchers have presented the P2P sharing framework for smart building microgrids. For instance, the research work in [102] proposes a P2P energy sharing platform for the residential houses to coordinate the demand response and renewable energy utilization. The work in [103] puts forward a novel concept of energy classes in accordance with the preferences of consumers and producers, to distinguish heterogeneous energy sources in P2P transactive market. Regarding the energy trading settlement, the works in [104] and [105] apply auction approaches to determine the market clearing price by all participants. It is pointed out that P2P market can help facilitate making full utilization of renewable energies, e.g. the rooftop solar PV with little or even no curtailment of renewables [106]. However, the frameworks presented in the aforementioned works are based on the centralized energy trading market with a coordinator. The information privacy of market participants is not well respected in the centralized market environment.

Distributed algorithms are favorable in resolving the energy sharing market due to their privacy-preserving properties. In this context, the work in [107] formulates the P2P trading problem into the game theoretic framework, and the profits of individual peers are guaranteed without exchanging each other's private information. Moreover, the authors in [74] and [108] model the behavior of prosumers in microgrids into mathematical forms and then apply the non-cooperative Stackelberg game theory to model the P2P energy sharing between

prosumers. The essence of Stackelberg game arises from master-follower game theoretic framework, and the Stackelberg equilibrium is proved efficient to reduce the total operational cost greatly and maximize the utility of all participants [77]. Also, similar results in [78] confirm that the cooperative energy management based on the coalition game can significantly improve the social welfare via direct energy trading among prosumers. The social welfare maximization problem can be decoupled into a series of decentralized sub-problems by decentralized algorithms [70].

Regarding the energy pricing in P2P energy trading schemes, Nash bargaining method is widely investigated [24, 109] where the system cost savings are allocated to all participants. In particular, a two-stage local trading framework is presented in [82], where the pricing issue is settled down subsequently to energy quantity settlement results. Essentially, the existence of the Nash equilibrium can be mathematically proved in [80], and thus its property of Pareto efficiency for the cost saving allocation is guaranteed. The work in [81], modifies the conventional Nash bargaining by market power, which seeks to distribute savings among all participants with varying weights. The authors in [110] suggest a novel allocation scheme by designing a metric named as the cost reduction ratio on the basis of acceptable price ranges for all agents. The underneath essence of the aforementioned approaches is to distribute the expense savings to participants according to the proportion of their contributions in the whole-day trading.

From the literatures, it is observed that there is a lack in the detailed design of the energy sharing framework for multiple microgrids. Taking a group of smart building microgrids as an example, this chapter aims to devise a novel cooperation optimization framework and investigate fully decentralized algorithms for the energy sharing among multiple microgrids. The main contributions of this chapter

are twofold:

- A practical framework for the peer-to-peer energy sharing is proposed for multiple microgrids. In the framework, each microgrid can control the local flexible loads, such as electric vehicles and storage. In addition, the framework can address the energy transmission loss and energy sharing price, which are two independent parts for the reality. In this regard, the optimal solutions can be acceptable for all participant microgrids.
- In addition, this chapter designs a decentralized algorithm for the formulated energy sharing problem. Due the admirable properties of the algorithm, the internal information of all microgrids is regarded as privacy for the individual agent. Furthermore, the communication is conducted in a peer-to-peer manner.

The rest of this chapter is structured as below. In Section 3.2, the individual elements in smart building microgrids are mathematically modeled. In Section 3.3, the cooperative energy trading details are presented and the social welfare maximization problem is formulated. In addition, Section 3.4 proposes a fully distributed algorithm for solving the cooperation problem. Section 3.5 presents the case study and discusses the results and performance. Section 3.6 summarizes this chapter.

## 3.2 Smart Building Microgrid Model

In this chapter, we take an example of DER embedded microgrids, i.e., smart buildings. In particular, interconnected buildings are considered, which are located geographically near each other. Fig. 3.1 illustrate an abstract description of such a community of buildings: the buildings are all connected with each other

**Table 3.1:** Nomenclature

$\mathbf{E}_i$	The graph adjacent matrix from nodes to lines
$i, v, t, k$	The index of building, EVA, time, iteration
$P_{i,t}^h$	HVAC power load of microgrid $i$ at $t$
$P_{i,t}^{\text{EVA}}$	EV aggregator power load of microgrid $i$ at $t$
$P_{i,t}^{\text{ch}}, P_{i,t}^{\text{dis}}$	Battery storage power of microgrid $i$ at $t$
$S_{i,t}$	Energy level of battery storage $i$ at $t$
$s_{i,t}^{\text{ch}}, s_{i,t}^{\text{dis}}$	0-1 variables indicating the charging or discharging states of battery storage $i$
$u_{i,t}^{\text{bat}}$	0-1 variables indicating the charging/discharging switch of battery storage $i$
$P_{i,t}^{\text{re}}, P_{i,t}^{\text{L}}$	The renewable output power and load power of building $i$
$P_{i,t}^{\text{buy}}, P_{i,t}^{\text{sell}}$	The purchasing power from the grid, the selling power to the grid of building $i$
$e_{j,t}^{j \rightarrow}, e_{j,t}^{i \rightarrow}$	The direct trading power transmitted from $j$ and received by $i$ on the link $(i, j)$ at $t$
$y_{j,t}^{i \rightarrow}, y_{j,t}^{i \leftarrow}$	0-1 variables indicating the direct energy trading direction on link $(i, j)$
$\lambda_{i,t}^j, \lambda_{j,t}^i$	Ancillary variable indicating the local estimates of the settlement price on link $(i, j)$
$\lambda_{(i,j),t}$	Lagrangian dual variables for the direct trading energy equality on link $(i, j)$

via direct lines, while each of them has access to the main grid through the distribution network. For clarity, the buildings are collected as  $\mathcal{N} := \{1, 2, \dots, N\}$  and the neighborhood of building  $i \in \mathcal{N}$  are denoted as  $\mathcal{N}_i$ .

In addition to the installed renewables and battery energy storage system (BESS), smart building microgrids have other electric appliances such and flexible load, i.e. HVAC system and lighting system, electric vehicles [111]. The elements of the building are controlled by the smart building energy management system (SBEMS) comprising of advanced techniques and communications. This chapter investigates the P2P energy sharing of building microgrids in the day-ahead market. That is, the hourly horizon window of the P2P local market in this chapter

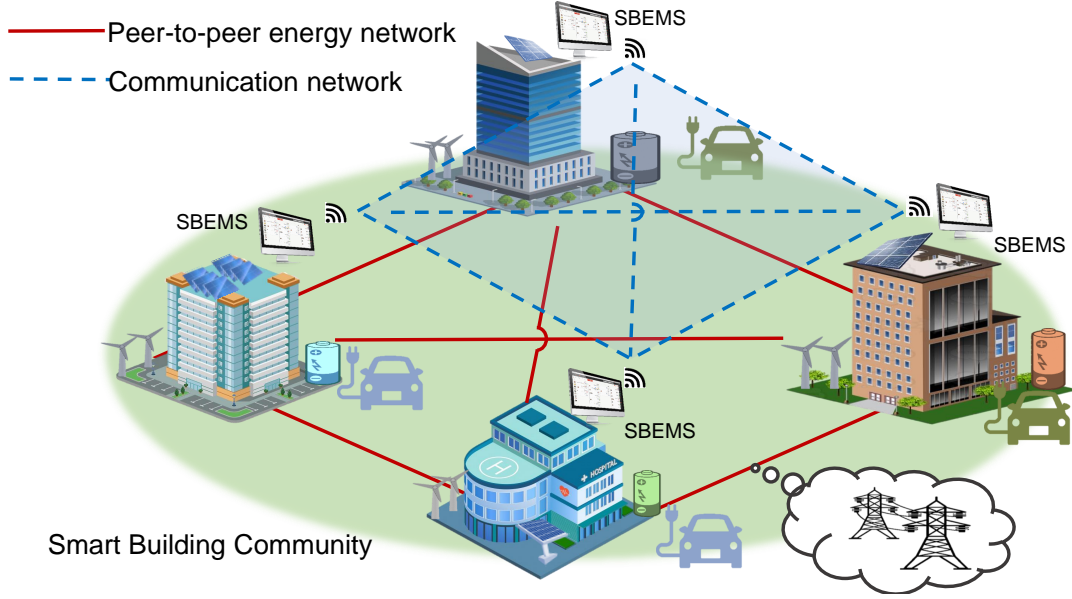


**Figure 3.1:** The structure of smart buildings community.

is  $\mathcal{T} := \{1, 2, \dots, H\}$  and  $H = 24$ .

### 3.2.1 HVAC Units in Building Microgrids

HVAC accounts for a large percentage of energy use (e.g. industrial factories, hostels, hospital complex, business center) [112]. In general, HVAC units keeps indoor temperature into a satisfying level by consuming the electric power. The room comfort is thus maintained for indoor occupants. The indoor temperature is controlled by the accumulative power consumption according to the outdoor temperature. The linearize form of this transformation is summarized as follows [110]:

$$T_{i,t}^{\text{in}} = \left(1 - \frac{1}{G_i R_i}\right) T_{i,t-1}^{\text{in}} + \frac{1}{G_i R_i} T_{i,t}^{\text{out}} - \frac{\eta_i}{G_i} P_{i,t}^{\text{h}}, \quad \forall t \quad (3.1)$$

where  $T_{i,t}^{\text{in}}$  and  $T_{i,t}^{\text{out}}$  indicate the temperature inside and outside the building  $i$ ;  $P_{i,t}^{\text{h}}$  suggests the real-time HVAC power consumption at time  $t$ ; the parameters  $G_i$  and  $R_i$  are those in HVAC units;  $\eta_i$  represents the energy transfer efficiency;

in the cooling mode  $\eta_i > 0$  and in the heating mode  $\eta_i < 0$ , in the building  $i \in \mathcal{N}$ , respectively.

The comfortable indoor temperature is a range for inside occupants (3.2), that is:

$$T_{i,\min}^{\text{in}} \leq T_{i,t}^{\text{in}} \leq T_{i,\max}^{\text{in}}, \quad \forall t \quad (3.2)$$

where  $T_{i,\min}^{\text{in}}$  is the lower bound and  $T_{i,\max}^{\text{in}}$  is the upper bound. In practice, occupants can define a set-point of the preferred indoor temperature e.g.  $T_{\text{set}}^{\text{in}}$ , and then HVAC units attempts to achieve and maintain this temperature by consuming the electric power. For example in [109, 112], the desired indoor temperature set-point is  $22^\circ\text{C}$ , and the allowable operating range is  $[20^\circ\text{C}, 24^\circ\text{C}]$  in summer. If the indoor temperature deviates from the set-point, it will result in a discomfort of occupants.

### 3.2.2 Electric Vehicle

Electric Vehicles (EVs) are typical kind of consumers/producers in modern buildings, due to the charging and discharging property. EVs can not only charge energy but also manage the charging according to the smart charging strategy. In this chapter, EV are supposed to connected to the smart building energy management system (SBEMS) via EV aggregators (EVA). In principle, EVAs are responsible for collecting the information from all EVs and schedule individual EVs accordingly. For example, the battery energy capacity, rated charging power, expected leaving time, and driver preferences. In this way, the privacy information are not directly revealed to the building system.

To begin with, when arriving at the charging stations in the building microgrids, EVs reveal their charging requirements and the EVA estimates and updates

the dispatch ability of the EVs. In other words, the EVA can flexibly make charging plans for EVs while meeting their demands within EV parking time.

$$t_{i,v}^{\text{req}} = d_{i,v}^{\text{EV}} / \min \{ \bar{p}_{i,v}^{\text{EV}}, \bar{p}^{\text{charger}} \} \quad (3.3)$$

where  $d_{i,v}^{\text{EV}}$  represents the total required charging energy of  $v$ -th EV in building  $i$ ; the allowable charging power is capped by the rated EV charging power  $\bar{p}_v^{\text{EV}}$  and the rated charger power  $\bar{p}_i^{\text{charger}}$ ; the EVA calculates the minima charging duration  $t_{i,v}^{\text{req}}$  accordingly; the arriving time  $t_v^{\text{st}}$  and the departure time  $t_{i,v}^{\text{end}}$  are information collected from individual EVs. In (3.3), the rated EV charging power is leveraged to calculate the minimal required charging time  $t_{i,v}^{\text{req}}$ . For simplicity, the rated charging power as  $p_{i,v}^{\text{rated}}$ , to denote the rated power ability of EVs:

$$p_{i,v}^{\text{rated}} = \min \{ \bar{p}_{i,v}^{\text{EV}}, \bar{p}_i^{\text{charger}} \} \quad (3.4)$$

In (3.5), the parking duration ( $t_{i,v}^{\text{end}} - t_{i,v}^{\text{st}}$ ) is leveraged to determine whether the EV is dispatchable. That is, the EVs are arranged with immediate charging or smart charging respectively.

$$\begin{cases} \text{immediate charging,} & \text{if } t_{i,v}^{\text{req}} > t_{i,v}^{\text{end}} - t_{i,v}^{\text{st}} + 1; \\ \text{smart charging,} & \text{if } t_{i,v}^{\text{req}} \leq t_{i,v}^{\text{end}} - t_{i,v}^{\text{st}} + 1 \end{cases} \quad (3.5)$$

where immediate charging means that the EVs are charging for all the parking time, while the smart charging means that the EVs are flexible and dispatchable. For the first group, EVs are regarded as uncontrollable load at the maximal charging power for the microgrid system. For the latter group, EVs with smart charging strategies can participate in the energy management of smart building microgrids. The charging requirement of EVs with smart charging strategies is

fulfilled during the parking duration:

$$d_{i,v}^{\text{EV}} = \sum_{t=t_{i,v}^{\text{st}}}^{t_{i,v}^{\text{end}}} \eta p_{i,v,t}^{\text{EV}} \Delta t \quad (3.6)$$

$$0 \leq p_{i,v,t}^{\text{EV}} \leq p_{i,v}^{\text{rated}}, t \in [t_{i,v}^{\text{st}}, t_{i,v}^{\text{end}}] \quad (3.7)$$

where  $d_{i,v}^{\text{EV}}$  represents the EV charging demand;  $\eta$  represents the charging efficiency;  $p_{i,v,t}^{\text{EV}}$  represents the charging power of EV  $v$  in the building microgrid  $i$  at  $t$ ; the charging power  $p_{i,v,t}^{\text{EV}}$  follows the bound constraint as in (3.7) on  $[t_v^{\text{st}}, t_v^{\text{end}}]$ .

According to [113], the EVA power instead of EV power is considered in this chapter. That is, the charging power of EVA is the sum of the charging power of all EVs. In this way, the number of variables is reduced.

$$P_{i,t}^{\text{EVA}} = \sum_{v=1}^{V_i} p_{i,v,t}^{\text{EV}} \quad (3.8)$$

where  $P_{i,t}^{\text{EVA}}$  is the total charging power of the EVA governing all EVs in the building microgrid  $i$ . Then, the model of EVA can be built accordingly.

$$E_{i,t}^{\text{EVA}} = \sum_{\tau=1}^t \eta P_{i,\tau}^{\text{EVA}} \Delta t \quad (3.9)$$

$$0 \leq E_{i,t}^{\text{EVA}} - E_{i,t-1}^{\text{EVA}} \leq P_{i,\text{max}}^{\text{EVA}} \quad (3.10)$$

$$E_{\text{min},i,t}^{\text{EVA}} \leq E_{i,t}^{\text{EVA}} \leq E_{\text{max},i,t}^{\text{EVA}} \quad (3.11)$$

where  $E_{i,t}^{\text{EVA}}$  represents the accumulated recharged energy of EVA,  $P_{i,t}^{\text{EVA}}$  represents the aggregated charging power of EVA. (3.10) implies that the EVA charging energy in one time interval is limited by the rated charging power power, and (3.11) suggests that the recharged energy of EVA is upper-bounded by  $E_{\text{max},i,t}^{\text{EVA}}$ ,

and lower-bounded by  $E_{\min,i,t}$ . The accumulated EVA energy is directly calculated by the retroactive method based on the EV rated charging power, as follows:

$$E_{\max,i,t}^{\text{EVA}} = \sum_{v=1}^{V_i} \left[ \sum_{\tau=t_{i,v}^{\text{st}}}^t \eta p_{i,v}^{\text{rated}} \Delta t \right]_0^{d_{i,v}^{\text{EV}}} \quad (3.12)$$

$$E_{\min,i,t}^{\text{EVA}} = \sum_{v=1}^{V_i} \left[ d_{i,v}^{\text{EV}} - \sum_{\tau=t}^{t_{i,v}^{\text{end}}} \eta p_{i,v}^{\text{rated}} \Delta t \right]_0^{d_{i,v}^{\text{EV}}} \quad (3.13)$$

where  $[\cdot]_a^b$  is notation of project onto the interval  $[a, b]$ ; in (3.12), the maximal energy trajectory is calculated by summing all EV charging energy supposing all EVs charge at the rated charging power immediately the vehicles arrived; in (3.13), the minimal energy trajectory is calculated by summing all EV charging energy assuming they wait for charging until the rated power-based charging time is just to the departure time[113].

### 3.2.3 Model of Battery Energy Storage System

Battery Energy Storage Systems (BESS) are widely deployed in smart building microgrids and are controlled by the energy management system. BESS can help building microgrids supply the load demand and store the excessive energy Via discharging and charging. Suppose that there BESS in  $i \in \mathcal{N}$ , the operation of battery energy storage should follow the operation constraints:

$$S_{i,t} = (1 - \eta_i^{\text{bat}}) S_{i,t-1} + \eta_i^{\text{ch}} P_{i,t}^{\text{ch}} \Delta t - P_{i,t}^{\text{dis}} / \eta_i^{\text{dis}} \Delta t \quad (3.14)$$

$$S_{i,\min} \leq S_{i,t} \leq S_{i,\max} \quad (3.15)$$

$$S_{i,H} \geq S_{i,0} \quad (3.16)$$

$$0 \leq P_{i,t}^{\text{ch}} \leq \bar{P}_i^{\text{ch}} S_{i,t} \quad (3.17)$$

$$0 \leq P_{i,t}^{\text{dis}} \leq \bar{P}_i^{\text{dis}}(1 - s_{i,t}^{\text{ch}}) \quad (3.18)$$

$$s_{i,t}^{\text{ch}} - s_{i,t-1}^{\text{ch}} \leq u_{i,t}^{\text{bat}}, s_{i,t-1}^{\text{ch}} - s_{i,t}^{\text{ch}} \leq u_{i,t}^{\text{bat}} \quad (3.19)$$

$$\sum_{t \in \mathcal{T}} u_{i,t}^{\text{bat}} \leq U_i^{\text{bat}} \quad (3.20)$$

where  $S_{i,t}$  represents the battery storage energy level,  $P_{i,t}^{\text{ch}}$  and  $P_{i,t}^{\text{dis}}$  represents the charging and discharging power in the building microgrid  $i$  at time slot  $t$ ;  $\eta_i^{\text{bat}}, \eta_i^{\text{ch}}, \eta_i^{\text{dis}} \in (0, 1)$  represent the self-discharging, charging and discharging efficiency;  $s_{i,t}$  is the binary variable representing the charging or discharging states;  $u_{i,t}^{\text{bat}}$  is the binary variable representing the charging-discharging switch states, respectively. specifically, (3.14) implies the energy level evolution process of BESS, (3.15) suggests the bound constraint of the battery energy level; (3.16) suggests that the final energy level is more than or equal to the beginning stored energy  $S_{i,0}$ ; (3.17) and (3.18) indicate the charging and discharging power limit; (3.19) and (3.20) imply that the total charging-discharging switch is capped by a pre-defined number on the scheduling horizon.

### 3.2.4 Operation Cost of Building Without Energy Sharing

In this subsection, the building microgrids without energy sharing is considered. In the building microgrids, the main source of energy supply involve the utility grid, renewables (PV energy, wind energy), and battery storage systems. The energy demand includes HVAC and EVs. In this regard, the energy balance in the building microgrids is:

$$P_{i,t}^{\text{buy}} + P_{i,t}^{\text{dis}} + P_{i,t}^{\text{re}} = P_{i,t}^{\text{L}} + P_{i,t}^{\text{h}} + P_{i,t}^{\text{EVA}} + P_{i,t}^{\text{ch}} + P_{i,t}^{\text{sell}} \quad (3.21)$$

where  $P_{i,t}^{\text{re}}$  represents the real-time renewable output,  $P_{i,t}^{\text{L}}$  represents the basic inflexible load,  $P_{i,t}^{\text{buy}} \geq 0$  represents the purchasing energy from the utility grid,  $P_{i,t}^{\text{sell}} \geq 0$  represents the selling energy to the utility grid, respectively, in the building microgrid  $i \in \mathcal{N}$  at time period  $t$ . In this regard, the left-hand side of (3.21) suggests the power supply, while the right-hand side of (3.21) suggests the power demand in the smart building microgrid. Meanwhile, because of the physical power line capacity  $F_i$ , the energy purchased or sold should follow:

$$-\bar{F}_i \leq P_{i,t}^{\text{buy}} - P_{i,t}^{\text{sell}} \leq \bar{F}_i \quad (3.22)$$

In this subsection, the microgrids with energy sharing is taken into considered. That is, when the building  $i$  does not involve in P2P energy sharing frameworks, the building energy management systems aim to minimize the cost of grid trading and occupant discomfort cost:

$$\tilde{C}_{i,t} = \beta_i (T_{i,t}^{\text{in}} - T_{\text{set}}^{\text{in}})^2 \Delta t + \kappa_i^{\text{bat}} (P_{i,t}^{\text{ch}} + P_{i,t}^{\text{dis}}) \Delta t + \left( \mu_t^{\text{b}} P_{i,t}^{\text{buy}} - \mu_t^{\text{s}} P_{i,t}^{\text{sell}} \right) \Delta t, \quad \forall t \quad (3.23)$$

where  $\beta_i$  is a coefficient to represent the discomfort level of occupants in the smart building  $i \in \mathcal{N}$ , and  $\kappa_i^{\text{bat}}$  is used to describe the degradation of batteries. That is, in (3.23), the first term denotes the occupant discomfort cost; the second term represents the degradation cost of battery energy storage systems; and the third term implies the power grid trading cost where the buying price and selling price are  $\mu_t^{\text{b}}$  and  $\mu_t^{\text{s}}$ , respectively. In general,  $\mu_t^{\text{b}} > \mu_t^{\text{s}}$ .

Given this context, the building energy management system aims to search for the economic operation plans by individually searching for solutions of the following optimization problem, **P0**:

### **P0: Operation Optimization Problem Without Energy Sharing**

$$\begin{aligned} \min \quad & \sum_{t \in \mathcal{T}} \tilde{C}_{i,t} \\ \text{s.t.} \quad & (3.1)-(3.22) \end{aligned}$$

where the objective function includes the total operational cost in the whole time interval  $\mathcal{T}$ . Note that **P0** is convex, which can be solved by cutting-edge commercial solvers. In this regard, let  $\bar{C}_i$  represent the objective value of **P0**, which is the cost of  $i \in \mathcal{N}$  without energy sharing.

It is noticed that the model above is a general case where all involved building microgrids are smart microgrids that are equipped with local battery energy storage systems. Generally, the proposed model in this chapter is extensive by properly reconstructing the constraints and cost functions: for example, some of the microgrids have no local storage systems, some microgrid communities have a centralized storage system. In the P2P energy sharing framework, private parameters (e.g. battery capacity, cost parameters) will be kept inside without sharing with others.

## **3.3 Energy Sharing Problem Formulation**

### **3.3.1 Operation Model of Energy Sharing**

As mentioned in the previous sections, P2P energy sharing is a prospective alternative to the energy trading with the power grid. Essentially, P2P energy sharing framework is a cooperative optimization problem, in which buildings can resolve the energy management problem by the cooperation with each other. In this way, the interconnected microgrids can fully utilize the diversities of renewables and

power supply patterns among different microgrids.

Taking a bilateral trading as an example, between  $i \in \mathcal{N}$  and  $j \in \mathcal{N}_i$ , the power transmission loss rate can be assumed as  $\epsilon \in (0, 1)$  through the link  $(i, j)$  [114]. Thus, the energy trading solution through this link can be described as follows:

$$e_{ij,t}^{i \rightarrow} (1 - \epsilon) = e_{ji,t}^{\rightarrow j}, \quad e_{ij,t}^{\rightarrow i} = e_{ji,t}^{j \rightarrow} (1 - \epsilon) \quad (3.24)$$

$$0 \leq e_{ij,t}^{i \rightarrow} \leq F_i^p y_{ij,t}^{i \rightarrow}, \quad 0 \leq e_{ij,t}^{\rightarrow i} \leq F_i^p y_{ij,t}^{\rightarrow i} \quad (3.25)$$

$$y_{ij,t}^{\rightarrow i} + y_{ij,t}^{i \rightarrow} \leq 1, \quad y_{ij,t}^{\rightarrow i}, y_{ij,t}^{i \rightarrow} \in \{0, 1\} \quad (3.26)$$

where the first equality in (3.24) represents the scenario where the electric power flows from microgrid  $i$  to microgrid  $j$ ;  $e_{ij,t}^{i \rightarrow}$  represents the total power ejected from  $i$  to the link and  $e_{ji,t}^{\rightarrow j}$  denotes the net power received by  $j$  from the link, respectively;  $\epsilon$  denotes the power loss on the link; similarly, the second equality in (3.24) describes another condition: the power flows from microgrid  $j$  to microgrid  $i$ , where  $e_{ji,t}^{j \rightarrow}$  and  $e_{ij,t}^{\rightarrow i}$  represent the total electric power ejected from microgrid  $j$  to the link and the net energy received by microgrid  $i$  from the link. In (3.25) and (3.26), the 0-1 variables  $y_{ij,t}^{i \rightarrow}$  and  $y_{ij,t}^{\rightarrow i}$  are introduced to indicate the energy flow directions, which means only one direction can exist through the link  $(i, j)$ : either from agent  $i$  to agent  $j$  or from agent  $j$  to agent  $i$ .

In order to simplify the equality equations of two cases in (3.24), new variables  $e_{i,t}^j$  and  $e_{j,t}^i$  can be introduced as below to replace the two direction conditions on the link  $(i, j)$ :

$$e_{i,t}^j = e_{ij,t}^{\rightarrow i} - e_{ij,t}^{i \rightarrow} (1 - \epsilon) \quad (3.27)$$

$$e_{j,t}^i = e_{ji,t}^{\rightarrow j} - e_{ji,t}^{j \rightarrow} (1 - \epsilon) \quad (3.28)$$

In this context, the number of variables can be reduced, and thus the link energy transfer equality in (3.24) is reformulated as follows:

$$e_{i,t}^j + e_{j,t}^i = 0, \quad \forall i \in \mathcal{N}, \forall j \in \mathcal{N}_i, \forall t \quad (3.29)$$

Meanwhile, when involving the energy sharing, the power energy balance equality are reformulated as follows:

$$P_{i,t}^{\text{buy}} + P_{i,t}^{\text{dis}} + P_{i,t}^{\text{re}} + \sum_{j \in \mathcal{N}_i} e_{ij}^{\rightarrow i} = P_{i,t}^{\text{L}} + P_{i,t}^{\text{h}} + P_{i,t}^{\text{EVA}} + \sum_{j \in \mathcal{N}_i} e_{ij}^{i \rightarrow} + P_{i,t}^{\text{ch}} + P_{i,t}^{\text{sell}} \quad (3.30)$$

### 3.3.2 Energy Sharing Pricing

The energy sharing pricing scheme concerns the cost saving and profit allocation in the P2P transaction. That is to say, the energy pricing agreement of each trading pairs should be satisfied as follows:

$$\lambda_{i,t}^j = \lambda_{j,t}^i, \quad \forall i \in \mathcal{N}, \forall j \in \mathcal{N}_i, \forall t \quad (3.31)$$

where  $\lambda_{i,t}^j$  represents the price of building  $i$  estimates of the energy on the link  $(i, j)$ , while  $\lambda_{j,t}^i$  represents the price of building  $j$  estimates of the energy on the link  $(i, j)$ , at  $t$ -th time slot. In this regard, with energy sharing, the cost function of smart building microgrid  $i \in \mathcal{N}$  is formulated as follows:

$$\sum_{t \in \mathcal{T}} \left( \tilde{C}_{i,t} + \boldsymbol{\lambda}_{i,t}^{\text{T}} \mathbf{e}_{i,t} \right) \quad (3.32)$$

where the column vectors  $\boldsymbol{\lambda}_{i,t} := \{\lambda_{i,t}^j\}_{j \in \mathcal{N}_i}$  represents the energy sharing price profiles with all neighborhoods at time slot  $t$ , while  $\mathbf{e}_{i,t} := \{e_{i,t}^j\}_{j \in \mathcal{N}_i}$  the is the

column vectors representing the energy trading profiles of microgrid  $i$  with all the neighboring microgrids at time slot  $t$ . The notation  $(\cdot)^T$  represents the transpose operation. In (3.32), the first term represents the local cost function defined in (3.23) and the second term represents the energy trading payment to neighboring buildings. It is also noted that, if  $\mathbf{e}_{i,t}$  is negative, the building microgrid  $i$  can gain profits by selling energy to neighboring buildings.

Therefore, the co-optimization problem of the considered building microgrids with energy sharing is summarized:

### SW-Social Welfare Maximization

$$\begin{aligned} & \text{maximize} && - \sum_{i \in \mathcal{N}} \sum_{t \in \mathcal{T}} \left( \tilde{C}_{i,t} + \boldsymbol{\lambda}_{i,t}^T \mathbf{e}_{i,t} \right) \\ & \text{subject to} && (3.1)-(3.22), (3.25)-(3.31) \end{aligned}$$

It is noticed that the objective function in **SW** maximizes the total welfare (minus total cost) of all smart building microgrids on the window horizon  $\mathcal{T}$ . With energy sharing, (3.29) and (3.31) are taken into account. It is observed in **SW** that, the total sum of energy sharing cost with each other (the second term) is zero, which means the equality  $\sum_{i \in \mathcal{N}} \boldsymbol{\lambda}_{i,t}^T \mathbf{e}_{i,t} = 0$  holds for all the time slots  $t \in \mathcal{T}$ .

It should be emphasized that though the cost function can be simplified as  $-\sum_{i \in \mathcal{N}} \sum_{t \in \mathcal{T}} \tilde{C}_{i,t}$ , the energy sharing payment term is added in **SW**. This helps determine the payment in the next sections.

### 3.3.3 Problem Decomposition

The optimization problem **SW** can be readily resolved by centralized algorithms, however, this chapter aims to devise a distributed algorithm for this problem due to privacy-preserving concerns. Towards this end, the optimization problem **SW** is firstly divided into  $N$  smaller optimization problems that can be solved by individual building microgrids. In this regard, each building can find solutions by solving **P1**:

#### **P1: Building's Operation with Energy Sharing**

$$\begin{aligned} \min \quad & \sum_{t \in \mathcal{T}} \left( \tilde{C}_{i,t} + \boldsymbol{\lambda}_{i,t}^T \mathbf{e}_{i,t} \right) \\ \text{subject to} \quad & (3.1)-(3.20), (3.22), (3.25)-(3.31) \end{aligned}$$

However, **P1** is coupled with other buildings because of the energy sharing involved, so it cannot be readily addressed by the building itself like **P0**. In essence,  $\boldsymbol{\lambda}_{i,t}$  and  $\mathbf{e}_{i,t}$  are variables related to other buildings, as explained in (3.29) and (3.31).

Specifically, there are  $N(N-1)/2$  pairs of buildings in the community, and let  $\mathcal{E}$  be the matrix collecting all the pairs  $(i, j)$  among  $N$  buildings. In this regard, (3.29) can result in  $|\mathcal{E}| = N(N-1)/2$  equations for every time period. In this regard, (3.29) can be modified:

$$\sum_{i \in \mathcal{N}} \mathbf{E}_i \mathbf{e}_{i,t} = \mathbf{0} \quad (3.33)$$

where  $\mathbf{E}_i \in \mathbb{R}^{|\mathcal{E}| \times (N-1)}$  denotes the mapping matrix from network nodes to lines. That is to say, for a specific smart building microgrid community, the matrix  $\mathbf{E}_i$  represents the topology relationship of nodes and links in the network. In

addition, the elements of  $\mathbf{E}_i$  is 0 and 1, and it is sparse with  $N - 1$  elements 1. For instance, if the  $m$ -th row and  $j$ -th column element in  $\mathbf{E}_i$  is 1, it implies that node  $j$  is a neighbor of node  $i$ , and the link  $(i, j)$  represents the  $m$ -th entry in the edge set  $\mathcal{E}$ .

Collect the Lagrangian variables regarding (3.33) in  $\boldsymbol{\lambda}_t := \{\lambda_{(i,j),t}\}_{(i,j) \in \mathcal{E}} \in \mathbb{R}^{|\mathcal{E}|}$ , and the vector  $\boldsymbol{\lambda}_t$  denotes the shadow price of the electric power flowing through the lines. In this regard, it is, from the economic perspective, reasonable for both the microgrid  $i$  and  $j$  to settle the energy sharing actions according to the price  $\lambda_{(i,j),t}$  at time slot  $t$ . In this regard, P2P energy trading pricing can be accordingly designed as follows:

$$\lambda_{i,t}^j = \lambda_{j,t}^i = \lambda_{(i,j),t}, \quad \forall (i, j) \in \mathcal{E}, \forall t \quad (3.34)$$

The equation (3.34) can be rewritten by  $\mathbf{E}_i$ :

$$\mathbf{E}_i^T \boldsymbol{\lambda}_t = \boldsymbol{\lambda}_{i,t} \quad (3.35)$$

Plugging (3.35) into **P1**, **P1** can be reformulated by the pricing scheme:

### **P2: Building's Optimization Problem with Sharing**

$$\begin{aligned} & \text{minimize} && \sum_{t \in \mathcal{T}} \left( \tilde{C}_{i,t} + \boldsymbol{\lambda}_t^T \mathbf{E}_i \mathbf{e}_{i,t} \right) \\ & \text{subject to} && (3.1)-(3.20), (3.22), (3.25)-(3.28), (3.30) \end{aligned}$$

where the neighbor-coupled energy sharing equality constraints (3.29) and (3.31) are relaxed thanks to the proposed pricing scheme. Particularly, (3.29) is removed from the optimization problem and replaced by KKT condition. That is,

the objective function becomes the Lagrangian objective function. Meanwhile, the energy sharing pricing agreement (3.31) is replaced by the Lagrangian dual variable  $\{\boldsymbol{\lambda}_t\}_{t \in \mathcal{T}}$  in the second term of the objective function. Consequently, the social welfare optimization problem can be decomposed into sub-problems in which individual agent aims to minimize the cost in **P2**. Lagrangian dual  $\{\boldsymbol{\lambda}_t\}_{t \in \mathcal{T}}$  is a global variable that prevents the local problem from being solved in a decentralized manner. In the next section, the manipulation of this issue will be presented. Also, the bi-linear term  $\boldsymbol{\lambda}_t^T \mathbf{E}_i \mathbf{e}_{i,t}$  is addressed in the meantime.

### 3.4 Proposed Decentralized Algorithm

Decentralized algorithm has the advantage of privacy protection and plug-and-play that are favorable in smart building energy management systems. In addition, decentralized algorithms has no central coordinators that is responsible for gathering and diffusing local variable. In this regard, this section develops a decentralized algorithm based on the ADMM algorithm [115].

#### 3.4.1 Algorithm Design

It is noticed that, the challenges in developing a decentralized algorithm for **P2** lie in dealing with the existence of global variable  $\boldsymbol{\lambda}_t$  and the bilinear term  $\boldsymbol{\lambda}_t^T \mathbf{E}_i \mathbf{e}_{i,t}$ . Traditional versions of ADMM is inapplicable. In this chapter, a modified version of ADMM named dual-consensus ADMM (DC-ADMM) is leveraged to solve the problem [115].

Under the DC-ADMM framework, in the reformulated local optimization problem **P2**, the primal variables include the power consumption and power trading while the dual variable includes the trading prices. Meanwhile, the primal

variables are not exchanged with others except dual variables. In this context, the dual price can reach a consensus after limited number of iterates. To be more specific, in the iterates, each building  $i \in \mathcal{N}$  estimates the energy sharing price for the traded energy on the line  $(i, j), (i, j) \in \mathcal{E}$ , i.e.,  $\boldsymbol{\lambda}_t^{(i)}$  and  $\boldsymbol{\lambda}_t^{(i)} := \{\lambda_{(i,j),t}^{(i)}\}_{(i,j) \in \mathcal{E}}$ . Through the P2P communication network, individual building microgrid  $i$  receive pricing estimates from neighborhoods,  $\boldsymbol{\lambda}_t^{(j)}, j \in \mathcal{N}_i$ . Once the building microgrid  $i$  received the estimates from neighbors, it constructs the following equality constraints in the optimization problem:

$$\hat{\boldsymbol{\lambda}}_t^{(i)} = \boldsymbol{\varepsilon}_{ij,t}, \quad (3.36)$$

$$\hat{\boldsymbol{\lambda}}_t^{(j)} = \boldsymbol{\varepsilon}_{ij,t}, \quad (3.37)$$

where the hat notation  $\hat{\cdot}$  denotes the information received from the previous iterate;  $\boldsymbol{\varepsilon}_{ij,t}$  represents the slack variable. Based on the Lagrangian dual theory,  $\mathbf{u}_{ij,t}$  and  $\mathbf{v}_{ij,t}$  are introduced as the dual variables regarding the equality (3.36) and (3.37). According to the ADMM theory, the variables are updated in an alternative way as follows:

$$\mathbf{u}_{ij,t} = \hat{\mathbf{u}}_{ij,t} + \frac{\rho}{2} \left( \hat{\boldsymbol{\lambda}}_t^{(i)} - \hat{\boldsymbol{\lambda}}_t^{(j)} \right) \quad (3.38a)$$

$$\mathbf{v}_{ij,t} = \hat{\mathbf{v}}_{ij,t} + \frac{\rho}{2} \left( \hat{\boldsymbol{\lambda}}_t^{(j)} - \hat{\boldsymbol{\lambda}}_t^{(i)} \right) \quad (3.38b)$$

where  $\rho$  is a step parameter. It is noted in the above equations that  $\boldsymbol{\varepsilon}_{ij,t}$  disappears in (3.38), this is because the closed form has been solved and directly used in the update. Here gives the detailed proof:

*Proof.* From traditional ADMM:

$$\begin{aligned}\mathbf{u}_{ij,t} &= \hat{\mathbf{u}}_{ij,t} + \rho(\hat{\boldsymbol{\lambda}}_t^{(i)} - \boldsymbol{\varepsilon}_{ij,t}) \\ \mathbf{v}_{ij,t} &= \hat{\mathbf{v}}_{ij,t} + \rho(\hat{\boldsymbol{\lambda}}_t^{(j)} - \boldsymbol{\varepsilon}_{ij,t})\end{aligned}\tag{3.39}$$

Then, the slack variables are attained by:

$$\begin{aligned}\text{minimize } & \hat{\mathbf{u}}_{ij,t}^T(\hat{\boldsymbol{\lambda}}_t^{(i)} - \boldsymbol{\varepsilon}_{ij,t}) + \hat{\mathbf{v}}_{ij,t}^T(\hat{\boldsymbol{\lambda}}_t^{(j)} - \boldsymbol{\varepsilon}_{ij,t}) \\ & + \frac{\rho}{2}\|\hat{\boldsymbol{\lambda}}_t^{(i)} - \boldsymbol{\varepsilon}_{ij,t}\|^2 + \frac{\rho}{2}\|\hat{\boldsymbol{\lambda}}_t^{(j)} - \boldsymbol{\varepsilon}_{ij,t}\|^2 \\ \text{variables: } & \boldsymbol{\varepsilon}_{ij,t}\end{aligned}\tag{3.40}$$

Next, the closed form solution of (3.40) is solved as follows:

$$\boldsymbol{\varepsilon}_{ij,t} = \frac{1}{2}(\hat{\boldsymbol{\lambda}}_t^{(i)} + \hat{\boldsymbol{\lambda}}_t^{(j)}) + \frac{1}{2\rho}(\hat{\mathbf{u}}_{ij,t} + \hat{\mathbf{v}}_{ij,t})\tag{3.41}$$

By plugging (3.41) into (3.39), the variables update can be simplified as follows without solving the optimization problems:

$$\begin{aligned}\mathbf{u}_{ij,t} &= \hat{\mathbf{u}}_{ij,t} + \frac{\rho}{2}(\hat{\boldsymbol{\lambda}}_t^{(i)} - \hat{\boldsymbol{\lambda}}_t^{(j)}) - \frac{1}{2}(\hat{\mathbf{u}}_{ij,t} + \hat{\mathbf{v}}_{ij,t}) \\ \mathbf{v}_{ij,t} &= \hat{\mathbf{v}}_{ij,t} + \frac{\rho}{2}(\hat{\boldsymbol{\lambda}}_t^{(j)} - \hat{\boldsymbol{\lambda}}_t^{(i)}) - \frac{1}{2}(\hat{\mathbf{u}}_{ij,t} + \hat{\mathbf{v}}_{ij,t})\end{aligned}\tag{3.42}$$

Moreover, the variable  $\mathbf{u}$  and  $\mathbf{v}$  can be further simplified by observing in (3.42) that,  $\mathbf{u}_{ij,t}[k] + \mathbf{v}_{ij,t}[k] = 0$  holds at all  $k$ , if initialized with  $\mathbf{u}_{ij,t}[0] + \mathbf{v}_{ij,t}[0] = 0$  [115].

Thanks to this observation, we have the updates shown in (3.38a) and (3.38b).  $\square$

Based on the closed-form solution, the updates of  $\boldsymbol{\varepsilon}$  in (3.41) can thus be simplified as below:

$$\boldsymbol{\varepsilon}_{ij,t} = \frac{1}{2}(\hat{\boldsymbol{\lambda}}_t^{(i)} + \hat{\boldsymbol{\lambda}}_t^{(j)}) \quad (3.43)$$

Here, by observing the location of  $i$  and  $j$  in (3.38) and (3.43), one can find their symmetric structures. In this regard, it is concluded that for the pair of  $(i, j) \in \mathcal{E}$ , the following equations hold for any pairs:

$$\begin{aligned} \boldsymbol{\varepsilon}_{ij,t} &= \boldsymbol{\varepsilon}_{ji,t} \\ \mathbf{u}_{ij,t} &= -\mathbf{u}_{ji,t} = \mathbf{v}_{ji,t} \end{aligned} \quad (3.44)$$

Based on the DC-ADMM algorithm, the variable  $\mathbf{z}_{i,t} = 2 \sum_{j \in \mathcal{N}_i} \mathbf{u}_{ij,t} = \sum_{j \in \mathcal{N}_i} (\mathbf{u}_{ij,t} + \mathbf{v}_{ji,t})$  is introduced, therefore, the min-max problem and updating equations.

Combining the update of primal variables and dual variables, a min-max optimization problem is accordingly formulated as follows:

$$\begin{aligned} \min_{\{\boldsymbol{\lambda}_t^{(i)}\}} \max_{\{\mathbf{x}_{i,t}, \mathbf{e}_{i,t}\}} \sum_{t \in \mathcal{T}} & \left( -\tilde{C}_{i,t} - \boldsymbol{\lambda}_t^{(i)\top} \mathbf{E}_i \mathbf{e}_{i,t} + \boldsymbol{\lambda}_t^{(i)\top} \hat{\mathbf{z}}_{i,t} \right. \\ & \left. + \rho \sum_{j \in \mathcal{N}_i} \left\| \boldsymbol{\lambda}_t^{(i)} - (\hat{\boldsymbol{\lambda}}_t^{(i)} + \hat{\boldsymbol{\lambda}}_t^{(j)})/2 \right\|^2 \right) \end{aligned} \quad (3.45)$$

where  $\mathbf{x}_{i,t}$  denotes local variables, such as battery discharging and charging power, electric vehicle charging, HVAC power of the building microgrid  $i$ ;  $\mathbf{z}_{i,t}$  represents the auxiliary variable which is introduced to remove  $\mathbf{u}$  and  $\mathbf{v}$ .

It should be mentioned that the formulated min-max problem (3.45) is convex in  $\{\boldsymbol{\lambda}_t^{(i)}\}_{t \in \mathcal{T}}$  and concave in  $\{\mathbf{x}_{i,t}, \mathbf{e}_{i,t}\}_{t \in \mathcal{T}}$  [115]. To resolve the dual and auxiliary variables, the variables are integrated into the quadratic term of the objective function in (3.45), and the initial values are from the previous iterate  $\hat{\boldsymbol{\lambda}}_t^{(j)}$  and  $\hat{\mathbf{z}}_{i,t}$ .

### Primal Variables Update

Primal variables include local power consumption and trading power with the utility grid. The updates are conducted in parallel:

$$\begin{aligned}
& \text{minimize} && \sum_{t \in \mathcal{T}} \left[ \tilde{C}_{i,t} + \frac{\rho}{4|\mathcal{N}_i|} \left\| \frac{1}{\rho} \mathbf{E}_i \mathbf{e}_{i,t} - \frac{1}{\rho} \hat{\mathbf{z}}_{i,t} \right. \right. \\
& && \left. \left. + \sum_{j \in \mathcal{N}_i} \left( \hat{\boldsymbol{\lambda}}_t^{(i)} + \hat{\boldsymbol{\lambda}}_t^{(j)} \right) \right\|^2 \right] \\
& \text{subject to} && (3.1)-(3.20), (3.22), (3.25)-(3.28), (3.30) \\
& \text{variables:} && \{\mathbf{x}_{i,t}, \mathbf{e}_{i,t}\}_{t \in \mathcal{T}}
\end{aligned} \tag{3.46}$$

where  $|\mathcal{N}_i|$  counts the neighborhood of  $i \in \mathcal{N}$ .

### Dual Variables Update

After calculating the local primal variables, each building microgrid  $i$  conducts (3.47) and communication.

$$\boldsymbol{\lambda}_t^{(i)} = \frac{1}{2|\mathcal{N}_i|} \left[ \sum_{j \in \mathcal{N}_i} \left( \hat{\boldsymbol{\lambda}}_t^{(i)} + \hat{\boldsymbol{\lambda}}_t^{(j)} \right) - \frac{1}{\rho} \hat{\mathbf{z}}_{i,t} + \frac{1}{\rho} \mathbf{E}_i \hat{\mathbf{e}}_{i,t} \right] \tag{3.47}$$

### Auxiliary Variables Update

Individual microgrid  $i$  updates the local auxiliary variable according to the following equation upon the previous communication:

$$\mathbf{z}_{i,t} = \hat{\mathbf{z}}_{i,t} + \rho \sum_{j \in \mathcal{N}_i} \left( \hat{\boldsymbol{\lambda}}_t^{(i)} - \hat{\boldsymbol{\lambda}}_t^{(j)} \right) \tag{3.48}$$

It is noticed that Algorithm 1 solves **P2** in a P2P fashion. That is, most information are stored in the building microgrid  $i$  itself with limited communication. In addition, though the proposed algorithm is based on the DC-ADMM,

---

**Algorithm 1:** DC-ADMM based P2P Algorithm to Solve **P2**

---

- 1: Initialize  $\boldsymbol{\lambda}_t^{(i)}, \mathbf{z}_{i,t} = \mathbf{0}, i \in \mathcal{N}$  with known  $\rho$ ; **Set**  $k = 0$ ;
  - 2: **repeat**
  - 3:   **for** Each  $i \in \mathcal{N}$  (in parallel) **do**
  - 4:     Update primal variables  $\mathbf{x}_{i,t}, \mathbf{e}_{i,t}$  according to (3.46);
  - 5:     Update dual variables  $\boldsymbol{\lambda}_t^{(i)}$  according to (3.47);
  - 6:     Transmit  $\boldsymbol{\lambda}_t^{(i)}$  to neighborhood  $j \in \mathcal{N}_i$ , and receive  $\boldsymbol{\lambda}_t^{(j)}$  from neighbors;
  - 7:     Update auxiliary variables  $\mathbf{z}_{i,t}$  according to (3.48);
  - 8:   **end for**
  - 9:    $k = k + 1$ ;
  - 10: **until** the stopping criterion.
- 

it has realistic market meanings regarding the dual and ancillary variable. For example, the convergence process and iterates in the optimization represent the negotiation of peers in the local energy trading market. The dual variable denote the energy sharing price consensus between trading pairs. In addition, the local and dual variables are obtained simultaneously, which suggests that the trading energy is settled together according to the marginal price. Further, the variables are exchanged in a peer-to-peer manner, which indicates that the energy sharing process can protect the individual privacy at a high level.

### 3.4.2 Features of the Framework

Based on the analysis in the previous sections, the proposed energy sharing framework and algorithm have admirable features and some advantages as compared to existing works.

- **Plug-and-play.** The proposed energy sharing framework can involve both

producers, consumers and prosumers. This is distinguished from most existing works that divide producers and consumers in advance by calculating the energy surplus and deficit. In the proposed work, smart building microgrids communicate with neighboring microgrids in a peer-to-peer manner. The model can be extended to a large-scale community, which only needs plug-and-play operations.

- **Optimality.** It is noticed that the problem formulated in **P1** has the property of strong duality and convexity. That is, the optimal solution resulted from **P2** is the same as that of **P1**. Thanks to the Lagrangian dual theory, the proposed framework can provide optimality for the energy sharing market.
- **Fairness.** The proposed framework can obtain the sharing energy and settlement price in a holistic manner. Each unit of the sharing energy is cleared based on the marginal cost. In addition, the marginal cost is the Lagrangian dual of the trading equality. From the perspective of economics, the framework offers a fair pricing settlement for the participant smart building microgrids.
- **Fully Decentralized.** The energy sharing algorithm does not need central coordinators in the variable updating process. To be more clear, Fig. 3.2 illustrated the problem decomposition and framework. The algorithm has the merit of privacy-protection. As compared to existing works, the proposed algorithm only transmit pricing estimates with others.

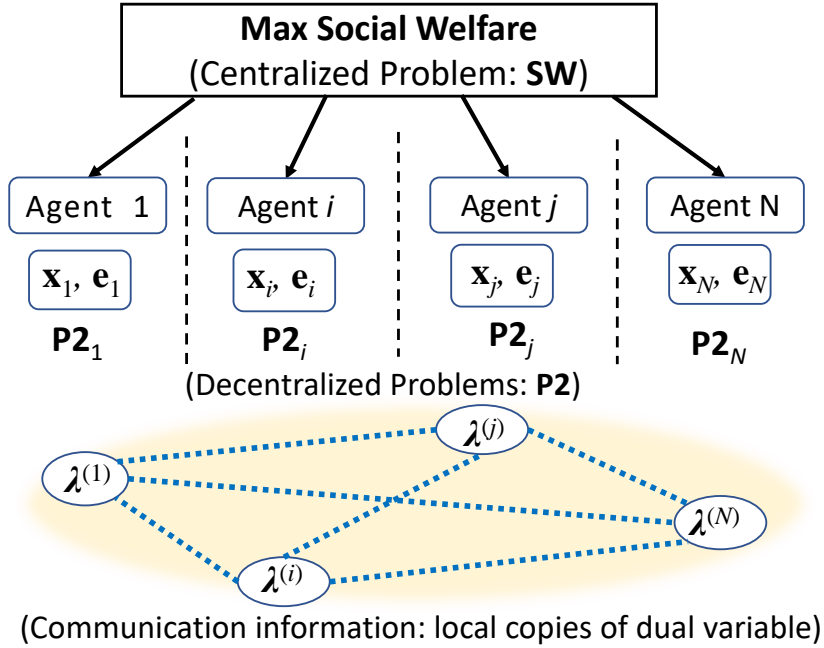


**Figure 3.2:** Problem decomposition of energy sharing.

## 3.5 Numerical Simulations

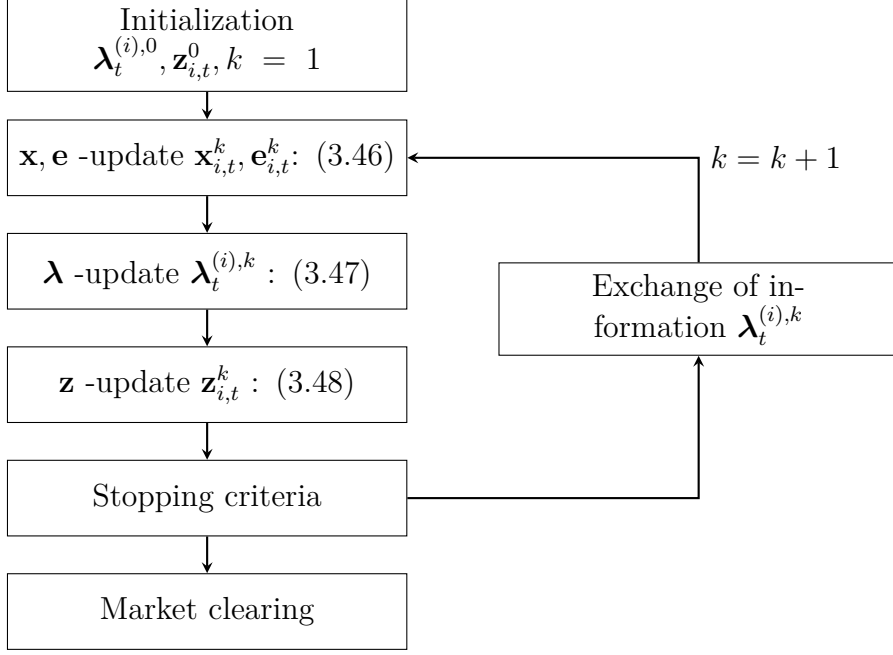
This section presents the numerical simulation results and makes discussions about the performance of the proposed energy sharing framework.

### 3.5.1 Case Configuration

In this section, a community of smart building microgrids including four smart buildings is considered in the case study. The load demand includes basic load, EV load, HVAC units. Each building is supposed to install a BESS and energy management system.

Fig. 3.4 plots the basic load in buildings, which is regarded as fixed and untrollable<sup>3</sup>. As for the HVAC units, the parameters are given as follows:  $G_i = 1.5\text{kWh}/^\circ\text{C}$ ,  $R_i = 1.33^\circ\text{C}/\text{kWh}$ , and  $\eta_i = 0.15$ ,  $i \in \mathcal{N}$ . The indoor occupant

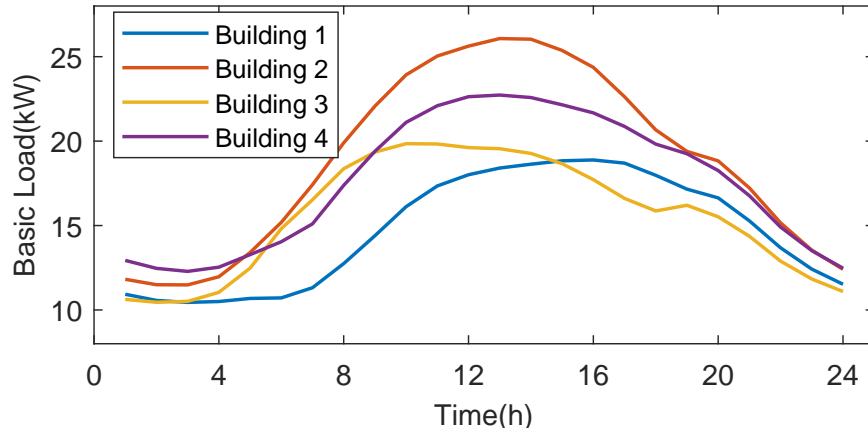
<sup>3</sup>Southern California Edison. "SCE Dynamic Load Profiles," <https://www.sce.com/regulatory/load-profiles/dynamic-load-profiles>.



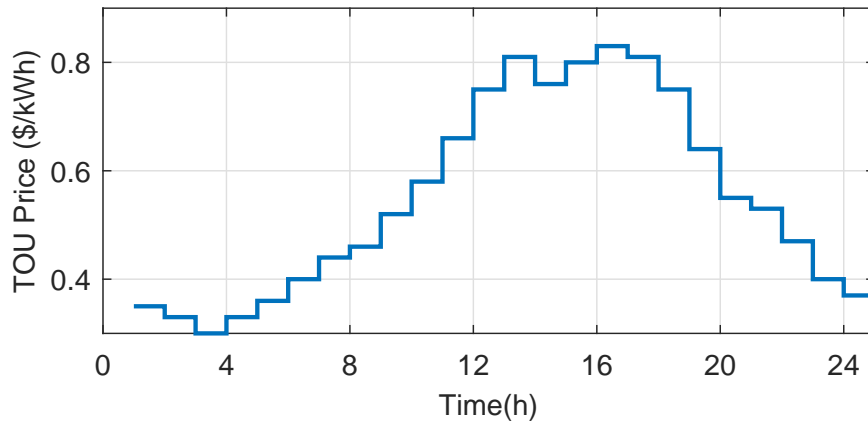
**Figure 3.3:** Algorithm flowchart of the decentralized algorithm implementation.

discomfort coefficient  $\beta_i$  is  $\{3.2, 3.6, 4, 4.4\}$  [110]. The electricity price is plotted in Fig. 3.5. When there is energy surplus in smart building microgrids, they are allowed to sell energy to the grid at half of the time-of-use price. The power line capacity from the utility grid to the microgrid is 200 kW, and the power line capacity between peers is 80kW. The energy sharing loss parameter  $\epsilon$  is set as 0.02 for each link. The degradation cost is  $\kappa_i^{\text{bat}} = 0.05\$/\text{kWh}$ . The battery energy level is bounded by the range  $[20, 200]$  kWh, and the battery power limit is 50 kW. The self-discharging, charging, discharging efficiency of BESS are set as 1, 0.95, 0.95. The daily charging/discharging state switch number is capped by 3. In the distributed algorithm,  $\rho = 4.5$ , and the stopping criterion is set as  $\|\lambda^{(i),k} - \lambda^{(i),k-1}\| \leq 0.02$ . The simulations are conducted on Matlab2021a using Yalmip by solver Gurobi on the personal computer.

Each smart building microgrid is supposed to have 20 EVs and the rated power is  $\{3, 6, 8, 10\}$  kW for four microgrids, respectively. The charging demands



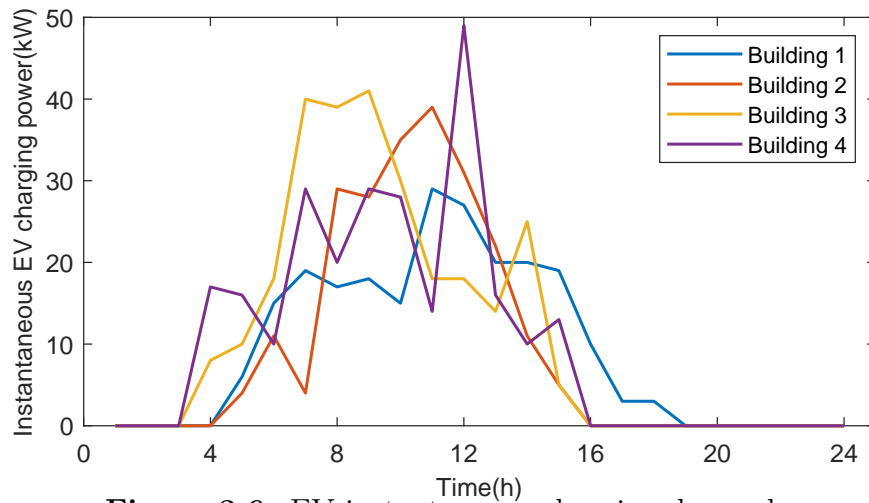
**Figure 3.4:** Basic uncontrollable load in buildings.



**Figure 3.5:** Time-of-use electricity price.

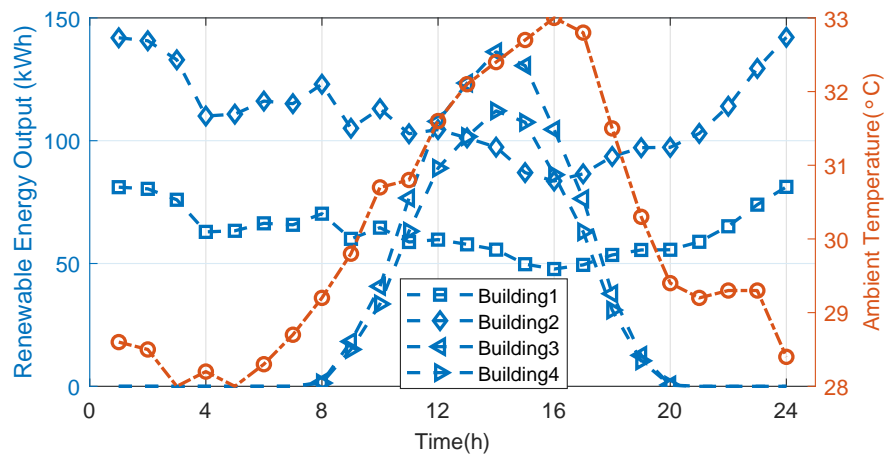
of EVs  $d_v^{EV}$  are estimated according to the daily travel mileage data and per mile energy consumption. On the basis of the survey report [116], the travel behaviors of EVs are analyzed by the statistical probability method. The mileage follows the logarithmic normal distribution  $\text{Log-}N(2.98, 1, 14^2)$ , and the charging start and end time follows the truncated normal distribution  $N(8.92, 3.2^2)$  and  $N(17.6, 3.4^2)$ . More specifically, Fig. 3.6 plots the EV charging power with instantaneous charging strategy.

Fig. 3.7 plots the wind, PV energy and outdoor temperature, on 15th June, 2020 from HK observatory [117, 118]. In Fig. 3.7, buildings 1 and 2 have wind



**Figure 3.6:** EV instantaneous charging demand.

turbines, and the other two are PV buildings.



**Figure 3.7:** Hourly data of buildings: renewable energy and load.

### 3.5.2 Results and Discussion

In the operation optimization, building microgrids aim to supply local loads by minimizing the total cost, as in **P0**.

It is noticed that buildings can leverage BESS energy before energy sharing, and make full utilization of renewables. As seen in Fig. 3.8 and Fig. 3.9, buildings

can purchase energy from the grid, when the local supply is not sufficient. Moreover, it is seen that utility trading profiles happens at many time slots. This is because that the microgrids should meet the balance requirement at every time slot. For example, for the building 1, the wind energy is more than the load demand at 1-8 hours. So, it sells excessive energy to the main grid during this time, and particularly, it charges local battery storage system at 3-4 hour. However, for the building 3, the solar PV energy can not solely meet the local demand at 1-8 hours (weak sunshine time). Hence, it needs purchase energy from the grid during these hours.

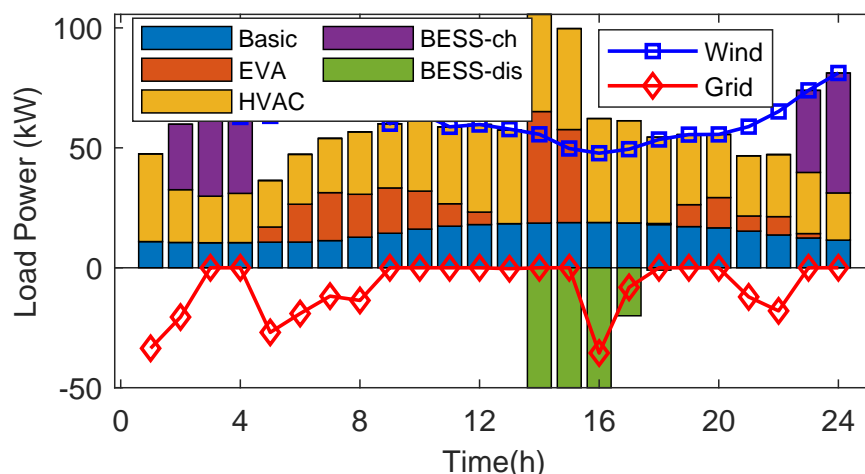


**Figure 3.8:** Energy management profiles: Building 1 before energy sharing.

After energy sharing, building microgrids can work together in energy management **P2**. In particular, they can cooperate with each other and reduce the dependence on the main grid. In this regard, the utility grid purchasing profiles are plotted before and after energy sharing. To be more clear, the grid energy trading profiles are compared in Fig. 3.10 of four building microgrids before and after energy sharing. In Fig. 3.10 (a), the energy trading profiles before energy sharing is firstly plotted. Similar to the observation in 3.8 and 3.9, it is seen that building 1 and 2 (wind microgrids) sell energy when wind energy supply is

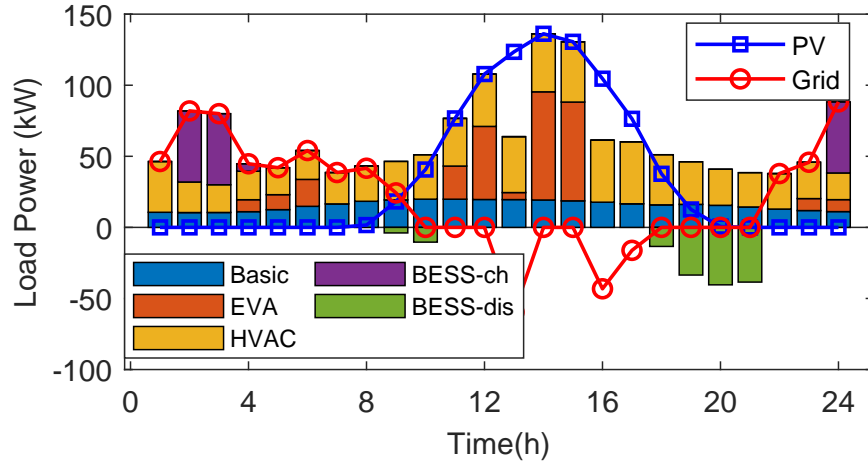
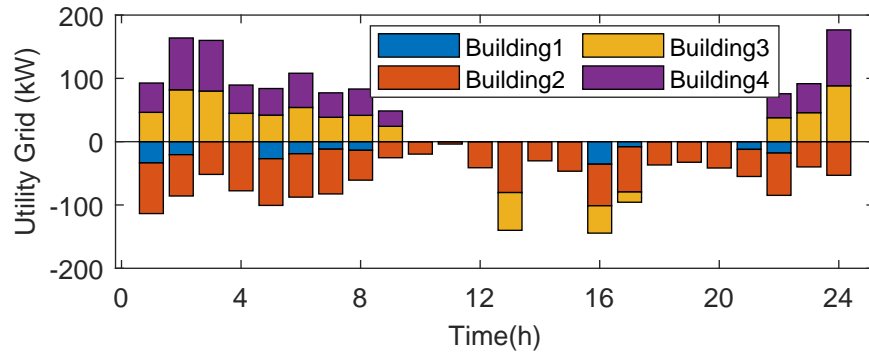


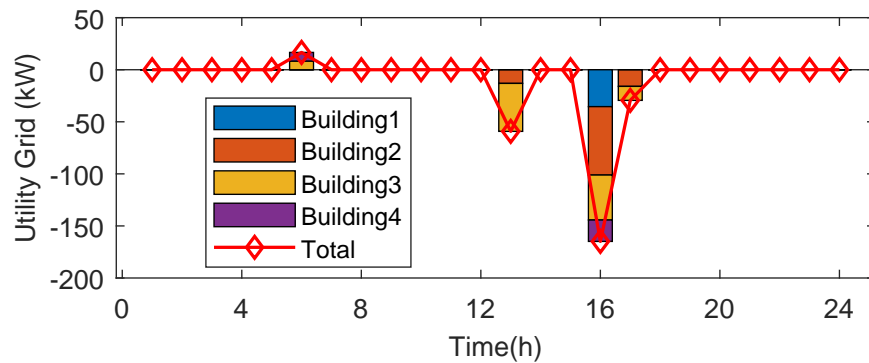
**Figure 3.9:** Energy management profiles: Building 3 before energy sharing.

sufficient at night time, while PV buildings 3 and 4 need purchase energy at night time. Further, it is seen that the purchasing and selling plans is relative to the time-of-use prices to a great extent. For example, when the time-of-use prices are low in midnight, PV buildings (3 and 4) purchase more energy; when the price is high at hour 13 and 16, wind buildings (1 and 2) sell more energy to the main grid. In Fig. 3.10 (b), the grid trading profiles of buildings after energy sharing is illustrated. The most obvious finding is that, the buildings have reduced the dependence on the main grids, and the trading energy becomes less after energy sharing. In addition, it is seen that all building microgrids have similar trading behaviors (buy or sell) after energy sharing. That is, four buildings all buy energy at a single hour or all sell energy at a single hour. For example, all of the buildings have surplus energy during e.g., at hour 13 and 16. This proves that there is a consensus in the grid trading of building energies.

After energy sharing, the energy management profiles of building microgrids are plotted in Fig. 3.11 (building 1, 2) and Fig. 3.11 (building 3, 4). As is observed, the microgrid loads (HVAC units, BESS and EVs) are controlled in a flexible way. Most importantly, due to the diverse features in various building



(a) Without energy sharing

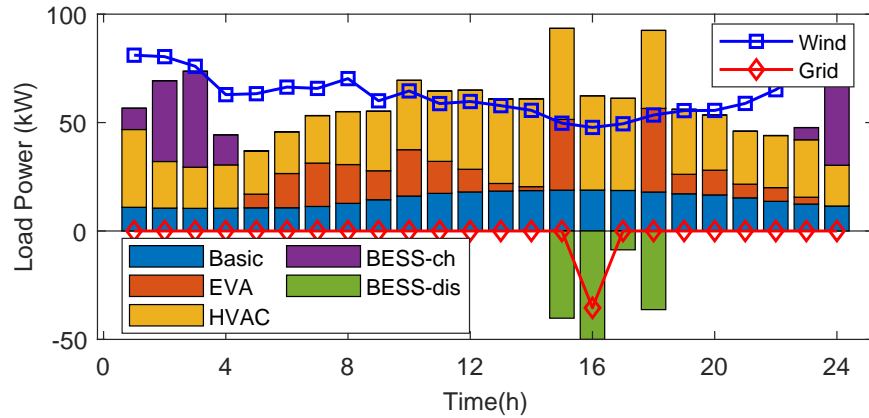


(b) With energy sharing

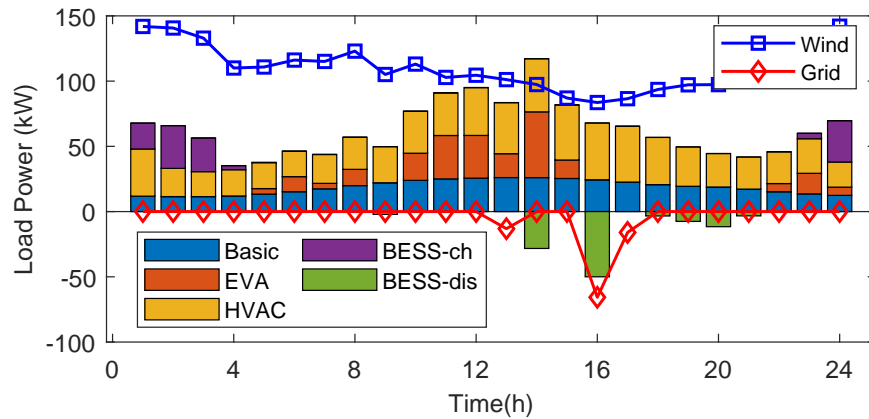
**Figure 3.10:** Grid power trading profiles in smart buildings: without and with energy sharing.

microgrids, they are able to cooperate in the trading market. For instance, the wind building 1 has surplus energy at hour 1-9 and 20-24. Meantime, the PV building 3 needs energy during these time because of the PV generation patterns. Moreover, the BESS and EV are flexible, which facilitates the cooperative management.

Fig. 3.13 plots the battery energy level trajectory. As can be seen, the battery storage systems behave actively in energy management, For example, in building 1 and 2, the battery charges in first four hours to store excessive energy as the wind energy generation is at the high level. It is also observed that the battery storage in building 3 and 4 also charge in the midnight, even though there is no solar energy in these hours. The rationale is that the time-of-use price is relatively



(a) Building 1

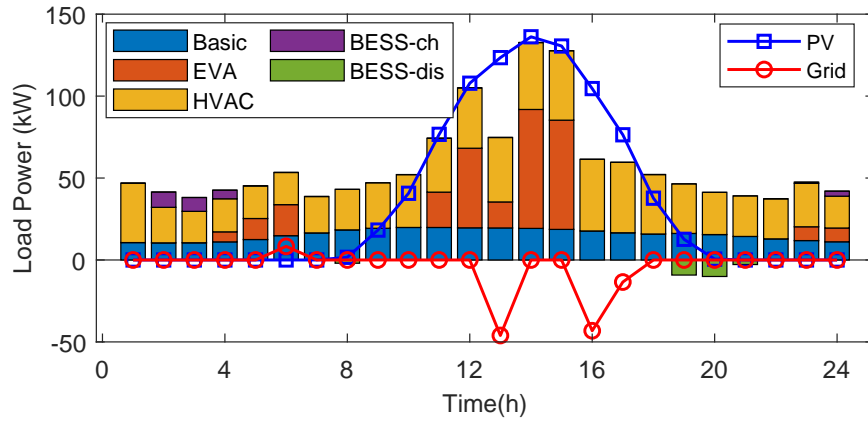


(b) Building 2

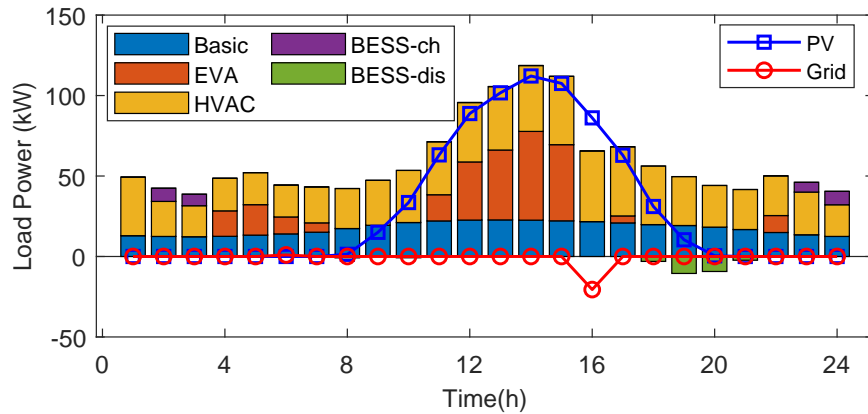
**Figure 3.11:** Energy management profiles of building 1 and 2: after energy sharing.

low at these hours. The battery storage systems store energy from the main grid, at low-price hours and then discharge at high-price hours. They can facilitate saving grid trading costs for building microgrids. Further, it is observed that the battery energy level becomes similar in four buildings after energy sharing. In this regard, the proposed framework can harmonize local battery storages efficiently with decentralized communication in buildings.

Fig. 3.14 plots the EV charging profiles and EV battery energy trajectories in four smart building microgrids. Recall that electric vehicles are integrated as an aggregator EVA in each microgrid. The dashed lines in each figure represent the



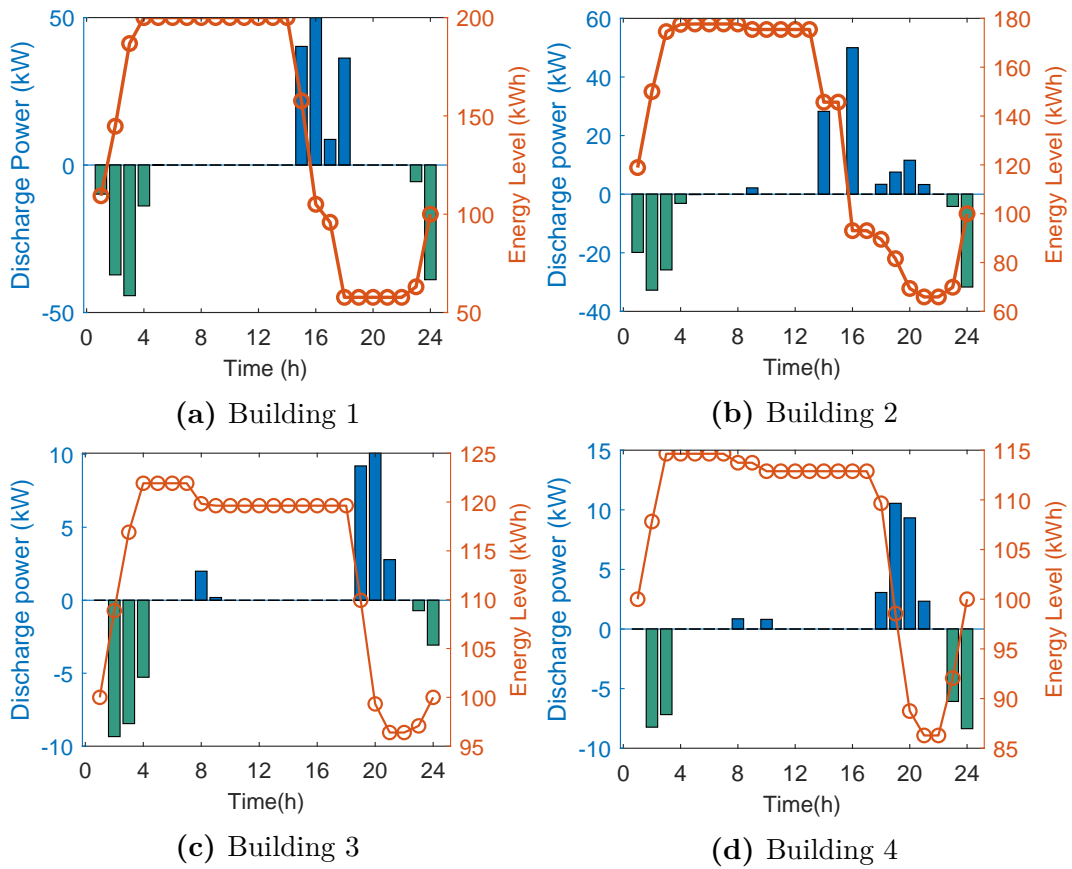
(a) Building 3



(b) Building 4

**Figure 3.12:** Energy management profiles of building 3 and 4: after energy sharing.

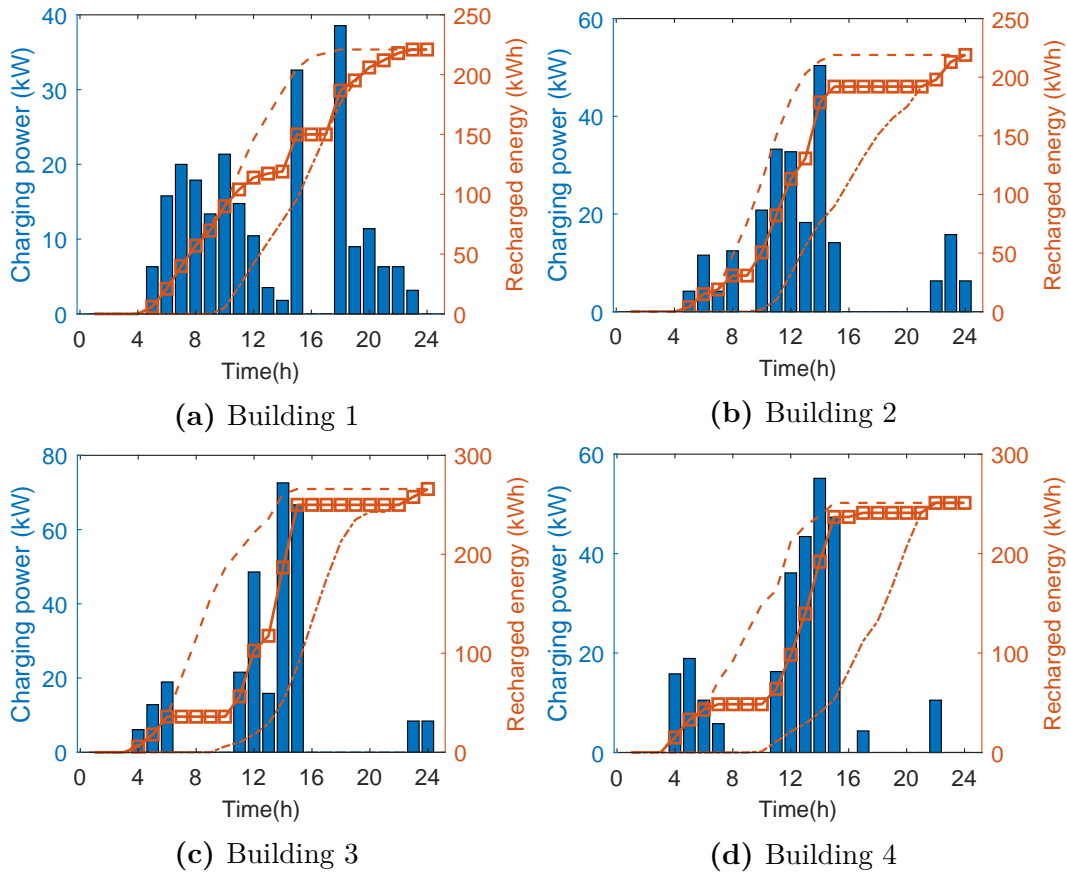
minimal charging curve  $E_{\min}^{\text{EVA}}$  and the maximal charging curve  $E_{\max}^{\text{EVA}}$  respectively, which are obtained offline according to (3.12) and (3.13). In particular, the upper dashed line means that the EVs are charging at the rated power as soon as they arrived at the station, while the lower dashed line means that EVs wait for charge at the rated power until the finishing time is just the departure time. That is, any charging curve between these two curves will satisfy the EV operation requirements, such as charging demand and rated charging power limit. Since the resulting recharged curve (the line with squares) lie between the two dashes boundaries, it demonstrates that EV charging demands are all satisfied within



**Figure 3.13:** Energy level of battery energy systems.

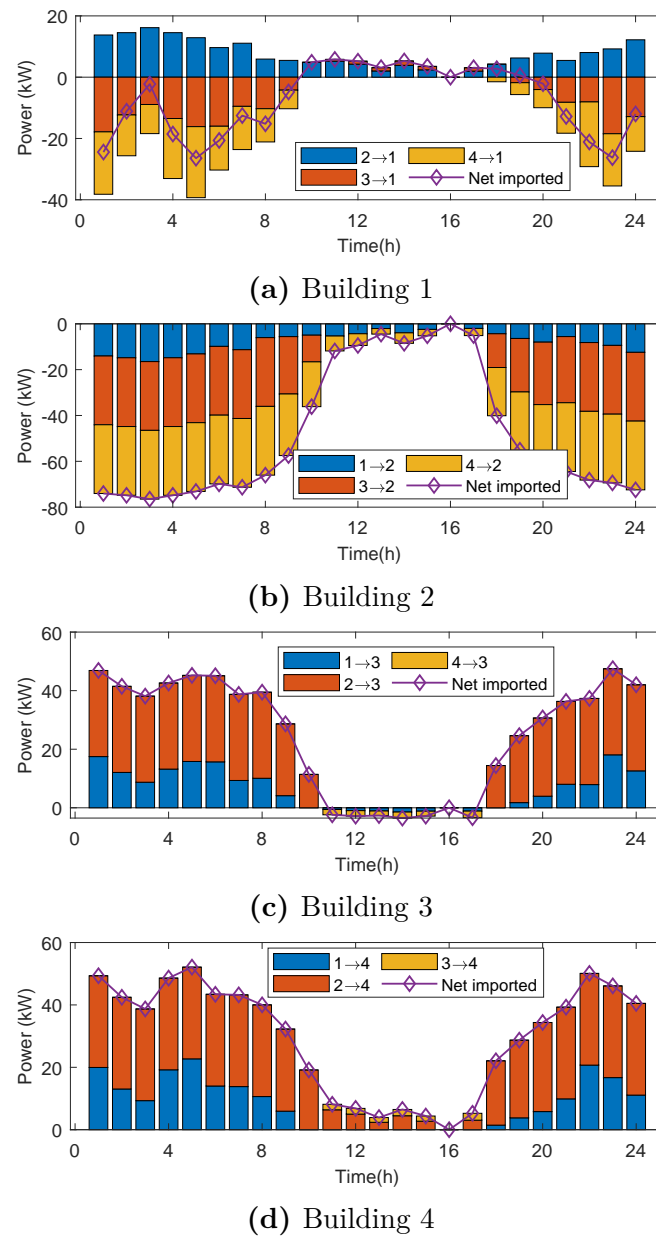
their parking duration.

Fig. 3.15 illustrates the internal P2P energy sharing profiles of building microgrid pairs. Compared with Fig. 3.15 and Fig. 3.10, building microgrids prioritize neighbors after energy sharing. PV building microgrids 3 and 4 imported power energy from wind building microgrids 1 and 2 at nighttime, during when the wind energy is sufficient. Moreover, one can obviously observe the exchange between PV and wind buildings, which demonstrates that P2P energy trading is enabled by the proposed framework and the power supply diversities in various categories of microgrids are complemented with each other. As such, the total social cost can be reduced.



**Figure 3.14:** Charging power profile and energy level of electric vehicle aggregators.

Fig. 3.16 shows the global sharing price consensus  $\lambda_t^{(i)}$  in the horizon window. As presented in the decentralized algorithm, each building microgrid has a local price estimate of the optimal energy sharing price and reaches a global consensus finally. The shallow price is negotiated simultaneously together with the energy sharing amount, in the proposed holistic framework. In addition, the energy sharing price profile is smaller than the power grid time-of-use buying price and larger than the grid energy selling price. This demonstrates the incentive for building microgrids to participate in the energy sharing; otherwise, they can choose to trade directly with the main power grid. Fig. 3.17 illustrates the convergence of four price estimates, which again demonstrates that the proposed



**Figure 3.15:** Energy sharing profiles between peers.

algorithm has a favorable converge property and the local estimates can reach a global consensus on price.

Table 3.2 gives the energy cost of microgrids with and without energy sharing. After energy sharing, the total cost includes the local cost (i.e., HVAC

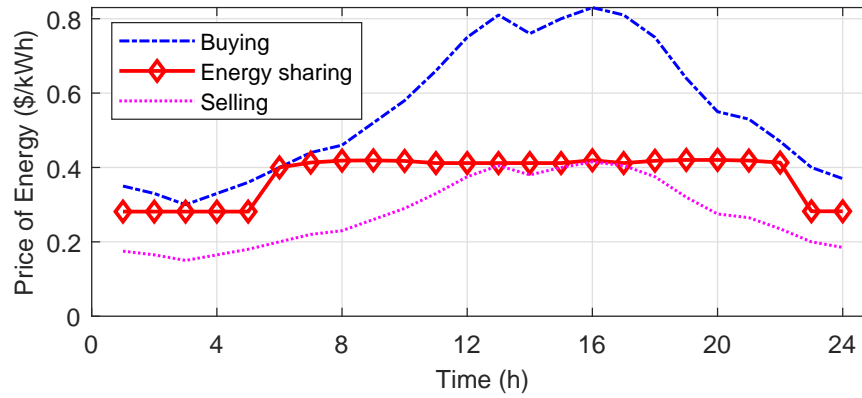


Figure 3.16: Consensus energy sharing price.

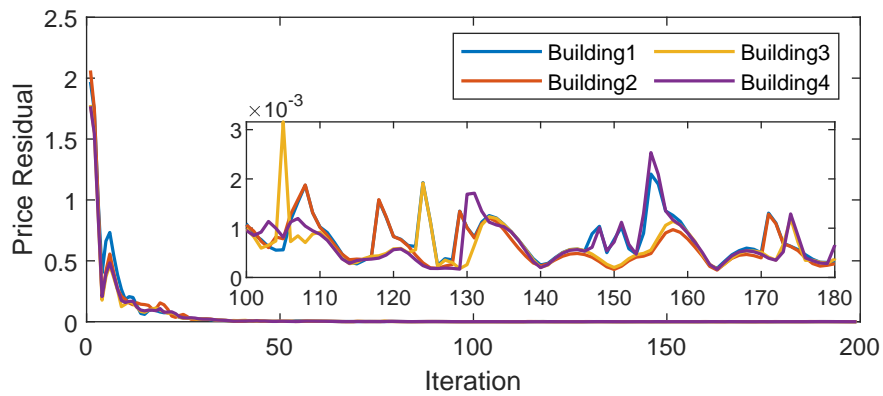


Figure 3.17: Convergence of the energy sharing price in each building.

discomfort cost, battery degradation cost, grid trading cost) and the energy sharing payment (or profit) with neighbors. It can be seen from the table that energy sharing can lead to a significant cost reduction for all building microgrids, ranging from \$19.9 to \$110.57. From the row of energy sharing payment to neighbors, it is obvious that four buildings have a large percentage of cost (profit) with others and proactively settle the payments issues, e.g.,  $\lambda_t^{(i)T} \mathbf{E}_i \mathbf{e}_{i,t}$  in the proposed model, which is similar as the energy sharing amount in Fig. 3.15.

**Table 3.2:** Cost Comparison with and without Energy Sharing (\$)

	Bldg 1	Bldg 2	Bldg 3	Bldg 4
Total cost without energy sharing	-26.34	-305.20	210.11	289.98
Local cost with energy sharing	6.75	-21.65	-30.31	0.07
Payment to neighbors	-52.99	-394.12	201.46	245.64
Total cost with energy sharing	-46.24	-415.77	171.15	245.72
Cost reduction	19.9	110.57	38.96	44.26

### 3.6 Summary for the Chapter

In this chapter, the P2P energy sharing among smart building microgrids is investigated. An peer-to-peer energy sharing framework is developed based on a cooperative welfare maximization problem for the P2P energy trading. In addition, the energy transmission loss and energy sharing price are both addressed in the model, which makes the research potential for future implementation. The P2P trading quantity and price are both negotiated between trading peers in a bilateral and privacy-preserving manner. The optimization problem is solved by a fully decentralized algorithm, where the dual and primal variables are both updated in a decentralized manner. The case study validates that the proposed P2P energy sharing framework can significantly improve the total welfare of participant microgrids by the cooperative management of distributed energy resources.

## Chapter 4

# Hierarchical Transactive Market based on Distributed MPC

### 4.1 Introduction

Over the last decades, power systems have witnessed a dramatic proliferation of small-scale distributed energy resources (DER) such as rooftop photovoltaic (PV) energy, wind energy, energy storage system (ESS) and flexible load demands. Microgrid is emerging to become a promising paradigm to integrate more and more DERs. Traditionally, various energy strategies have been adopted, on both the supply side and demand side, to promote the economic energy utilization of microgrids. However, distribution system operation constraints might be violated, if all microgrids in the distribution network (DN) directly trade with retailers or the utility grid [119]. A favorable solution involves local energy cooperation at the community level, which enables bilateral energy trading among multi-microgrids[108]. Such mechanism designs are called P2P energy trading, which are typically user-centric to fulfill the preference of agents, such as user comfort and financial privacies [99].

As reviewed in Chapter 1, plenty of recent research works have shown that P2P energy trading is a promising solution to smart microgrid transactive energy management [67]. In addition, among the most popular P2P frameworks, the decentralized P2P market models are more favorable and reasonable in practical implementation, in terms of their advantages including independence, self-interest and privacy protection. To address the financial conflict of participant microgrids in the P2P energy trading network, Nash bargaining theory is deployed in [80] to obtain the namely Pareto-efficient solution for the profit allocation among participants. Likewise, market power is adopted as a metric to fairly allocate the cost savings in [81]. A two-stage framework is put forward to sequentially determine the payment and the energy trading strategy [82]. The bilateral double auction scheme is formulated in [83] to determine the P2P trading price in a stable Stackelberg game. It is noticed that most of the above methods require solving the energy trading sub-problem and payment subproblem separately, which naturally leads to the semi-optimal solutions of compromised fairness. As a consequence, an optimal P2P trading solution including the price and quantity is pursued in this chapter.

Another key challenge associated with P2P local transactive market implementation relates to the uncertainty issues e.g. forecasting errors in renewable generation [120]. The recent work in [121] proposes a local energy market design under uncertainty, but a central community manager in the network is necessary. In fact, the deployment of multi-microgrids firstly takes place in the day-ahead market (DM), where preliminary schedule plans would be made before the gate closure[122]. Intra-day market (IM) sessions are widely incorporated in most existing electricity markets over the world, allowing participants to take corrective actions in response to unforeseen scenarios [102, 123]. Moreover, the regulation

market (RM) assists in the power balancing process at the energy scheduling level [124].

From the literature review, most existing works have proposed different P2P market designs with respect to trading frameworks, market mechanisms and profit allocations. Nevertheless, a computationally tractable and practical framework that fits the existing hierarchical electricity market framework requires elaborate design. In this chapter, a hierarchical P2P energy trading framework is proposed for interconnected microgrids. The main contributions of this chapter are twofold:

- A practical hierarchical P2P energy trading framework is newly proposed for the energy cooperative management of multiple microgrids. The optimization problems are formulated in detail for microgrids at different market stages (i.e. day-ahead market, intra-day market and real-time regulation market). This coincides with the multi-stage structure of the existing electricity market, which can effectively manage the uncertainty induced by e.g. forecasting errors which can inevitably incur penalty costs, etc.
- Distributed transactive market framework is proposed for the realization of the privacy-preserving energy trading based on distributed MPC method. A decomposition strategy based on dual-consensus Alternating Direction Method of Multipliers (DC-ADMM) is proposed to solve the P2P trading settlement problem in a fully distributed manner, in which the zero-sum payment term is explicitly determined. The bilateral trading prices can reach the global optimal consensus through iterative P2P communications by privacy-preserving negotiations.

The rest of this chapter is structured as follows: The multi-stage problem overview is given in Section 4.2, and Section 4.3 presents the mathematical agent

model in the market. Section 4.4 formulates the market optimization problems in the multiple stages. The fully distributed algorithm is developed in Section 4.5. Numerical simulation results are reported in Section 4.6. Section 4.7 summarizes this chapter.

**Table 4.1:** Nomenclature of Chapter 4

$\mathcal{N}$	Set of microgrids
$\mathcal{N}_i$	Set of neighbors of microgrid $i$
$\mathcal{T}$	Set of time slots
$T_s$	Time slot interval
$\mu_t^b, \mu_t^s$	Electricity price of microgrids purchased from/sold to grid[\$/kWh]
$B_i$	Battery capacity of ESS $i$
$\eta_i^c, \eta_i^d$	Charging and discharging efficiency of ESS $i$
$\bar{c}_i, \bar{d}_i$	Rated charging and discharging power of ESS $i$
$\kappa^c, \kappa^d$	Cost parameters of ESS charging and discharging
$\hat{l}_{i,t}$	Forecasted load demand in microgrid $i$
$i_{\min}$	Minimal flexible load in microgrid $i$
$\mu_d$	Load demand response price
$F_{ij}$	Power line capacity limit of peer line $(i, j)$
$\bar{b}_i, \bar{s}_i$	Power line capacity of microgrid $i$ with utility grid
$\delta$	Power loss on P2P trading line
$b_i, s_i$	Electricity power of microgrid $i$ purchased from/sold to grid
$SoC_i$	State of Charge level of ESS $i$
$c_i, d_i$	Charging and discharging power of ESS $i$
$r_i$	Renewable energy available in microgrid $i$
$l_i$	Flexible load power in microgrid $i$
$\pi_{i,t}^j$	P2P price of microgrid $i$ set for microgrid $j \in \mathcal{N}_i$

## 4.2 Overview of the Local Transactive Market

### Design

In this section, the structure of the proposed local transactive market is conceptually described. Each agent in the market is named as a prosumer or microgrid in

this chapter, which may proactively buy or sell power energies among themselves.

As Table 4.2 shows, taking the Iberian market as an example, the existing market includes several sessions for each particular day. For example, the day-ahead session opens at 12:00 of the day before the scheduling day, and the intra-day session 5 opens at 8:00, three hours before its actual execution timeline, to allow for bids from all agents. This timeline nature of the electricity market necessitates a hierarchical framework solving the energy scheduling problems in DM, followed by the different sessions of IM and RM. In addition, the length of time horizon, affecting the forecast error in the renewable generation and load demand, also determines the priorities among various measurements against uncertainty: ESS charging/discharging, load shedding, utility trading and P2P trading.

**Table 4.2:** Day-ahead Market and Intra-day Market Sessions

	DM	IM1	IM2	IM3	IM4	IM5	IM6
Session opening	12:00	17:00	21:00	01:00	04:00	08:00	12:00
Execution starting	00:00	21:00	00:00	04:00	07:00	11:00	15:00
Schedule horizon	24h	27h	24h	20h	17h	13h	9h

In this chapter, we aim to propose a practical P2P transactive market align with the existing market mechanism. A key feature of the proposed market framework is that a detailed operating regime is provided to integrate decentralized P2P market into existing market structure, which can be extended to integrate most works dealing with P2P trading issues.

Fig. 4.1 illustrates the hierarchical electricity market framework based on MPC for the community energy cooperation in different stages of the transactive market. MPC-based optimization is essentially a look-ahead multi-period optimization problem with only the first element being implemented, which shows potentials to handle the uncertainty of the controlled system. In the hierarchical

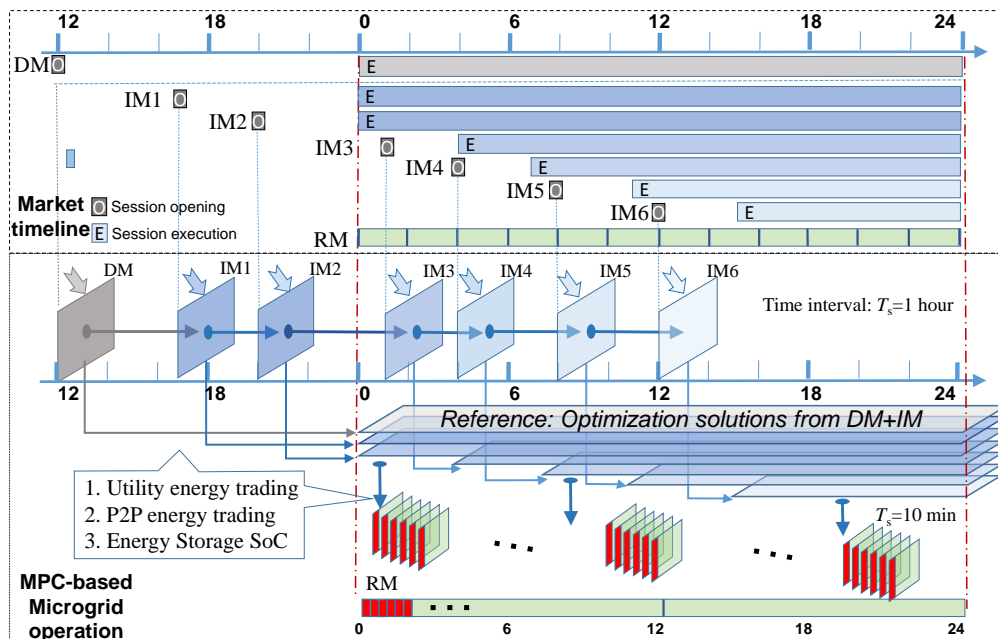


**Figure 4.1:** Illustration of the hierarchical framework of the proposed P2P local transactive market.

framework, DM and IM operation are treated as upper-level cooperative optimizations that generate preliminary decision references based on rough forecasted information, while the short-term RM operation is seen as the lower-level independent optimization that makes corrections in hand with up-to-date available data.

### 4.2.1 DM: Pre-schedule Problem

The day-ahead problem takes place at the noon before the targeted energy schedule day, which is a cooperative hourly energy pre-schedule problem. This problem can be cast as a market clearing process to preliminarily decide the local trading energy prices and the quantities of energy traded by each prosumer. Even though this clearing problem can be solved in a centralized manner, the P2P market prefers decentralized realization, to protect the privacy of agents. In addition, the communication procedure in the network is another concerned issue of

agents, of which the communication burden should be as small as possible, while the communication failures should be tolerant.

In order to tackle these two challenges, the setting of day-ahead problem is as follows: the centralized market optimization problem is fully decomposed into multiple sub-problems allocating to market participants. Unlike most exiting works, the market coordinator is removed and the trading energy information is kept secret in the proposed clearing process, considering privacy concerns. Each agent manages its own data, i.e., electricity load, ESS operation data, and utility trading energy, if any. The problem thus becomes a fully decentralized and iterative pricing negotiation process. Each agent sends/receives pricing information to/from neighboring agents in the P2P network for every hour of the next day. After the iteration stops, the preliminary energy scheduling results includes utility trading energy, P2P trading energy and price, ESS charging/discharging energy, and load shedding, if any. The mathematical model of the DM clearing problem is formulated in Section 4.3.

### **4.2.2 IM: Adjustment Problem**

The DM clearing problem provides pre-scheduling references, i.e., utility trading energy, ESS charging/discharging, and P2P trading profiles, for the first session of IM, which opens at 17:00 and executed at 21:00 before the targeted day based on the forecast information. Then, the reference of the following five sessions of IM are given by the previous session, which opens 3 hours before the execution starts. However, among all reference values, only the pre-scheduled utility trading energy is under contract, while P2P cooperative energy trading plans can be freely adjusted in IM sessions irrespective of the DM pre-scheduling results. This is rational in terms of temporal match considering the 1-hour schedule internal

of IM, much longer than the P2P communication process. Each IM session aims to correct the hourly scheduling plan upon the updated forecast information. In this regard, the intra-day problem is an iterative adjustment problem. The mathematical model of the IM adjustment problem is explained in Section 4.3.

### 4.2.3 RM: Real-time Problem

The RM has a smaller time interval than DM and IM, e.g., 5-15 min, which aims to balance the real-time power supply and demand. In RM, each agent has to make its actual energy operational decisions, including actual ESS charging/discharging power, load shedding power, the utility trading power and P2P trading quantity and price. All these decisions are determined taking into account both the references of previous market sessions and available information of forecast information. On the one hand, the violation of utility trading contracts is allowed but will incur a regulation cost, while the P2P trading profiles should be strictly complied. SoC of ESS resulted from previous sessions is treated as the state trajectory to follow in RM. Rolling optimization, i.e., MPC, is used in this chapter to hedge against the uncertainty. On the other, the actual output of DER is updated, and the available renewables should be fully utilized. The mathematical model of the RM real-time problem is explained in Section 4.3.

### 4.2.4 Settlement Issue

The last stage of the proposed market is the settlement stage. Distinguished from most recent works, the market coordinator is removed in the proposed market framework when dealing with the settlement issues. Since the energy cooperation is performed in a P2P manner, each agent in the community network is treated as a selfish prosumer. That is, the agents in the community need not send any

private information, e.g., trading quantities and bids, to a central market manager for settling the payment issues. Instead, the mutual payment is settled in a fully decentralized fashion. After the closure of all IM sessions, the P2P trading quantities and prices are finally negotiated by each agent pairs. Likewise, after the closure of the whole-day markets, the actual commitment of the utility trading is determined. In this way, the P2P local transactive market is settled in an autonomous and fully decentralized way.

### 4.3 Microgrid Operation Model

In this section, the microgrid community in consideration is firstly described and modeled. The mathematical formulation of the cost functions and operation constraints is then explained.

#### 4.3.1 System Description

A microgrid community  $\mathcal{N} := \{1, 2, \dots, N\}$  is considered in this chapter. Under the deregulated market environment, microgrids are qualified to independently participate in the local transactive energy market, at a community level, as in Fig. 4.2. Each microgrid contains various components, e.g., ESS, renewable sources, and elastic loads, which are managed by an Energy Management System (EMS) to ensure the local power balance. Without loss of generality, it is assumed that the microgrids can carry out P2P energy trading with each other. In addition, the bilateral information exchange is only based on the local decisions made by the individual EMS, while the internal information, e.g., key parameters and DER capacities, is considered as privacy.

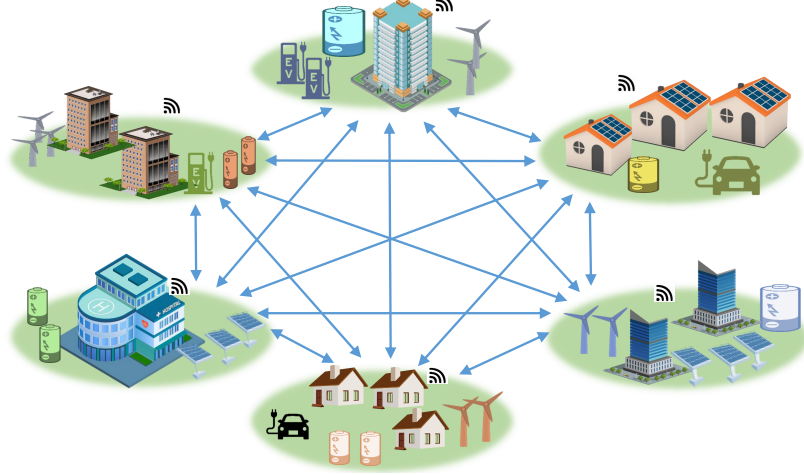


Figure 4.2: Peer-to-peer market structure of multi-microgrids.

### 4.3.2 Cost Function

**Utility Trading Cost** The microgrids can purchase deficient energy directly from the utility grid, or sell excessive energy to the grid:

$$C_{i,t}^U = (\mu_t^b b_{i,t} - \mu_t^s s_{i,t}) T_s, \quad \forall i \in \mathcal{N}, \forall t \in \mathcal{T} \quad (4.1)$$

**Battery Degradation Cost** The battery degradation cost is resulted from frequent charging and discharging. The quadratic cost function is adopted:

$$C_{i,t}^S = (\kappa_2^c c_{i,t}^2 + \kappa_1^c c_{i,t} + \kappa_2^d d_{i,t}^2 + \kappa_1^d d_{i,t}) T_s, \quad \forall i \in \mathcal{N}, \forall t \in \mathcal{T} \quad (4.2)$$

**Load Response Cost** Flexible load response cost in microgrids (e.g., thermal load) is roughly aggregated as:

$$C_{i,t}^L = \mu_d (\hat{l}_{i,t} - l_{i,t})^2 T_s, \quad \forall i \in \mathcal{N}, \forall t \in \mathcal{T} \quad (4.3)$$

**P2P Energy Trading cost** The trading cost of microgrid  $i \in \mathcal{N}$  includes all bilateral cost with neighbors  $j \in \mathcal{N}_i$ :

$$C_{i,t}^P = \sum_{j \in \mathcal{N}_i} (\pi_{i,t}^j q_{i,t}^j) T_s, \quad \forall i \in \mathcal{N}, \forall t \in \mathcal{T} \quad (4.4)$$

### 4.3.3 Constraints

**Energy Storage System** In this chapter, we suppose that each microgrid  $i \in \mathcal{N}$  installs a lithium-ion battery – the most popular option today. The secure operation of ESS should satisfy:

$$SoC_{i,t} = SoC_{i,t-1} + (\eta_i^c c_{i,t} - d_{i,t}/\eta_i^d) T_s/B_i, \quad \forall t \in \mathcal{T} \quad (4.5)$$

$$0 \leq c_{i,t} \leq w_{i,t} \bar{c}_i, \quad \forall t \in \mathcal{T} \quad (4.6)$$

$$0 \leq d_{i,t} \leq (1 - w_{i,t}) \bar{d}_i, \quad \forall t \in \mathcal{T} \quad (4.7)$$

$$SoC_{i,\min} \leq SoC_{i,t} \leq SoC_{i,\max}, \quad \forall t \in \mathcal{T} \quad (4.8)$$

$$SoC_{i,T} = SoC_{i,0} \quad (4.9)$$

Specifically, (4.5) represents the State of Charge (SoC) evolution process of ESS; (4.6)-(4.7) suggest that the charging and discharging power is limited by their maximal values, where  $w_{i,t} \in \{0, 1\}$ ; (4.8) implies that the energy level is bounded into a secure permissible range; (4.9) regulates the terminal energy level no less than the initial level.

**Flexible Load** Flexible load are common in microgrids, e.g., thermal appliances, electric vehicles, of which the consumption can be rearranged within a permissible range. Together with the basic inelastic load, the total load demand

$l_{i,t}$  of the microgrids is controlled as follows:

$$l_{i,\min} \leq l_{i,t} \leq \hat{l}_{i,t}, \quad \forall t \in \mathcal{T} \quad (4.10)$$

For example, HVAC units, dominating the energy consumption in buildings, are expected to adjust the indoor temperature  $T_{i,t}^{\text{in}}$  evolved by  $T_{i,t}^{\text{in}} = T_{i,t-1}^{\text{in}} + \eta(T_{i,t}^{\text{out}} - T_{i,t-1}^{\text{in}}) + \theta l_{i,t}^{\text{h}}$ . The discomfort for users can be defined proportional to the squared difference between the actual temperature and desired temperature, i.e.,  $(T_{i,t}^{\text{in}} - T_i^{\text{ref}})^2$ . In this regard, this HVAC load can be integrated into (4.10) by regarding the power required to track  $T_i^{\text{ref}}$  as rated power and the actual consumption as part of  $l_{i,t}$ .

**Energy Trading with the Utility** We assume that all microgrids share the same buying/selling price at the time slot  $t$ , since we consider a community of microgrids that are connected to the same utility. The trading amount is subject to:

$$0 \leq b_{i,t} \leq \bar{b}_i, \quad 0 \leq s_{i,t} \leq \bar{s}_i, \quad \forall t \in \mathcal{T} \quad (4.11)$$

**P2P Energy Trading** Consider a bilateral energy trading between  $i \in \mathcal{N}$  and  $j \in \mathcal{N}_i$ , and a  $\delta \in (0, 1)$  power loss is assumed on the line  $(i, j)$ . Then, the power exchange on the line is as follows:

$$q_{ij,t}^i(1 - \delta) = q_{ji,t}^j, \quad q_{ij,t}^i = q_{ji,t}^j(1 - \delta) \quad (4.12)$$

$$0 \leq q_{ij,t}^i \leq F_{ij} u_{ij,t}^i, \quad 0 \leq q_{ij,t}^j \leq F_{ij} u_{ij,t}^j \quad (4.13)$$

$$u_{ij,t}^i, u_{ij,t}^j \in \{0, 1\}, \quad u_{ij,t}^i + u_{ij,t}^j \leq 1 \quad (4.14)$$

In (4.12), the first equation indicates the case where the energy flows from  $i$  to  $j$ ,  $q_{ij,t}^i$  is the output energy from  $i$ , and  $q_{ji,t}^j$  is the input energy to  $j$ ; the second equation indicates the case, where energy flows from  $j$  to  $i$ , where  $q_{ji,t}^j$  is the output energy from  $j$ , and  $q_{ij,t}^i$  is the energy received by  $i$ . In (4.13) and (4.14),  $u_{ij,t}^i$  and  $u_{ij,t}^j$  are binary variables standing for the energy trading directions.

In this context, two state variables  $q_{i,t}^j$  and  $q_{j,t}^i$  are introduced to denote the energy at two ends of line  $(i, j)$  as follows:

$$q_{i,t}^j := q_{ij,t}^i - q_{ij,t}^i(1 - \delta), \quad q_{j,t}^i := q_{ji,t}^j - q_{ji,t}^j(1 - \delta) \quad (4.15)$$

And then, (4.12) is reformulated as follows:

$$q_{i,t}^j + q_{j,t}^i = 0, \quad \forall i \in \mathcal{N}, \forall j \in \mathcal{N}_i, \forall t \in \mathcal{T} \quad (4.16)$$

Similar to the previous chapter, for any successful trading quantity agreement (4.16), the associated price agreement should be also reached:

$$\pi_{i,t}^j = \pi_{j,t}^i = \pi_{(i,j),t}, \quad \forall (i, j) \in \mathcal{E}, \forall t \in \mathcal{T} \quad (4.17)$$

where  $\pi_{(i,j),t}$  is the Lagrangian dual variable of (4.16) representing the optimal P2P trading price on the edges  $(i, j) \in \mathcal{E}$ .

## 4.4 Multi-stage Market Problem Formulation

In this section, the multi-stage transactive market is firstly described. The MPC-based P2P energy trading problem is then formulated for each stage.

#### 4.4.1 Cooperative DM Operation Problem

The day-ahead problem takes place at the noon before the targeted energy schedule day, which is a cooperative hourly energy pre-schedule problem. This problem can be cast as a market clearing process to preliminarily decide the local trading energy prices and the quantities of energy traded by each prosumer. Even though this clearing problem can be solved in a centralized manner, the P2P market prefers decentralized realization, to protect the privacy of agents. The DM, normally closed before noon, aims to handle the power transactions for the following day. As such, the daily schedule problem of participants is solved with the schedule horizon ahead from 12 to 36 hours, and is structured in 24 slots corresponding to 24 hours of each day. In DM, all microgrids participate in setting the preliminary P2P energy cooperation plan based on day-ahead forecasting data. Given this context, in DM, microgrids aim to minimize the total cost including load demand response cost, storage degradation cost, utility grid trading cost, and P2P trading cost over the scheduling horizon:

$$C_i^{\text{DM}} = \sum_{k=12}^{36} (C_{i,t+k}^{\text{L}} + C_{i,t+k}^{\text{S}} + C_{i,t+k}^{\text{U}} + C_{i,t+k}^{\text{P}}) \quad (4.18)$$

In DM, the power energy supply and demand balance is characterized by (4.19) in every microgrid  $i \in \mathcal{N}$ :

$$b_{i,t} - s_{i,t} + \sum_{j \in \mathcal{N}_i} (q_{ij,t}^i - q_{ij,t}^j) = l_{i,t} - \hat{r}_{i,t}^{\text{DM}} + c_{i,t} - d_{i,t}, \quad \forall t \in \mathcal{T} \quad (4.19)$$

where  $\hat{r}_{i,t}^{\text{DM}}$  denotes the day-ahead forecast renewable energy generation in the microgrid  $i \in \mathcal{N}$  at  $t$ -th time slot.

### 4.4.2 Cooperative IM Operation Problem

The DM clearing problem provides pre-scheduling references, i.e., utility trading energy, ESS charging/discharging, and P2P trading profiles, for the first session of IM, which opens at 17:00 and executed at 21:00 before the targeted day based on the forecast information. Then, the reference of the following five sessions of IM are given by the previous session, which opens 3 hours before the execution. However, among all reference values, only the pre-scheduled utility trading energy ( $g^{\text{ref}} = b^{\text{ref}} - s^{\text{ref}}$ ) is under contract, while P2P cooperative energy trading plans can be freely adjusted in IM sessions irrespective of the DM pre-scheduling results. This is rational in terms of temporal match considering the 1-hour schedule interval of IM, much longer than the P2P communication process. Each IM session aims to correct the hourly scheduling plan upon the updated forecast information. In this regard, the intra-day problem is an iterative adjustment problem.

The DM scheduling problem provides reference power values for the first session of IM. Then, the reference of the following sessions of IM are given by the previous session. However, among all reference values, only the scheduled utility exchanging energy ( $g^{\text{ref}} = b^{\text{ref}} - s^{\text{ref}}$ ) is under contract. Each IM session aims to correct the energy plan upon the updated forecasting information.

In consideration of the corrective actions in IM, the power balance equation (4.19) is modified by:

$$g_{i,t}^{\text{IM}} + g_{i,t}^{\text{ref}} + \sum_{j \in \mathcal{N}_i} (q_{ij,t}^i - q_{ij,t}^j) = l_{i,t} - \hat{r}_{i,t}^{\text{IM}} + c_{i,t} - d_{i,t}, \quad \forall t \in \mathcal{T} \quad (4.20)$$

where  $\hat{r}_{i,t}^{\text{IM}}$  denotes the updated forecasting renewable output. The grid exchanging power  $g_{i,t}^{\text{IM}} = b_{i,t}^{\text{IM}} - s_{i,t}^{\text{IM}}$  is to be optimized in the current IM session. In this

regard, the new hourly utility power is the sum of decisions in DM and corrections in all previous IM sessions:

$$g_{i,t} = g_{i,t}^{\text{DM}} + \sum_{s=1}^{N_s} g_{i,t}^{\text{IM}^s}, \quad \forall t \in \mathcal{T} \quad (4.21)$$

where  $N_s$  is the number of IM sessions that have occurred till the current time slot.

As such, the cost function of microgrids in the IM sessions is expressed in (4.22), considering the demand response management.

$$C_i^{\text{IM}} = \sum_{k=IM_{st}}^{IM_{end}} (C_{i,t+k}^{\text{L}} + C_{i,t+k}^{\text{S}} + C_{i,t+k}^{\text{U}} + C_{i,t+k}^{\text{P}}) \quad (4.22)$$

where  $IM_{st}$  and  $IM_{end}$  represent the starting and ending time instants of the scheduling horizon in the corresponding IM session. Normally, the time interval of IM is one hour or half an hour. In this chapter, 1-hour is chosen in accordance with the Iberian Market.

### 4.4.3 RM Operation Problem

The RM assists in avoiding real-time imbalances between the power supply and consumption in microgrids within a smaller time interval, e.g., 5-15 min. In the designed P2P electricity market framework, the P2P energy trading contracts, determined in previous market sessions, must be fulfilled in the RM. This is achieved by rescheduling local flexible load, ESSs, or utility power exchange. Moreover, in this stage, any further additional exchanging power plan with the

grid is considered as a deviation from the contract, which may incur up/down-regulation cost:

$$C_{i,t}^{\text{reg}} = \mu_t^{\text{up}} b_{i,t}^{\text{RM}} + \mu_t^{\text{dn}} s_{i,t}^{\text{RM}}, \quad \forall t \in \mathcal{T} \quad (4.23)$$

where  $\mu_t^{\text{up}}$  and  $\mu_t^{\text{dn}}$  denote the up-regulation price and down-regulation price, respectively. In consideration of the corrective actions in the regulation market, the power balance constraint (4.19) is modified by (4.24) in RM.

$$g_{i,t}^{\text{RM}} + g_{i,t}^{\text{ref}} + \sum_{j \in \mathcal{N}_i} (q_{ij,t}^{i,\text{ref}} - q_{ij,t}^{j,\text{ref}}) = l_{i,t} - \hat{r}_{i,t}^{\text{RM}} + c_{i,t} - d_{i,t}, \quad \forall t \in \mathcal{T} \quad (4.24)$$

where  $\hat{r}_{i,t}^{\text{RM}}$  is the updated forecasting renewable output,  $g_{i,t}^{\text{ref}}$ , expressed in (4.21), is the latest reference utility power, and  $(q_{ij,t}^{i,\text{ref}} - q_{ij,t}^{j,\text{ref}})$  is the latest P2P trading energy reference value determined by the IM session therein.

It is obvious that the renewable energy generation in RM will deviate from the intra-day forecasts. In order to avoid further deviations, microgrids aim to follow the reference ESS energy level over the RM scheduling horizon, especially at the last time instant. Towards this end, MPC-based optimization problems of multi-microgrids in the RM are summarized as follows.

$$\begin{aligned} C_i^{\text{RM}} = & \sum_{k=H_0}^H (C_{i,t+k}^{\text{L}} + C_{i,t+k}^{\text{S}} + C_{i,t+k}^{\text{reg}}) \\ & + \omega_1 \sum_{k=H_0}^{H-1} (S_{i,t+k} - S_{i,t+k}^{\text{ref}})^2 + \omega_2 (S_{i,t+H} - S_{i,t+H}^{\text{ref}})^2 \end{aligned} \quad (4.25)$$

where  $H_0$  and  $H$  represent the starting time and the length of the corresponding RM scheduling horizon,  $S_{i,t} = B_i \text{SoC}_{i,t}$  is the energy level of ESS  $i$ ,  $S_{i,t+k}^{\text{ref}}$  represents the given reference energy level trajectory of ESS  $i$  in the current schedule horizon,  $\omega_1$  and  $\omega_2$  are the weighting coefficient. The first line of the objective function is the internal cost of the microgrid, the second line steers the actual

SoC trajectory to the reference one, given by the IM sessions. Note that since the reference P2P trading energy is strictly followed and cleared in this stage, the P2P trading cost is omitted in the objective function (4.25). As such, the RM optimization problem of the microgrids under uncertainty is thus formulated as a look-ahead multi-period cost-minimization problem, which can be independently solved by microgrids without cooperation [122].

#### 4.4.4 Unified Market Optimization Problem

With the microgrid problems formulated above, the cooperative optimization problems in DM and IM are summarized as a social fare minimization:

$$\text{minimize } \sum_{i \in \mathcal{N}} \sum_{t \in \mathcal{T}} C_{i,t}^M(\mathbf{x}_{i,t}, \mathbf{q}_{i,t}, \boldsymbol{\pi}_{i,t}) \quad (4.26)$$

where  $C_{i,t}^M$  denotes the DM or IM operation cost. The associated constraints are denoted as  $\mathcal{X}^M$ . The variables include two groups: local variables  $\mathbf{x}_{i,t} = \{c_{i,t}, d_{i,t}, b_{i,t}, s_{i,t}, l_{i,t}\}$  collecting internal decision variables in the microgrid  $i \in \mathcal{N}$  and coupling variables  $\mathbf{q}_{i,t} = \{q_{i,t}^j\}_{j \in \mathcal{N}_i}$ ,  $\boldsymbol{\pi}_{i,t} = \{\pi_{i,t}^j\}_{j \in \mathcal{N}_i}$  coupled with other agents, as in (4.16),(4.17).

### 4.5 Distributed Algorithm Design

Even though the centralized market optimization problem for DM and IM can be solved efficiently by off-the-shelf tools, this chapter aims to design a distributed framework for privacy-preserving concern. In this section, we firstly propose a decomposition strategy to address the coupling constraint. After that, a dual-consensus distributed algorithm is put forward, in which the communication lossy network is modeled toward a robust version of the algorithm in practice.

### 4.5.1 Problem Decomposition

It is seen that (4.16) includes  $|\mathcal{E}|$  equations over all links at every period. Then, (4.16) is modified:

$$\sum_{i \in \mathcal{N}} \mathbf{Q}_i \mathbf{q}_{i,t} = \mathbf{0}, \quad \forall t \in \mathcal{T} \quad (4.27)$$

where  $\mathbf{q}_{i,t} \in \mathbb{R}^{N-1}$  denotes the neighboring trading energy vector,  $\mathbf{Q}_i \in \mathbb{R}^{|\mathcal{E}| \times (N-1)}$  is the mapping matrix. For a specific microgrid community,  $\mathbf{Q}_i$  is considered as a given fixed sparse matrix with entries 1 and 0.

Note that  $\boldsymbol{\pi}_{i,t} \in \mathbb{R}^{N-1}$  collects the neighboring prices of agent  $i$ . Let  $\boldsymbol{\pi}_t = \{\pi_{(i,j),t}\}_{(i,j) \in \mathcal{E}} \in \mathbb{R}^{|\mathcal{E}|}$  contain dual variables of (4.16), i.e., the optimal price of P2P trading defined in (4.17). Observing the structure of (4.16), one can rewrite the optimal pricing scheme (4.17):

$$\mathbf{Q}_i^T \boldsymbol{\pi}_t = \boldsymbol{\pi}_{i,t}, \quad \forall t \in \mathcal{T} \quad (4.28)$$

Accordingly, the P2P trading cost (4.4) can be rewritten as:

$$C_{i,t}^P = \boldsymbol{\pi}_{i,t}^T \mathbf{q}_{i,t} = \boldsymbol{\pi}_t^T \mathbf{Q}_i \mathbf{q}_{i,t}, \quad \forall i \in \mathcal{N}, \forall t \in \mathcal{T} \quad (4.29)$$

where the time slot  $T_s$  has been omitted for simplicity. Hence, the centralized market problem (4.26) is split into  $N$  sub-problems in agent  $i \in \mathcal{N}$ :

$$\text{minimize} \quad \sum_{t \in \mathcal{T}} (C_{i,t}^{\text{int}}(\mathbf{x}_{i,t}) + \boldsymbol{\pi}_t^T \mathbf{Q}_i \mathbf{q}_{i,t}) \quad (4.30)$$

where  $C_{i,t}^{\text{int}} = C_{i,t}^S + C_{i,t}^L + C_{i,t}^U$  represents the internal energy cost of microgrid  $i \in \mathcal{N}$ . The first term implies the internal cost counterpart, which contains local private information, while the second term stands for the P2P energy trading

cost counterpart.

Compared to (4.26), (4.30) replaces the coupling constraint (4.16) by the KKT condition in the objective function. Note that the convexity ensures the optimality and equivalence of the reformulation. In doing so, agents only have to solve the convex optimization problem (4.30) on the local constraint set, provided the global dual variable  $\boldsymbol{\pi}_t$ . Thus, the challenge lies in the coupling term  $\boldsymbol{\pi}_t^T \mathbf{Q}_i \mathbf{q}_{i,t}$  in (4.30), where the price vector  $\boldsymbol{\pi}_t$  is essentially the dual variable of the energy agreement (4.16). Toward this end, we leverage dual-consensus Alternating Direction Method of Multipliers (DC-ADMM) to address the aforementioned challenge [79].

## 4.5.2 Communication-Loss-Robust Distributed Algorithm

In principle, DC-ADMM contains the following steps, at iteration  $k = 1, 2, \dots$ , for agents  $i \in \mathcal{N}$ :

$$\{\mathbf{x}_{i,t}^k, \mathbf{q}_{i,t}^k\}_{t \in \mathcal{T}} = \arg \min_{\mathcal{X}} \sum_{t \in \mathcal{T}} \left[ C_{i,t}^{\text{int}} + \rho \left\| \frac{1}{\rho} \mathbf{Q}_i \mathbf{q}_{i,t} - \frac{1}{\rho} \mathbf{y}_{i,t}^{k-1} + 2 \sum_{j \in \mathcal{N}_i} \mathbf{v}_{ij,t}^{k-1} \right\|^2 \right] / 4|\mathcal{N}_i| \quad (4.31)$$

$$\boldsymbol{\pi}_t^{(i),k} = \left[ 2 \sum_{j \in \mathcal{N}_i} \mathbf{v}_{ij,t}^{k-1} - \frac{1}{\rho} \mathbf{y}_{i,t}^{k-1} + \frac{1}{\rho} \mathbf{Q}_i \mathbf{q}_{i,t}^k \right] / 2|\mathcal{N}_i| \quad (4.32)$$

$$\mathbf{v}_{ij,t}^k = \left[ \boldsymbol{\pi}_t^{(i),k} + \boldsymbol{\pi}_t^{(j),k} \right] / 2, \forall j \in \mathcal{N}_i \quad (4.33)$$

$$\mathbf{y}_{i,t}^k = \mathbf{y}_{i,t}^{k-1} + 2\rho \sum_{j \in \mathcal{N}_i} \left( \boldsymbol{\pi}_t^{(i),k} - \mathbf{v}_{ij,t}^k \right) \quad (4.34)$$

where  $\rho > 0$  is the given parameter and  $\mathbf{v}_{ij,t}$  and  $\mathbf{y}_{i,t}$  are auxiliary variables stored in agent  $i \in \mathcal{N}$ . Primal variables are solved in (4.31). In (4.32), each agent  $i$  keeps a local estimate of the global dual variable, i.e.,  $\boldsymbol{\pi}_t^{(i)}$ . In (4.33), every agent

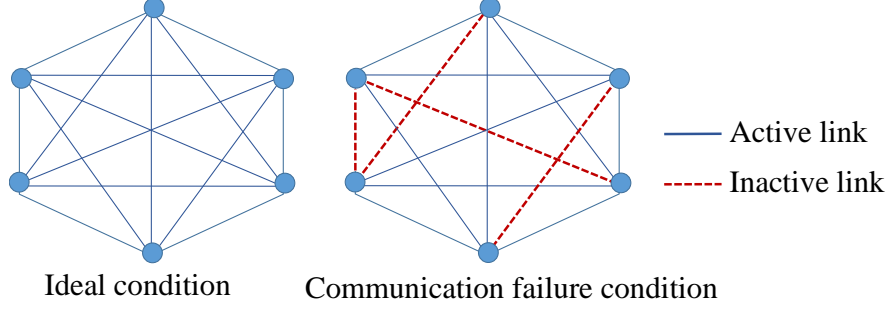


**Figure 4.3:** Illustration of the communication failure on the lossy P2P network.

$i$  exchanges the up-to-date  $\boldsymbol{\pi}_t^{(i)}$  to its neighbors. It is noticed that the updates in (4.31) involves a convex optimization problem, and the updates in (4.32)–(4.34) are simple algebraic operations, at every time slot  $t \in \mathcal{T}$ .

The DC-ADMM enjoys several desirable features: Firstly, the aforementioned updates are parallel and distributed. Secondly, each agent  $i$  has access to only local information, i.e.,  $C_{i,t}^{\text{int}}$ ,  $\mathbf{Q}_i$ ,  $\mathbf{q}_{i,t}^k$ , and local auxiliary variables. More importantly, the DC-ADMM can be implemented in a lossy network, e.g., communication links between agents may fail at computing iterations. This is specially pointed out as frequent message exchanges (4.33) may be impractical in the real-world electricity market. This observation motivates us to develop the following algorithm.

To model such a lossy network, we assume that, for each communication link  $(i, j)$ , there is a probability  $\xi_{ij} \in (0, 1]$  that the message exchange between agent  $i$  and  $j$  fails. In such a case, the link is called inactive at this iteration, as shown in Fig. 4.3. At each iteration  $k$ , let  $\Phi^k \subseteq \mathcal{E}$  be the set of all active communication links, on which the message exchange is successful. Otherwise, the associated agents of the link would not update  $\mathbf{v}_{ij,t}^k$  as in (4.33), but keep it unchanged:  $\mathbf{v}_{ij,t}^k = \mathbf{v}_{ij,t}^{k-1}$ . Likewise,  $\mathbf{y}_{i,t}^k$  is updated using only  $\mathbf{v}_{ij,t}^k$  on  $(i, j) \in \Phi^k$ . Algorithm

2 summarizes the proposed communication-loss-robust P2P Consensus algorithm based on DC-ADMM.

---

**Algorithm 2:** Communication-Loss-Robust Distributed Energy Trading Algorithm

---

- 1: Initialize  $\mathbf{x}_{i,t}^0, \mathbf{q}_{i,t}^0, \boldsymbol{\pi}_t^{(i),0}, \mathbf{y}_{i,t}^0, \mathbf{v}_{ij,t}^0 = \mathbf{0}$ , for each microgrid  $i \in \mathcal{N}, \forall t$ . Set iteration  $k = 1$ ;
  - 2: **repeat**
  - 3:   **for** all  $i \in \mathcal{N}$  (*in parallel*) **do**
  - 4:     Update  $\mathbf{x}_{i,t}^k, \mathbf{q}_{i,t}^k$  according to (4.31);
  - 5:     Update  $\boldsymbol{\pi}_t^{(i),k}$  according to (4.32);
  - 6:     Transmit  $\boldsymbol{\pi}_t^{(i),k}$  to neighbors  $j \in \mathcal{N}_i$ , and receive  $\boldsymbol{\pi}_t^{(j),k}$ ,  $j \in \{j | (i, j) \in \Phi^k\}$  from active links;
  - 7:     Update  $\mathbf{v}_{ij,t}^k$  according to (4.33) if  $(i, j) \in \Phi^k$ ; otherwise  $\mathbf{v}_{ij,t}^k = \mathbf{v}_{ij,t}^{k-1}$ ;
  - 8:     Update  $\mathbf{y}_{i,t}^k = \mathbf{y}_{i,t}^{k-1} + 2\rho \sum_{j | (i,j) \in \Phi^k} \left( \boldsymbol{\pi}_t^{(i),k} - \mathbf{v}_{ij,t}^k \right)$ ;
  - 9:   **end for**
  - 10:   Set  $k = k + 1$ ;
  - 11: **until** a predefined stopping criterion is satisfied.
- 

### 4.5.3 Algorithm Implementation and Scalability

Algorithm 2 summarizes the proposed distributed algorithm, through which are able to participate in the cooperative P2P energy trading in DM and IM sessions. It is worth mentioning that all microgrids solve their own problems in parallel, with only the dual variables (peer pricing information) exchanged among neighborhoods to reach a global pricing consensus, which ensures the agent privacy preservation as well as the fairness. Particularly, each microgrid  $i \in \mathcal{N}$  holds a pricing estimate, i.e.,  $\boldsymbol{\pi}_t^{(i)}$  of the global variable  $\boldsymbol{\pi}_t$  and exchanges it to each other. Until the predefined stopping criterion, all local estimates converge to a consensus value, which represents the optimal P2P trading price on all peers. The novelty of this work is that there are no any coordinators to gather and diffuse

information during the iterations, namely fully distributed in this chapter. As such, the proposed algorithm is scalable to a large number of microgrids.

## 4.6 Case Study

In this section, the proposed market model and algorithm are demonstrated by numerical experiments. The uncertainty in consideration includes the PV forecast errors and intra-day component failure.

### 4.6.1 Simulation Setup

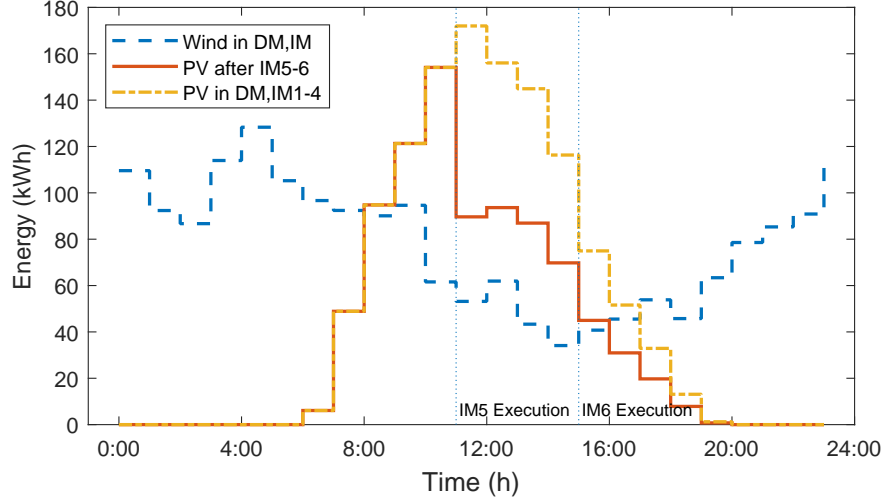
A microgrid community composed of six microgrids is used to test the proposed framework. Table 4.3 shows the basic data setup of the community. Fig. 4.4 illustrates the basic forecast outputs of solar energy in MG1 and wind energy in MG4. Note that the solar PV generation is modified at IM5 session that opens at 8:00 and executes from 11:00 (see Table 4.2), owing to up-to-date weather conditions. All data are based on scaled real-world electricity data of Belgium<sup>1</sup>. In the proposed market design, the time slot interval is 1 hour for DM and IM sessions. Provided the references and uncertainties, the MPC-based RM optimization is performed on the 2-hour horizon at a 10-min interval, and  $\omega_1 = 2\text{p.u.}$ ,  $\omega_2 = 5\text{p.u.}$  In the algorithm,  $\rho = 4.5$ ,  $\xi_{ij} = 0.2$ ,  $\delta = 0$ , the stopping criterion is primal residual smaller than 0.1. All implementations are conducted in Matlab 2019b on a personal computer with CPU Intel Core i7 2.6GHz and 16GB memory. The formulated optimization problem is performed by YALMIP with CPLEX 12.9 as a solver.

---

<sup>1</sup>“Solar Power Generation, NRWL Wind Data and Load Data in Belgian Power Grid,” website: <http://www.elia.be/en/grid-data/>.

**Table 4.3:** Microgrid Data Setup of Simulations

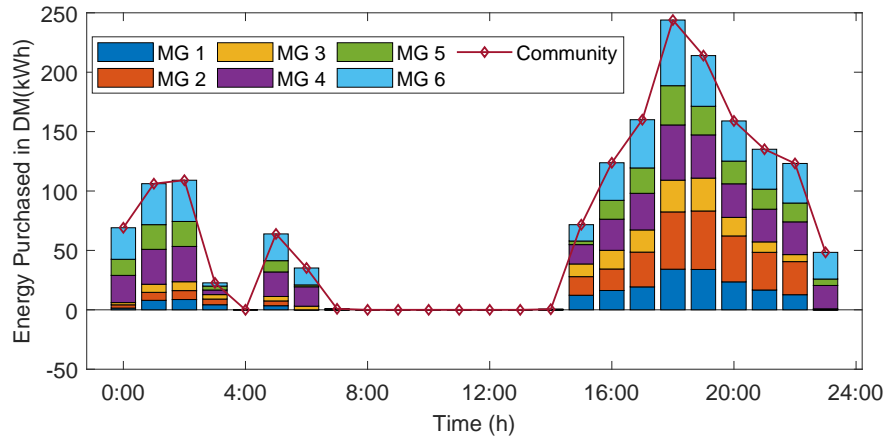
MG 1,2,3: PV energy=base PV capacity $\times\{1,1.2,0.8\}$ ;
MG 4,5,6: wind energy=base wind capacity $\times\{1,0.8,1.2\}$ .
Load ( $\forall i$ ): peak value range (79-95kW, at 12:00-20:00), off-peak value range (59-66kW, at 2:00-6:00), $l_{\min} = 0.8\hat{l}$ , $\mu_d = 0.1\$/\text{kWh}$ .
ESS ( $\forall i$ ): $B = 600\text{kWh}$ , $\kappa_2^c = \kappa_2^d = 10^{-5}\$/\text{kW}^2\text{h}$ , $\kappa_1^d = 10\kappa_1^c = 0.225\$/\text{kWh}$ , $\eta^c = \eta^d = 0.92$ , $\bar{c} = \bar{d} = 120\text{kW/h}$ , $SoC_{\min} = 0.2$ , $SoC_{\max} = 0.9$ .
Line( $\forall i$ ): $\bar{b} = \bar{s} = 100\text{kW}$ , $F_{ij} = 50\text{kW}$ .

**Figure 4.4:** Forecasting generation of base solar PV energy and wind energy in DM and updates in IM sessions.

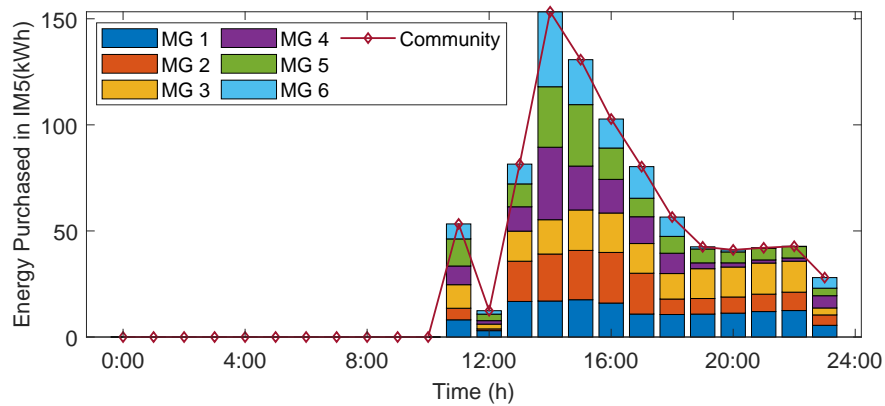
## 4.6.2 Results and Discussion

Firstly, the cooperative energy schedule problem is tentatively cleared in the DM. In Fig. 4.5(a), the utility grid energy purchasing plan in DM is displayed for six microgrids and the community. It is observed in DM that the purchasing energy actions only occur at the community net-energy deficient periods, e.g., 0:00-4:00, 5:00-7:00, and 15:00-24:00. The reason for this observation is that the cooperative P2P trading enables mutual transactions among community agents, instead of separately trading with the utility. At IM sessions, all microgrids make necessary corrections in case of any updated forecast condition. As the grid buying price

in IM is much lower than regulation fees in RM, all microgrids are motivated to participate in IM to avoid deviation penalties.



(a) DM preliminary plans.



(b) Adjustment in the IM5 session.

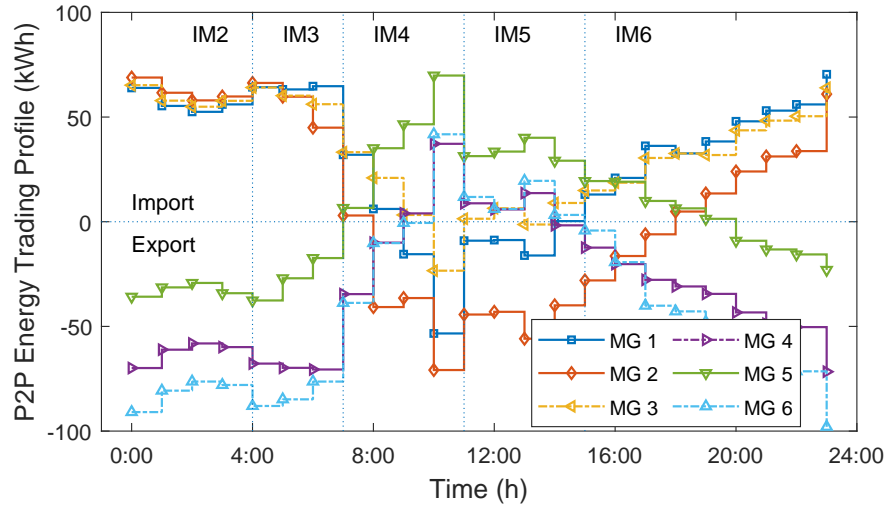
**Figure 4.5:** Purchasing energy plan.

Since the forecast PV generation in Fig. 4.4 is somehow lower than expected from 11:00, we find that all agents modify their previous plans at IM5 session that regulates the time period 11:00-24:00. For instance, as illustrated in Fig. 4.5(b), microgrids have to purchase more energy from the utility to compromise the PV energy deficit, in the IM5 session. It is also noticed that, even though all decisions are made in a fully distributed manner, the energy purchasing plans are consistent for all agents, in terms of purchasing periods. This result suggests

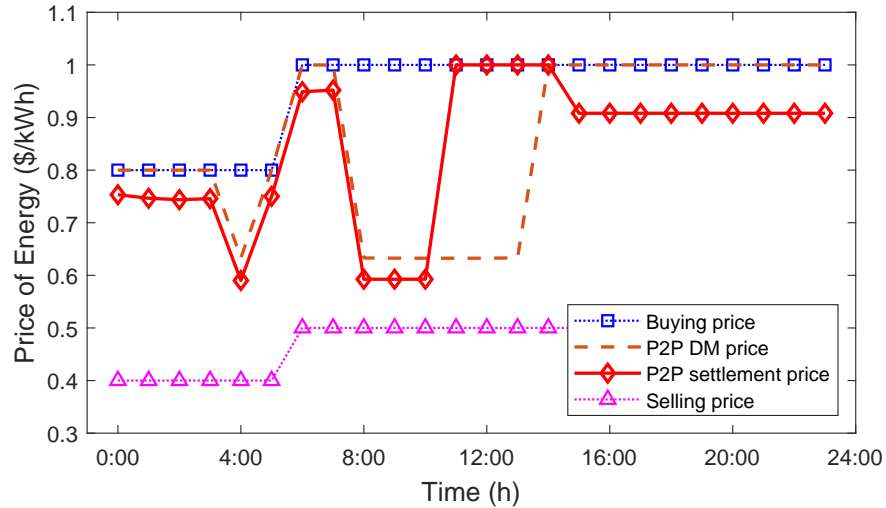
that the proposed P2P energy trading market succeeds in achieving a cooperative energy schedule plan.

Secondly, the P2P energy trading contracts are determined in six consecutive IM sessions, including the trading quantity and price, as shown in Fig. 4.6. It is observed that, the energy cooperation profile is proactive in the community, in terms of the energy quantity and temporal evolving profile. Particularly, it is obvious to see the energy exchange to PV microgrids (MG1,2,3) from wind microgrids (MG3,4,5) in the nighttime. This is reasonable because the wind energy dominates the nighttime while the solar energy arises only during the daytime. In the meantime, the P2P settlement price estimates in each agent would finally reach a consensus, as the red line shows in Fig. 4.6(b), which is below the buying price and above the selling price. This observation suggests that the P2P trading in the proposed framework is incentive for all participant microgrids. It should be noticed that, the tentative P2P trading decisions resulted from the DM clearing problem is not under contract, since the microgrids are entitled to modify their P2P decisions in IM sessions.

Thirdly, in RM, each microgrid makes individual scheduling decisions, taking into account the available solar PV and wind generation, actual load demands, as well as the utility energy trading reference from previous sessions. In RM, a up/down regulation fee  $\mu^{\text{up}} = \mu^{\text{dn}} = 10\$/\text{kWh}$  will be regulated to penalize deviations in RM. Fig. 4.7 illustrates the energy level of ESSs in six microgrids, and Fig. 4.8 shows the scheduling results for the MG1 and MG4. As illustrated, microgrids achieve the short-term power supply-demand balance mainly by means of local ESS charging and discharging, provided the grid energy contract and P2P trading contract. Interestingly, one can observe that the ESS energy level trajectories tend to be almost identical after incorporating P2P energy trading. This



(a) Imported P2P Energy.

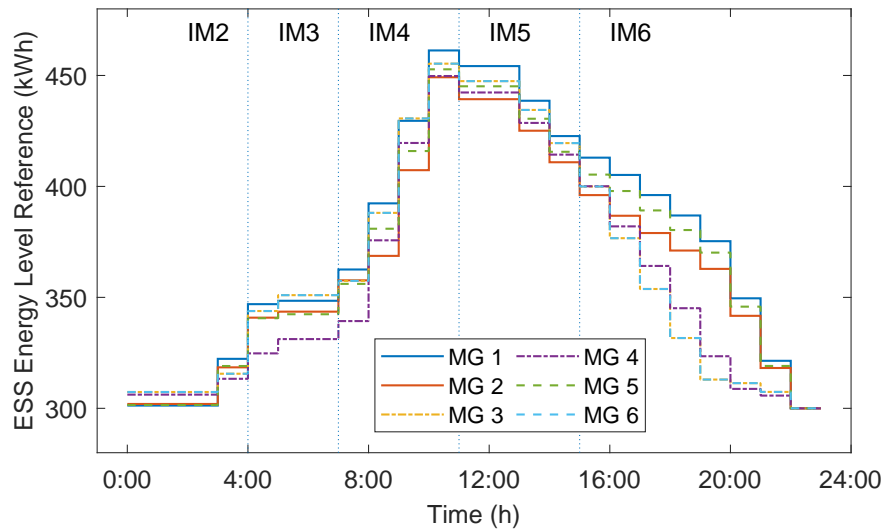


(b) Bilateral P2P price consensus.

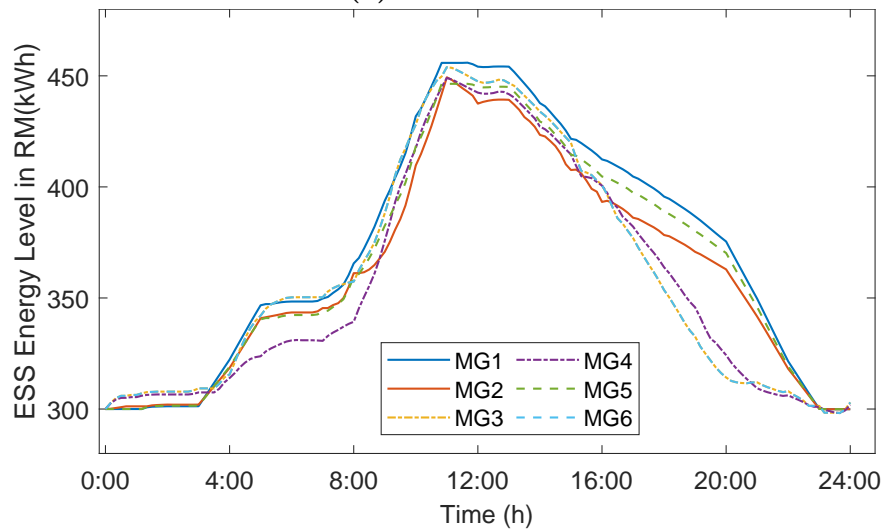
**Figure 4.6:** P2P trading profiles and optimal P2P price consensus.

implies that the ESSs in all microgrids are motivated to coordinately schedule the energy storage.

As such, the proposed P2P trading model can harmonize the distributed ESSs efficiently via distributed communication among microgrids. In addition, Fig. 4.9 depicts the flexible load profiles in the simulations. As is seen, the flexible load can be also regarded as a source of flexibility provision, which has limited capacity to adjust between the IM and RM.



(a) IM session.



(b) RM sessions.

**Figure 4.7:** SoC profiles of battery energy storage systems.

Fig. 4.10(a) and Fig. 4.10(b) depict the convergence performance of the proposed algorithm, in terms of primal and dual residuals, taking DM clearing problem as an example. In addition, the actual number of active links in the iterative processes are explicitly shown in Fig. 4.10(c). Even though a larger link failure probability leads to a sparse communication network with more inactive links, it is observed that the proposed algorithm has almost the similar

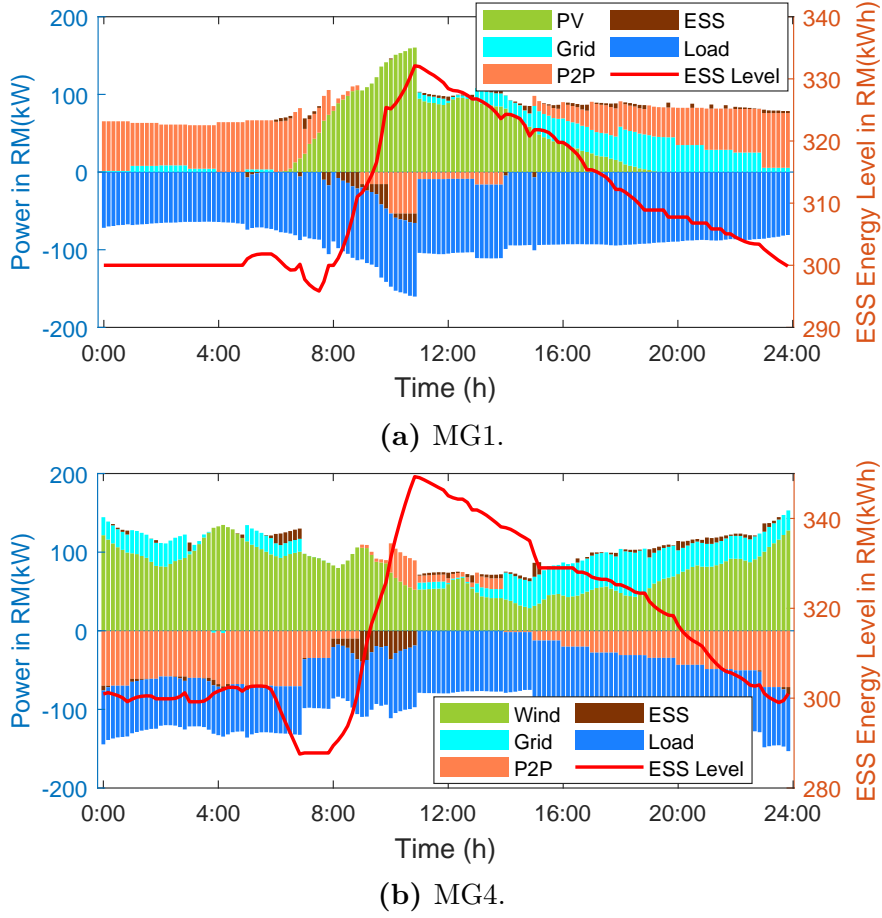
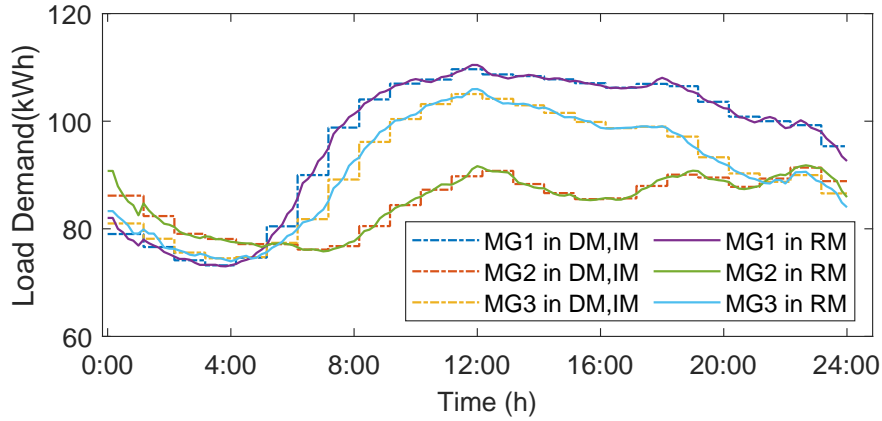


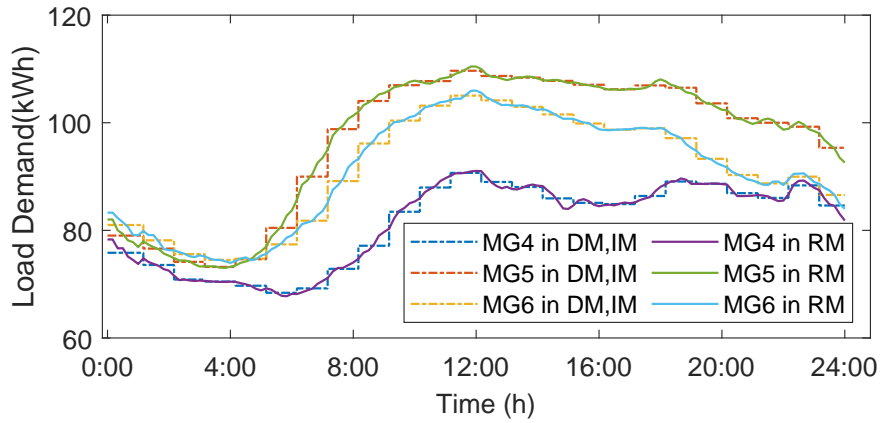
**Figure 4.8:** Energy profiles of microgrids in RM.

convergence rate at  $\xi = 0.2$  and  $\xi = 0.4$ , as compared to that on the ideal communication network at  $\xi = 0$ . It is seen that the worst case in the iteration is that, only 4 of total communication links are active, which implies a high robustness level to communication losses. Moreover, the average computational time for DM is 51.96 seconds for each microgrids with the stopping criteria primal residual  $\leq 0.1$ , which is acceptable in practice. Though the case study is a small scale composed of six microgrids, the proposed framework is promising to be extended to a larger case without compromising computational tractability, since it allocates the computational burden to agents in parallel.

Lastly, another intra-day component-maintenance case is also simulated to



(a) MG 1,2,3.



(b) MG 4,5,6.

**Figure 4.9:** Flexible load profiles in RM.

validate the effectiveness of the proposed framework in dealing with such uncertainties. It is supposed that, at the opening of IM6, the EMS of MG4 somehow schedules an intra-day maintenance of ESS from 18:00. That is, the ESS of MG4 can only serve for the first three hours of IM6 session. Under this circumstance, the proposed P2P trading market framework allows EMS of MG4 to adjust the scheduling plans in IM6. As can be seen in Fig. 4.11, the ESS in MG4 is out of service after the scheduled maintenance time. Also, MG4 schedules its ESS to discharge more energy during the service time than the case without maintenance plan.

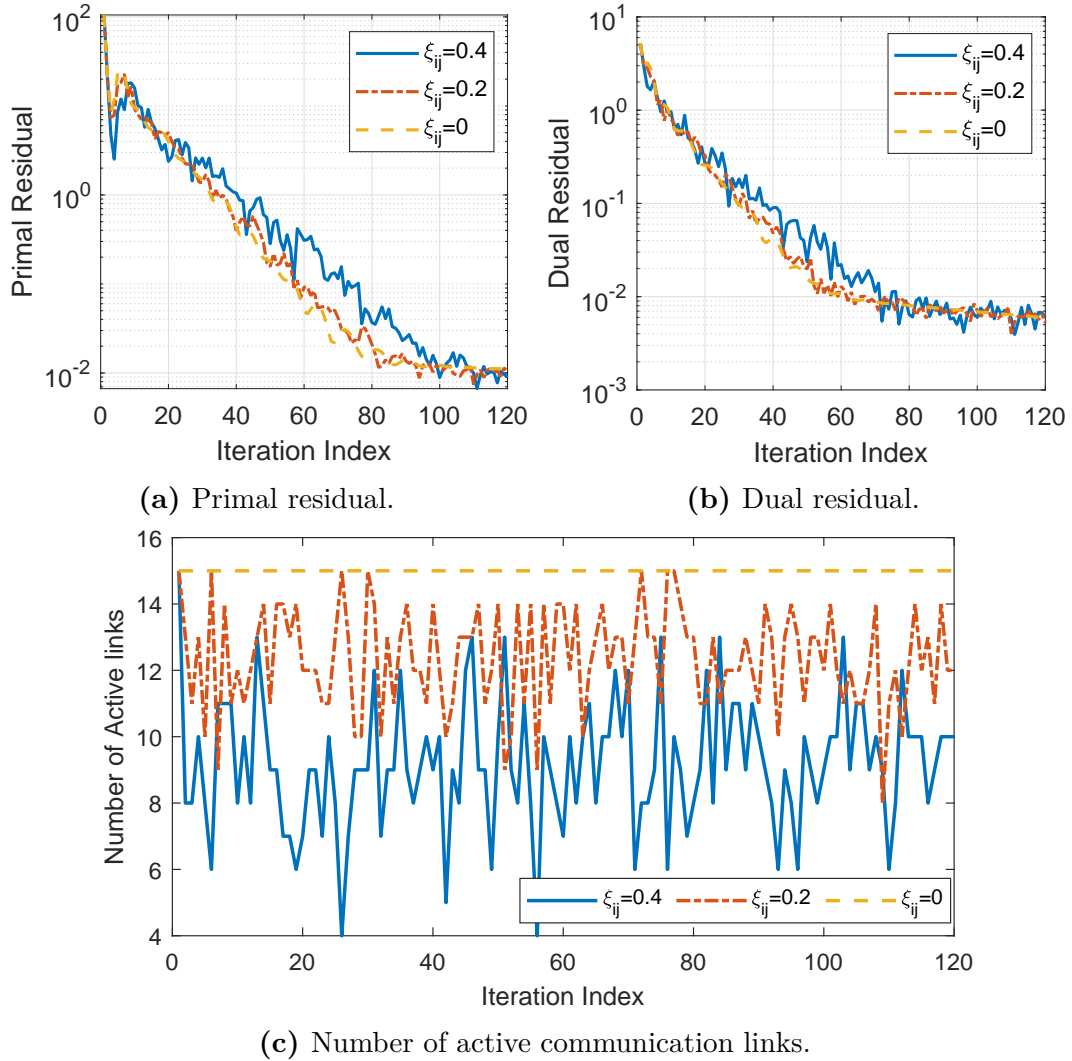


**Figure 4.10:** Performance of proposed algorithm.

In addition, Fig. 4.12 compares the P2P imported energy of MG4 from peers in IM 6 (9 hours), where the negative value implies the exporting energy. MG4 exports more energy to neighbors in the first three hours before its maintenance, since its ESS is re-scheduled to discharge more energy in this interval. Meanwhile, in the remaining six hours, MG4 is observed to export less energy to others in Fig. 4.12(b) than that in Fig. 4.12(a), owing to the shut-down of ESS. Though microgrids can trade with the utility to compensate for the shutdown of ESS, the microgrid community prioritizes bilateral trading, since it is much economic.

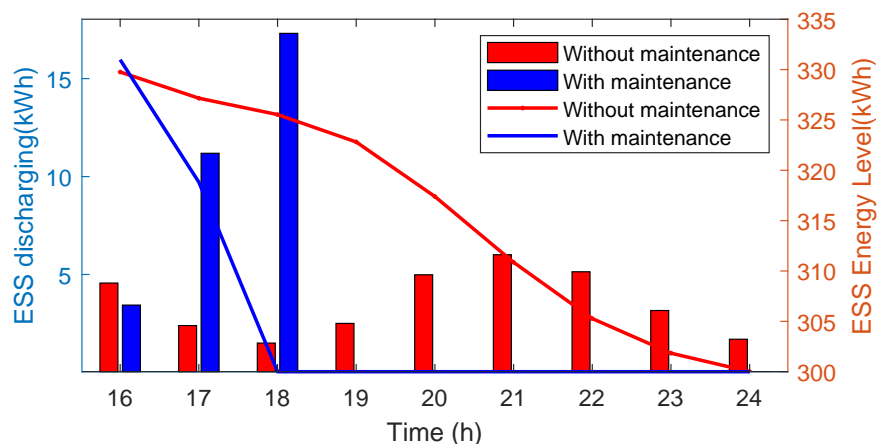


**Figure 4.11:** Operation status of ESS in MG4 when maintenance plan is scheduled at the opening of IM6.

This result once again validates the robustness of the proposed P2P electricity framework in dealing with real-world practical uncertain issues.

## 4.7 Summary for the Chapter

This chapter designed an effective hierarchical P2P transactive energy trading framework in line with the existing market framework. Considering the possible forecasting errors in renewable energy outputs, distributed MPC-based market operation problems are formulated in detail for microgrids in both DM and IM. The RM aims to schedule local energies such as ESS and flexible load, based on operational instructions given by previous market sessions. A distributed algorithm is designed to account for privacy concerns and potential communication failures during computing iterations. Case study results validate that the proposed framework can effectively hedge against DER uncertainties within the energy cooperation. The profits of participants can be significantly increased by the proposed hierarchical energy trading framework.

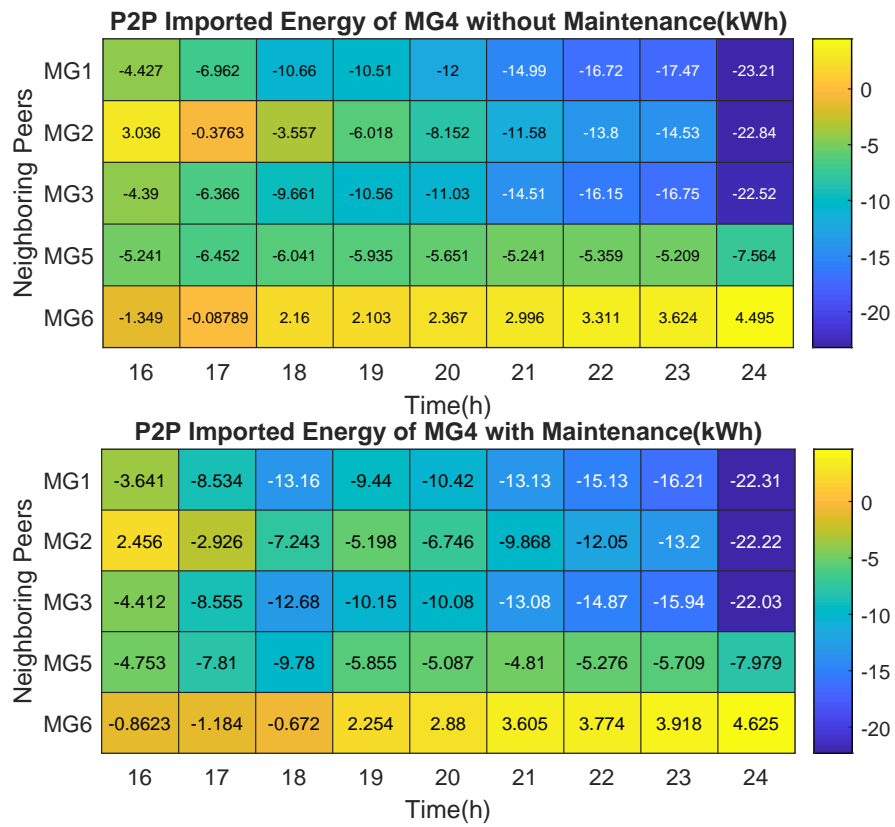


**Figure 4.12:** Comparison of P2P imported energy of MG4 from neighboring peers without and with maintenance plan scheduled at the opening of IM6.

## Chapter 5

# Network Constrained P2P Energy Trading in Unbalanced DNs

### 5.1 Introduction

The distribution system is facing the proliferation of distributed energy resources (DER) such as distribution generations (DGs) and energy storage systems [79]. Market participation of these small-scale flexible assets is envisioned via aggregators [25]. In this regard, the local transaction market becomes a promising paradigm to integrate such DERs in the active distribution network[125].

To maintain the stability of the distribution networks (DN) while making full utilization of renewable energy, the operator has to exploit flexibility locally provided by assets, e.g., elastic load and reactive power resources [126]. Further, in recent years, P2P energy trading has been suggested at the distribution system level as an extension of local transaction markets towards a privacy-preserving framework. Such mechanism designs are typically user-centric to enhance the

preference of agents, such as user comfort and financial privacy. Several research attempts have been made in designing peer-to-peer trading frameworks.

As reviewed in Chapter 1, P2P energy trading has become a trending paradigm for the energy transaction in power grids with high penetration of DERs. However, as mentioned before, there are still some practical challenges for the real-world implementation of P2P transactive market in existing power systems. The previous chapters have already well addressed some concerns with respect to e.g., hierarchical P2P market framework, bilateral pricing scheme and energy transmission losses. In this chapter, the challenge considered for P2P energy trading is the network constraint: local energy trading would pose challenges to the upper layer network, especially with the rapid penetration of DERs. Due to the unforeseen renewable generation and load demand, the market programs of players may be infeasible for the DN. Most existing works neglect the voltage violation issues when modeling the energy trading market [127]. Though the voltage regulation service target is previously regarded as another reactive power (VAR) control problem to be resolved sequentially, a low-voltage distribution system indeed features a relatively high R/X ratio as compared to the transmission networks. In this context, both active and reactive power shall be coordinated to provide voltage control in DNs [128]. Demand response (DR) is also regarded as a promising method for increasing the renewable energy penetration, and peer-to-peer business model based on the market mechanism for shared energy storage units is proposed in [129]. Decentralized algorithms are proposed in [75] for microgrid energy trading which maximizes the welfare considering the network voltage management through local information exchange among neighbors. Authors in [130] formulate the physical network power flow loss as the network usage fee and then allocate the total network utilization fee to the energy trading peers. While

these works primarily point out the importance of integrating voltage control issues into the energy trading mechanisms, most of them are mainly designed for three-phase balanced networks. As a matter of fact, the unbalance condition of a distribution system is common in practice: the common assumption of three-phase balanced DN is rather unrealistic in practice, due to e.g. unbalanced loads and untransposed distribution lines [131]. Therefore, it is necessary to design a market framework to address the aforementioned crucial yet cross-coupled issues in unbalanced DNs.

In this regard, this chapter is aimed to achieve both economic and secure operations for P2P energy trading. The contributions of this chapter are summarized as below:

- Considering that P2P trading may worsen the power flow and voltage violation issues, we integrate the three-phase optimal power flow of unbalanced DNs in the energy market model. The market-clearing results respect the network constraints and therefore reflect the realistic operation condition.
- A flexible P2P energy trading market framework is proposed in the unbalanced distribution network. Both the sellers and buyers are flexible in the P2P market, which is realistic in real-world transactions. Simulations on modified 37-bus cases verify that the proposed co-operative optimization can provide economic results and better voltage profiles.

The following table generally compares the chapter with recent works in the literature.

The remaining part of this chapter is organized as follows: Section 5.2 presents the three-phase unbalanced power flow model; Section 5.3 formulates

	P2P	Vol control	DR	VAR	Unbalanced DN
P2P Trading	✓	×	×	×	×
Voltage regulation	×	✓	×	✓	×
Network-trading	✓	✓	×	×	×
This work	✓	✓	✓	✓	✓

the co-operative optimization problem; Section 5.4 gives the simulation results on a modified distribution system and Section 5.5 summarizes the chapter.

## 5.2 Multi-phase Distribution Network Model

The underlying radial three-phase grid with  $N+1$  buses can be represented by the graph  $\mathcal{G} = (\{0\} \cup \mathcal{N}, \mathcal{E})$ , of which nodes  $\mathcal{N} = \{1, 2, \dots, N\}$  correspond to buses and edges  $\mathcal{E}$  correspond to the distribution lines with cardinality  $|\mathcal{E}| = N$ . The substation bus is specially indexed as  $i = 0$ . Every bus  $i \in \mathcal{N}$  is connected to a unique parent bus  $\pi_i$ , and owns a set of child buses  $\mathcal{C}_i$ . Without loss of generality, the nodes can be numbered such that  $\pi_i < i$  for all  $i \in \mathcal{N}$ . The line pointing from  $\pi_i$  to bus  $i$  is labeled as line  $i$ . The branch-bus incidence matrix  $\mathbf{A}^0 \in \mathbb{R}^{N \times (N+1)}$  denotes the line-bus mapping relationships. Hence, we have  $A_{ij}^0 = 1$  if  $j = \pi_i$ ,  $A_{ij}^0 = -1$  if  $j = i$ , and  $A_{ij}^0 = 0$  otherwise. That is,

$$A_{ij}^0 = \begin{cases} 1, & \text{if } j = \pi_i, \\ -1, & \text{if } j = i, \\ 0 & \text{otherwise} \end{cases}$$

Divide  $\mathbf{A}^0$  into two parts:  $\mathbf{A}^0 = [\mathbf{a}_0 \ \mathbf{A}]$  where  $\mathbf{A}$  is reduced branch-bus incidence matrix. For every bus  $i \in \mathcal{N}$ , let complex vector  $\mathbf{V}_i := [V_i^a \ V_i^b \ V_i^c]^T$  denote the three-phase voltage of bus  $i$ ; similarly, let complex vectors  $\mathbf{I}_i := [I_i^a \ I_i^b \ I_i^c]^T$

and  $\mathbf{S}_i := [S_i^a S_i^b S_i^c]^T \in \mathbb{C}^3$  denote the line current and power flow on line  $i$ , respectively. Phases are coupled with each other through the multivariate version of Ohm's law [131]:

$$\mathbf{V}_i = \mathbf{V}_{\pi_i} - \mathbf{z}_i \mathbf{I}_i \quad (5.1)$$

where the symmetric matrix  $\mathbf{z}_i := \mathbf{r}_i + j\mathbf{x}_i \in \mathbb{C}^3$  denotes the impedance matrix of line  $i$ . To obtain the voltage drop, (5.1) is multiplied by its complex conjugate (\*) of on both sides:

$$\mathbf{v}_i = \mathbf{v}_{\pi_i} - 2\text{Re}[\mathbf{V}_{\pi_i} \odot (\mathbf{z}_i^* \mathbf{I}_i^*)] + (\mathbf{z}_i \mathbf{I}_i) \odot (\mathbf{z}_i^* \mathbf{I}_i^*) \quad (5.2)$$

where  $\mathbf{v}_i = [v_i^a v_i^b v_i^c]^T = \mathbf{V}_i \odot \mathbf{V}_i^* \in \mathbb{R}^3$  denotes the squared voltage magnitudes at bus  $i$ ,  $\odot$  is the element-wise product operator,  $\text{Re}[\cdot]$  takes the real part of a complex matrix. The multiphase power flow balance at bus  $i$  is given by [131]:

$$-\mathbf{s}_i = \mathbf{S}_i - \sum_{j \in \mathcal{C}_i} \mathbf{S}_j - (\mathbf{z}_i \mathbf{I}_i) \odot \mathbf{I}_i^* \quad (5.3)$$

where  $\mathbf{s}_i = \mathbf{p}_i + j\mathbf{q}_i \in \mathbb{C}^3$  is the power injection at bus  $i$ . Note that  $\mathbf{z}_i$ 's have relatively small entries, the last term in the right-hand side of (5.2) and (5.3) thus can be dropped. Regarding the second term in the right-hand side of (5.2), it is further assumed that phase voltages are approximately balanced by surrogating  $\mathbf{V}_i = \tilde{V}_i \boldsymbol{\alpha}$ , where  $\tilde{V}_i$  denote the voltage magnitude  $\boldsymbol{\alpha} = [1, \alpha, \alpha^2]^T$  and  $\alpha = e^{-j2\pi/3}$ . Thus, the conjugate complex of line current  $\mathbf{I}_i^*$  can be roughly expressed by

$$\mathbf{I}_i^* \approx \frac{1}{\tilde{V}_{\pi_i}} \mathbf{S}_i \odot \boldsymbol{\alpha}^* \quad (5.4)$$

and then the term  $\mathbf{V}_{\pi_i} \odot (\mathbf{z}_i^* \mathbf{I}_i^*)$  can be simplified as:

$$\begin{aligned} \mathbf{V}_{\pi_i} \odot (\mathbf{z}_i^* \mathbf{I}_i^*) &= \boldsymbol{\alpha} \odot [\mathbf{z}_i^* (\mathbf{S}_i \odot \boldsymbol{\alpha}^*)] \\ &= \text{diag}(\boldsymbol{\alpha}) \mathbf{z}_i^* \text{diag}(\boldsymbol{\alpha}^*) \mathbf{S}_i \\ &= \tilde{\mathbf{z}}_i^* \mathbf{S}_i \end{aligned} \quad (5.5)$$

where  $\tilde{\mathbf{z}}_i := \text{diag}(\boldsymbol{\alpha}^*) \mathbf{z}_i \text{diag}(\boldsymbol{\alpha})$ . The first equality follows by plugging in (5.4) and  $\mathbf{V}_{\pi_i} = \tilde{\mathbf{V}}_{\pi_i} \boldsymbol{\alpha}$ ; the second equality follows from the property:  $\mathbf{x} \odot \mathbf{y} = \text{diag}(\mathbf{x}) \mathbf{y} = \text{diag}(\mathbf{y}) \mathbf{x}$ . Hence, the approximate linearized multi-phase distFlow model reads for all  $i \in \mathcal{N}$  [132]:

$$\mathbf{v}_{\pi_i} - \mathbf{v}_i = 2\text{Re}(\tilde{\mathbf{z}}_i^* \mathbf{S}_i) \quad (5.6)$$

$$\mathbf{S}_i - \sum_{j \in \mathcal{C}_i} \mathbf{S}_j = -\mathbf{s}_i \quad (5.7)$$

For notational brevity, collect all nodal variables related to non-substation buses in vectors:  $\mathbf{v} := [\mathbf{v}_1^T \cdots \mathbf{v}_N^T]^T \in \mathbb{R}^{3N}$ ,  $\mathbf{s} := [\mathbf{s}_1^T \cdots \mathbf{s}_N^T]^T \in \mathbb{C}^{3N}$ . Similar for lines, one can denote  $\mathbf{S} := [\mathbf{S}_1^T \cdots \mathbf{S}_N^T]^T \in \mathbb{C}^{3N}$ . In this context, (5.6) and (5.7) can be rewritten in a compact form as:

$$(\mathbf{A} \otimes \mathbf{I}_3) \mathbf{v} = 2\text{Re}[\text{bdiag}(\tilde{\mathbf{z}}_i^*) \mathbf{S}] - v_0 \cdot (\mathbf{a}_0 \otimes \mathbf{1}_3) \quad (5.8a)$$

$$(\mathbf{A}^T \otimes \mathbf{I}_3) \mathbf{S} = \mathbf{s} \quad (5.8b)$$

where  $\text{bdiag}(\cdot)$  constructs the block-wise diagonal matrix using a set of square matrices,  $\mathbf{I}_3$  is the 3-dimensional identity matrix,  $v_0$  is the squared voltage magnitude of bus 0 and  $\otimes$  denotes the Kronecker product. Plugging (5.8b) into (5.8a), and eliminating the line power  $\mathbf{S}$ , the voltage magnitudes in multi-phase

distribution networks are related to nodal power injections as:

$$\mathbf{v} = \mathbf{R}\mathbf{p} + \mathbf{X}\mathbf{q} + v_0\mathbf{1}_{3N} \quad (5.9)$$

where the involved matrices are defined as  $\mathbf{R} := 2\mathbf{M}^T \text{bdiag}([\text{Re}(\tilde{\mathbf{z}}_i)])\mathbf{M}$ ,  $\mathbf{X} := 2\mathbf{M}^T \text{bdiag}([\text{Im}(\tilde{\mathbf{z}}_i)])\mathbf{M}$  and  $\mathbf{M} := \mathbf{A}^{-T} \otimes \mathbf{I}_3$ .

## 5.3 Co-operative Optimization Problem Formulation

In this section, the abstract function for the co-operative optimization problem is given first, and then the two detailed operation problems including constraints are presented.

### 5.3.1 Objective Function

In the active distribution network, each bus is represented by an agent on behalf of local aggregated demand and generations, including buyers  $\mathcal{N}_b$  and sellers  $\mathcal{N}_s$  in the P2P market. In addition, the active distribution network are assumed to install photovoltaic (PV) inverters  $\mathcal{N}_v$  for the free-of-charge provision of energy generation.

$$\min_{\mathbf{x}, \mathbf{y}} F_1(\mathbf{x}) + \beta F_2(\mathbf{y}; \xi) \quad (5.10)$$

where the forecast uncertainties are considered and let  $\xi := \{\mathbf{p}_g, \mathbf{p}_d, \mathbf{q}_d\}$  denote a realization of uncertain variables. The decision variables include the P2P buying/selling power of prosumers in the P2P market  $\mathbf{x} := \{\mathbf{e}_{mn}, \mathbf{p}_m, \mathbf{p}_n\}_{m \in \mathcal{N}_b, n \in \mathcal{N}_s}$  and the reactive power output of PV inverters and the nodal voltage  $\mathbf{y} := \{\mathbf{v}_i, \mathbf{q}_i\}_{i \in \mathcal{N}}$ .  $\beta$  is the weighting parameter between the P2P market cost and

voltage regulation cost. In general, its value can be determined either by the system or by the agents.

### 5.3.2 Prosumer Cost in P2P Market

For buyers  $m \in \mathcal{N}_b$  in the P2P market, the utility function represents the satisfaction for electricity usage, and is expressed as a function of energy demand  $C_m(\mathbf{p}_m)$ . For sellers  $n \in \mathcal{N}_s$ , the cost function represents the fuel consumption for energy generation, and is represented as a function of energy generation  $U_n(\mathbf{p}_n)$ . Let  $F_1$  denotes the social cost in the P2P energy trading market:

$$F_1 = \sum_{m \in \mathcal{N}_b} C_m(\mathbf{p}_m) - \sum_{n \in \mathcal{N}_s} U_n(\mathbf{p}_n) \quad (5.11)$$

where we consider a quadratic utility function for sellers and a quadratic cost function for buyers[75]:

$$C_m(\mathbf{p}_m) = \frac{1}{2} \mathbf{p}_m^T \mathbf{A}_m \mathbf{p}_m + \mathbf{b}_m^T \mathbf{p}_m \quad (5.12)$$

$$U_n(\mathbf{p}_n) = -\frac{1}{2} \mathbf{p}_n^T \mathbf{A}_n \mathbf{p}_n + \mathbf{b}_n^T \mathbf{p}_n \quad (5.13)$$

The cost function parameters  $\mathbf{A}_m \in \mathbb{R}^{3 \times 3}$ ,  $\mathbf{b}_m \in \mathbb{R}^3$  are private information for buyer  $m$ , and the utility function parameters  $\mathbf{A}_n \in \mathbb{R}^{3 \times 3}$ ,  $\mathbf{b}_n \in \mathbb{R}^3$  are the private information of seller  $n$ . Let  $\mathbf{e}_{mn} = [e_{mn}^a \ e_{mn}^b \ e_{mn}^c]^T \in \mathbb{R}^3$  denote the active power trading results between buyers  $m \in \mathcal{N}_b$  and sellers  $n \in \mathcal{N}_s$ . Hence, the P2P trading between prosumers can be characterized by:

$$\sum_{n \in \mathcal{N}_s} \mathbf{e}_{mn} = \mathbf{p}_m \quad (5.14)$$

$$\sum_{m \in \mathcal{N}_b} \mathbf{e}_{mn} = \mathbf{p}_n \quad (5.15)$$

where (5.14) represents the P2P trading for buyers whereas (5.15) represents the trading condition for sellers. Considering the flexible operation of prosumers, as well as the power line capacity, the operation constraints for P2P trading peers are:

$$\underline{\mathbf{p}}_m \leq \mathbf{p}_m \leq \bar{\mathbf{p}}_m, \underline{\mathbf{p}}_n \leq \mathbf{p}_n \leq \bar{\mathbf{p}}_n \quad (5.16)$$

$$\mathbf{0} \leq \mathbf{e}_{mn} \leq \bar{\mathbf{e}}_{mn} \quad (5.17)$$

It is noticed that (5.17) is a general constraint to represent the power capacity of cable/line between any two peers.

### 5.3.3 Voltage Regulation Cost

In renewable-embedded active distribution networks, PV inverters can provide voltage control service via adjusting reactive power output. In this context, the voltage control cost includes the reactive power provision cost and demand response cost:

$$F_2 = \sum_{g \in \mathcal{N}_v} \|\mathbf{q}_g\|_2^2 + \sum_{i \in \mathcal{N}} (\|\mathbf{v}_i - \boldsymbol{\mu}\|_2^2 + \|\Theta\|_2^2 + \|\Delta\|_2^2) + \sum_{d \in \mathcal{N}_d} \|\bar{\mathbf{p}}_d - \mathbf{p}_d\|_2^2 \quad (5.18)$$

where  $\boldsymbol{\mu}$  is the desired admiring voltage profile, and  $\|\cdot\|_2$  is the Euclidean norm operator. A popular choice is the flat voltage profile  $\boldsymbol{\mu} = \mathbf{1}$  (i.e.,  $v_i^\phi = 1, \forall i \in \mathcal{N}, \forall \phi = \{a, b, c\}$ ) which can also be adjusted in practical cases to meet particular operational conditions. During the flexible operation of PV inverters, the active power outputs are at maximum power points to fully harvest the solar energy.

The reactive power output of PV inverter on phase  $\phi$  of bus  $g$  is constrained by:

$$-\sqrt{(S_g^\phi)^2 - (p_g^\phi)^2} \leq q_g^\phi \leq \sqrt{(S_g^\phi)^2 - (p_g^\phi)^2} \quad (5.19)$$

where  $S_g^\phi$  and  $p_g^\phi$  are the rated apparent power of PV inverter and instantaneous maximum active power available. As such, the available reactive power of PV inverters are:

$$-\bar{\mathbf{q}}_g \leq \mathbf{q}_g \leq \bar{\mathbf{q}}_g \quad (5.20)$$

In addition, the admissible ranges of nodal voltage at all buses are:

$$\underline{\mathbf{v}} - \Theta \leq \mathbf{v} \leq \bar{\mathbf{v}} + \Theta \quad (5.21)$$

where  $[\underline{\mathbf{v}}, \bar{\mathbf{v}}]$  denotes the bound constraint for squared voltage magnitude,  $\Theta$  and  $\Delta$  denote the voltage violation if there are not adequate voltage regulation resources.

All load demand are assumed to be flexible and the demand response is considered in this chapter:

$$\underline{\mathbf{p}}_d \leq \mathbf{p}_d \leq \bar{\mathbf{p}}_d \quad (5.22)$$

Combining nodal power injections from all kinds of agents at buses(i.e., flexible load demand, PV inverters, buyers and sellers), the active and reactive power injections of the distribution network are summarized as:

$$\mathbf{p} = \sum_{g \in \mathcal{N}_v} \mathbf{H}_g \mathbf{p}_g - \sum_{d \in \mathcal{N}_d} \mathbf{H}_d \mathbf{p}_d - \sum_{m \in \mathcal{N}_b} \mathbf{H}_m \mathbf{p}_m + \sum_{n \in \mathcal{N}_s} \mathbf{H}_n \mathbf{p}_n \quad (5.23a)$$

$$\mathbf{q} = \sum_{g \in \mathcal{N}_v} \mathbf{H}_g \mathbf{q}_g - \sum_{d \in \mathcal{N}_d} \mathbf{H}_d \mathbf{q}_d \quad (5.23b)$$

where  $\mathbf{H}_g, \mathbf{H}_d, \mathbf{H}_m, \mathbf{H}_n$  stand for the topology location for PV inverters, flexible

load demand, buyers and sellers, respectively. Note that, the constant load demand can be regarded as negative renewable generation with fixed output, while the nodes without load demand installation can be regarded as zero renewable output with  $\mathbf{p}_g = \mathbf{0}$  and  $\bar{\mathbf{q}}_g = \mathbf{0}$  as well. Hence, the load demand nodes  $\mathcal{N}_d$  and renewable energy nodes  $\mathcal{N}_v$  (e.g., PV inverters) are not explicitly distinguished in the model for simplicity. That is, it is assumed that  $\mathcal{N}_g = \mathcal{N}$  in the rest of the chapter.

It is worth noting that this study aims to jointly optimize the P2P energy trading, flexibility management and voltage control in a holistic manner, which is a novel while useful research attempt in this field. To better highlight the proposed framework, Fig. 5.1 compares traditional sequential methods<sup>1</sup> and the proposed market framework.

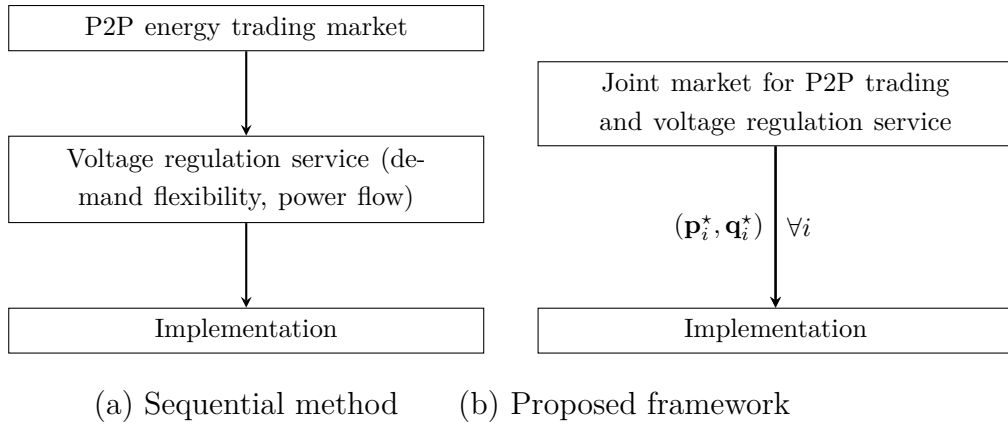


**Figure 5.1:** Comparison of sequential methods and the proposed framework.

<sup>1</sup>Sequential method means that the P2P trading market is cleared firstly within P2P sellers and buyers, while the voltage control is solved subsequently by the system operator.

## 5.4 Case Study

### 5.4.1 Simulation Setup

In this section, an illustrative case study is conducted to validate the proposed model. Fig. 5.2 illustrates the modified three-phase IEEE 37-bus distribution system. It is assumed that five nodes are installed with PV inverters of 100kWh capacity, three nodal agents are P2P buyers and three nodal agents are sellers. The coefficients of P2P peers are taken from [75]. The remaining nodes are loads agents. The objective functions are weighted by proper coefficients to a comparative level. We have multiple costs in consideration, for instance:

- 1) the P2P trading cost  $\sum_{m \in \mathcal{N}_b} C_m(\mathbf{p}_m) - \sum_{n \in \mathcal{N}_s} U_n(\mathbf{p}_n)$ ;
- 2) reactive power provision cost  $\sum_{g \in \mathcal{N}_v} \|\mathbf{q}_g\|_2^2$ ;
- 3) voltage regulation cost  $\sum_{i \in \mathcal{N}} \|\mathbf{v}_i - \boldsymbol{\mu}\|_2^2$ ;
- 4) voltage violation penalty  $\sum_{i \in \mathcal{N}} (\|\Theta\|_2^2 + \|\Delta\|_2^2)$  and 5) demand response cost  $\|\bar{\mathbf{p}}_d - \mathbf{p}_d\|_2^2$ .

Each of the cost functions deploys a weighting parameter to match with each other. So, we have five weighting parameters, which are set as 100, 2000, 10,  $10^9$ ,  $10^5$  in the simulation. It is noticed that this choice is based on experimental experience.

To elaborate the real operation condition, all the load agents and P2P agents are assumed to be flexible in managing local demand range in  $[p, \bar{p}]$  where  $\underline{p} = 0.8\bar{p}$ : the three-phase power load  $\bar{p}$  is list in Table 5.1. The power capacity of peer label/line is set as 100 kW. Among the P2P prosumers and load demands, the agents have the fixed power factor. The PV active power output forecast

is 80kW. The base voltage is 4.8kV with acceptable voltage range  $[0.95, 1.05]$ , and the voltage magnitude are expressed in per-unit value. The seller capacity is 100kW in all phases for node 3, 19, 25 and the three-phase buyer capacity is  $[126; 85; 140]$ ,  $[126; 85; 85]$ ,  $[85; 85; 85]$ kW for node 10, 28, 34 respectively.

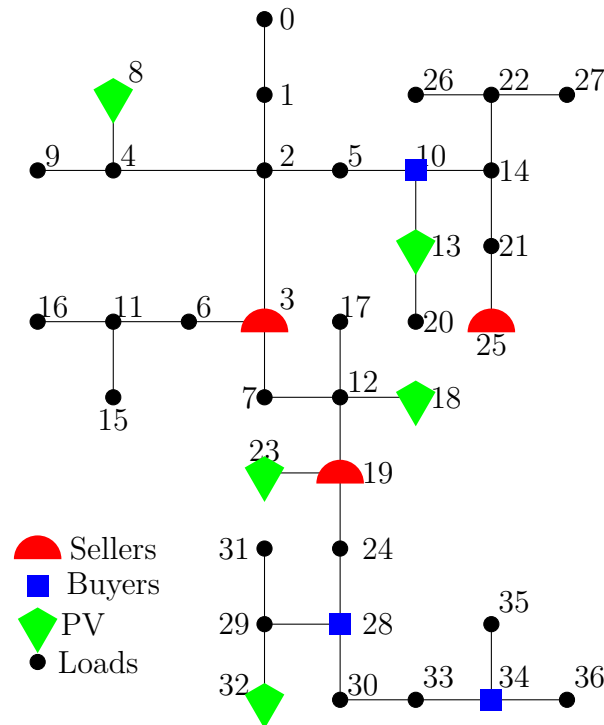


Figure 5.2: Modified IEEE 37-bus distribution system.

## 5.4.2 Results and Discussion

**Three-phase voltage profile** The voltage profile result generated from the proposed model is plotted in Fig. 5.3. It is seen that after deploying the proposed joint optimization problem, the three-phase voltage profile comes into the acceptable range  $[0.95, 1.05]$ . It is also observed that nodes with larger indices have lower voltage magnitudes, which indicates that these nodes play a crucial role in improving the voltage profile.

**Table 5.1:** Active(kW) and Reactive Power(kVar) of Load Agents

No.	Phase A		Phase B		Phase C		No.	Phase A		Phase B		Phase C	
	P	Q	P	Q	P	Q		P	Q	P	Q	P	Q
1	168	84	168	84	420	210	2	151.2	74.4	50.4	25.2	168	84
4	168	84	102	48	102	48	5	102	48	168	84	168	84
6	168	84	102	48	168	84	7	102	48	168	84	25.2	12
9	50.4	25.2	168	84	151.2	74.4	11	102	48	168	84	151.2	74.4
12	102	48	50.4	25.2	151.2	74.4	14	151.2	74.4	102	48	168	84
15	50.4	25.2	102	48	168	84	16	102	48	168	84	168	84
17	151.2	74.4	102	48	151.2	74.4	20	168	84	50.4	25.2	151.2	74.4
21	151.2	74.4	168	84	50.4	25.2	22	50.4	25.2	168	84	102	48
24	50.4	25.2	102	48	151.2	74.4	26	102	48	102	48	168	84
27	151.2	74.4	168	84	151.2	74.4	29	50.4	25.2	151.2	74.4	151.2	74.4
30	102	48	50.4	25.2	102	48	31	102	48	168	84	50.4	25.2
33	102	48	168	84	102	48	35	168	84	151.2	74.4	50.4	25.2
36	102	48	102	48	50.4	25.2							

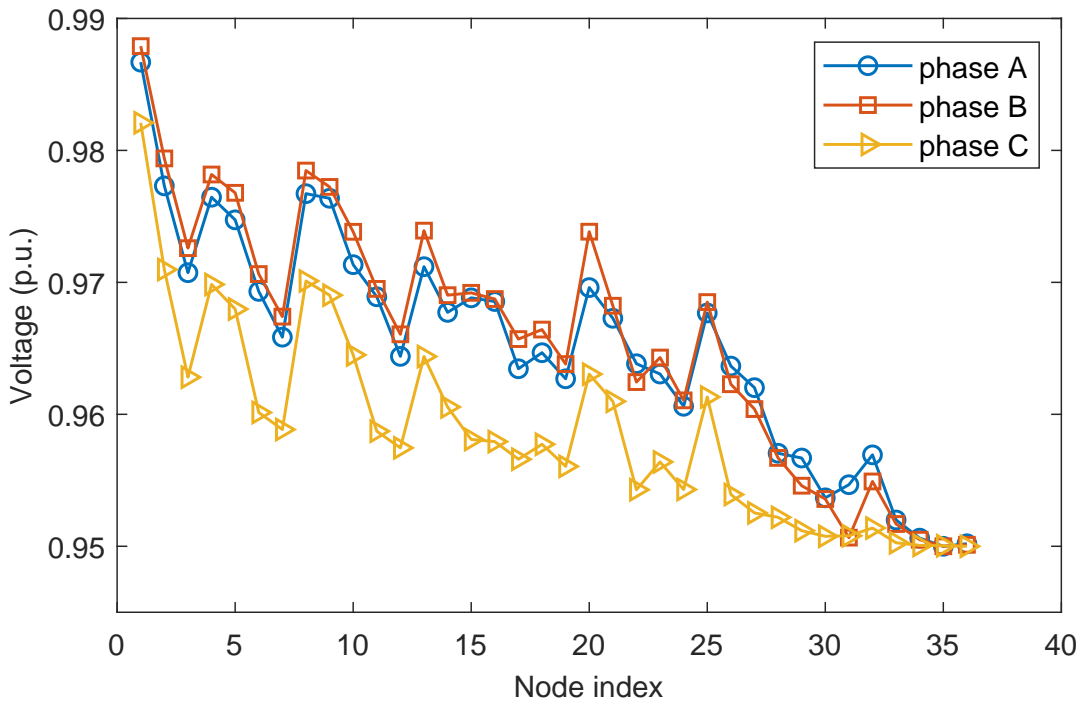
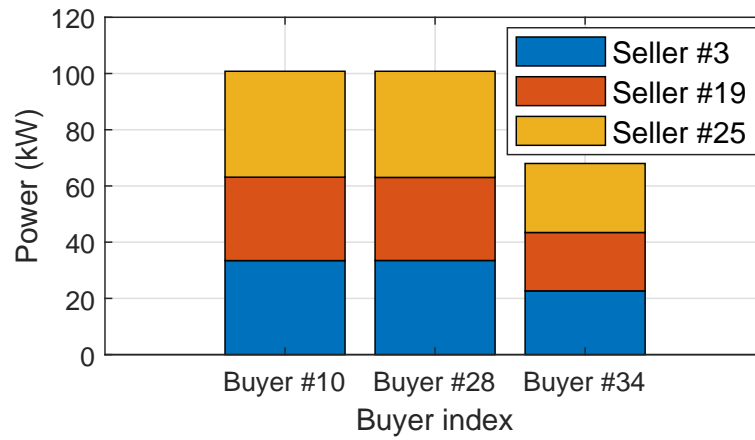


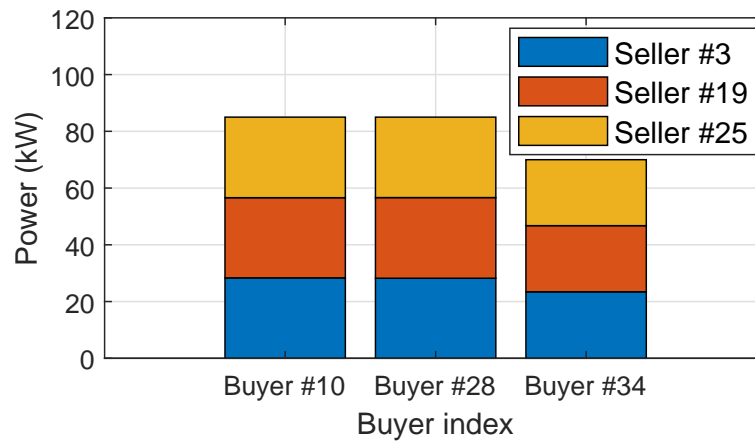
**Figure 5.3:** Three-phase bus voltage profile after the proposed model.

**P2P active power trading** The proactive three-phase P2P energy trading profiles are shown in Fig. 5.4. It is noted that all the buyers are sellers can flexibly adjust their trading quantity from 0.8 to 1 of the rated power. In this

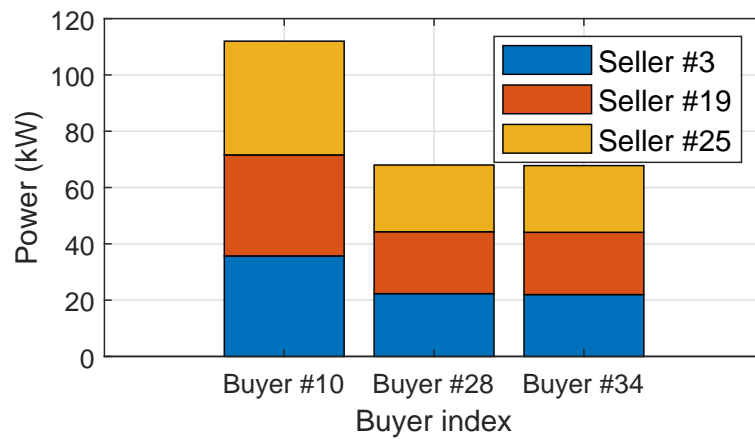
regard, they are entitled to trade their three-phase energy in the joint market.



(a) Phase A



(b) Phase B



(c) Phase C

**Figure 5.4:** Three-phase P2P energy trading profiles after proposed co-operative optimization.

**Comparison with sequential methods** The voltage magnitudes for different methods are plotted in Fig. 5.5, where the proposed distributed model outperforms sequential method which conducted voltage control (VC) after P2P solutions. Specially, the P2P solution is observed to result in voltage violation issues. Subsequently, the system deploy demand response and reactive power to tackle this voltage issue. In contrast, the proposed joint model coordinates the P2P trading and potential issues together, and generates the solution. Even though the final instructions in two cases may be similar, the joint model searches optimal solution at a higher level.

Table 5.2 further compares the individual cost components, which reveals a total cost reduction of the proposed joint model from \$175.00 to \$160.74. Note that the costs in the table include 1) P2P: P2P prosumers, 2) Load: load demand response cost, 3) VAR: reactive power provision cost, 4) Voltage: voltage regulation cost and voltage violation penalty. This observation could be tentatively explained by the optimal trade-off between the P2P market cost and voltage control cost. The Co-operative optimization can simultaneously achieve the P2P trading profile respecting network constraints. Both the load demands and prosumers are flexible, while their price for offering flexibility are diverse. In this context, the joint optimization can provide a preferable solution from the global perspective.

**Table 5.2:** Cost Comparison Between Different Models (\$)

Model	P2P	Load	VAR	Voltage	Total
Sequential method	45.25	27.15	43.46	59.14	175.00
Proposed framework	58.40	11.32	31.34	59.67	160.74

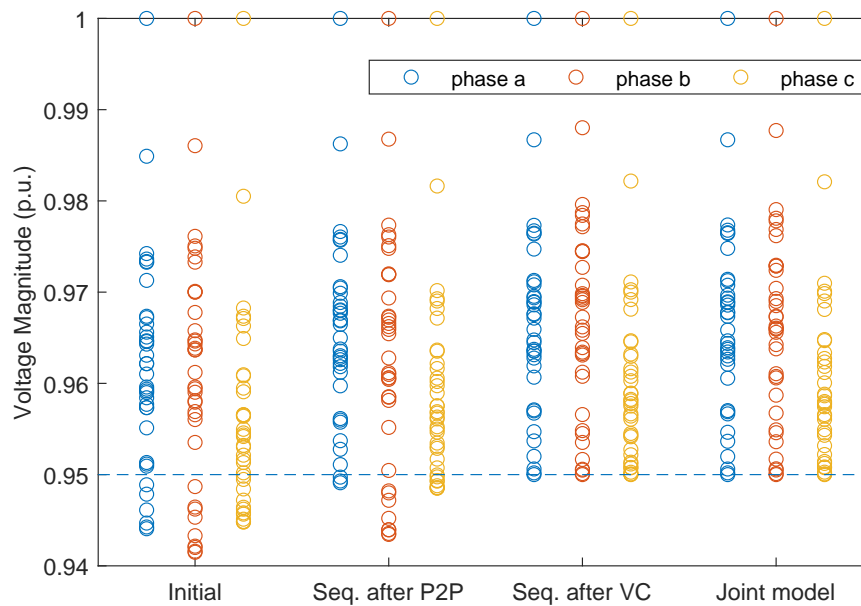


**Figure 5.5:** Three-phase bus voltage magnitude comparison: initial case (Initial), sequential model (Seq.) and proposed joint model.

## 5.5 Summary for the Chapter

Considering the distribution system operation constraints, a two-stage network-constrained P2P transaction framework is proposed in this chapter. In the first stage, distribution network power flow is incorporated with P2P transactions which can preliminarily determine the energy trading quantity based on forecasting information. In the second stage, the network operation constraints are respected by fully utilizing local flexible resources. A co-operative optimization model is formulated to solve the two-stage operation problem. Simulations on modified 37-bus cases verify that the proposed co-operative optimization framework can well address the implementation concerns of P2P energy transactions at the distribution network level. In addition, the social welfare can be greatly improved for the system operator since the P2P energy transaction and local flexibility resources are co-optimized.

## Chapter 6

# Conclusion and Future Work

### 6.1 Conclusion

The trending adoption of microgrids as the paradigm may bring about many economic and environmental benefits. However, it also poses challenges to the power system operation and energy management due to the uncertainty and intermittency of DERs. In view of this, economic operation and transactive energy management strategies are proposed for a single microgrid and multiple microgrids in smart grids. Several important technical and economic issues are carefully addressed: (i) the DER uncertainty in the multi-period microgrid operation optimization and (ii) P2P energy sharing framework for microgrids in the deregulated market.

The main conclusions of the thesis are summarized as below:

1. A short-term economic operation framework is proposed for microgrids with BESSs and uncertain renewable productions. A novel real-time degradation model is specially developed for lithium-ion BESSs to resemble the battery material degradation as much as possible. In addition, considering the short-term forecasting errors of renewable output, the microgrid operation

optimization is formulated into a weighted MPC framework. Case study validates that the proposed framework can significantly improve the computing efficiency in solving the uncertainty-embedded economic operation problem.

2. A comprehensive P2P energy sharing framework is proposed for smart microgrid energy cooperative management based on the social welfare maximization problem. The P2P trading quantity and price are both negotiated between trading peers in a bilateral and private-preserving manner. The optimization problem is solved by a fully decentralized algorithm based on a modified ADMM, where the dual and primal variables are both updated in a decentralized manner. The case study validates that the proposed P2P energy sharing framework can significantly improve the total welfare of participant microgrids by the cooperative management of distributed energy resources.
3. An effective hierarchical P2P transactive market framework is proposed in line with the existing market timescales. Considering the possible forecasting errors in renewable energy outputs, distributed MPC-based market operation problems are formulated in detail for microgrids in different stages of the electricity market. A distributed algorithm is designed to account for privacy concerns and potential communication failures during computing iterations. Case study results validate that the proposed framework can effectively hedge against DER uncertainties within the energy cooperation. The profits of participants can be significantly increased by the proposed hierarchical energy trading framework.
4. A holistic co-optimization framework is proposed to address the two-stage

network-constrained P2P transaction problem considering the distribution system operation constraints. In the first stage, distribution network power flow is incorporated with P2P transactions which can preliminarily determine the energy trading quantity based on forecasting information. In the second stage, the network operation constraints are respected by fully utilizing local flexible resources. Simulations on modified 37-bus cases verify that the proposed co-operative optimization framework can well address the implementation concerns of P2P energy transactions at the distribution network level. In addition, the social welfare can be greatly improved for the system operator since the P2P energy transaction and local flexibility resources are co-optimized.

## 6.2 Directions for Future Work

In this thesis, economic operation and transactive management strategies are proposed for smart microgrids with DERs in the active distribution networks. Following the thesis purpose in Chapter 1, the objectives of the thesis have been achieved. Based on a number of achievements made in this research, several directions for further research are suggested as below:

1. Based on the segmental battery degradation model in Chapter 2, the linear optimization model for the microgrid is established. One of the future attentions will therefore be paid to studying how to improve the accuracy of the degradation cost model of lithium-ion battery energy storage systems, as well as other modern batteries, so that it is able to capture more types of microgrids. This is of vital importance for future power system planning, operation and control.

2. Although this thesis includes the P2P trading loss, embodied in the trading energy equality in Chapter 3 and Chapter 4, the network-distance fee and its allocation are not taken into consideration in order to reduce the complexity of the model. However, this is an essential problem for the implementation of P2P energy transaction. As trading costs and profits are still the major concern affecting peers' decision-making, a reasonable formulation of distance-based network cost and allocation strategy will incentivize more participants into the transactive market. It is of vital importance for the extension of the transactive market with large number of proactive microgrids.
3. Although Chapter 5 considers voltage variations and demand response in the local market, the local P2P trading voltage will definitely incur unbalance problems across different phases in practice. The across-phase unbalance should be maintained within a specific level; otherwise, it may damage electric devices, e.g. transformers and motors. In addition, since DER uncertainty can provide flexibility resources for the network operation, incorporating the energy market and flexibility market will deploy the potential of DERs and thus increase the market efficiency. It is of importance for market operator to take DER effects into consideration as much as possible.

# Bibliography

- [1] GEC IRENA. “Renewable capacity statistics 2021”. In: *International renewable energy agency* (2021).
- [2] Mudathir Funsho Akorede, Hashim Hizam, and Edris Pouresmaeil. “Distributed energy resources and benefits to the environment”. In: *Renewable and sustainable energy reviews* 14.2 (2010), pp. 724–734.
- [3] Hannah E Murdock, Duncan Gibb, Thomas Andre, Janet L Sawin, Adam Brown, Lea Ranalder, Ute Collier, Christopher Dent, Baerbel Epp, Chetna Hareesh Kumar, et al. *Renewables 2021-Global status report*. REN21 Renewables Now, 2021.
- [4] Solar Energy Industries Association. “Solar Market Insight Report 2021 Q4”. In: *SEIA. org* (2021).
- [5] Yu Wang, Jijiang He, and Wenying Chen. “Distributed solar photovoltaic development potential and a roadmap at the city level in China”. In: *Renewable and Sustainable Energy Reviews* 141 (2021), p. 110772.
- [6] Jiayong Li. “Active management of distribution systems with distributed energy resources”. In: *Hong Kong Polytechnic University Electronic Theses* (2018).

- 
- [7] Camilo A Cortes, Sergio F Contreras, and Mohammad Shahidehpour. “Microgrid topology planning for enhancing the reliability of active distribution networks”. In: *IEEE Transactions on Smart Grid* 9.6 (2017), pp. 6369–6377.
- [8] Lubna Mariam, Malabika Basu, and Michael F Conlon. “Microgrid: Architecture, policy and future trends”. In: *Renewable and Sustainable Energy Reviews* 64 (2016), pp. 477–489.
- [9] Sheetal Chandak and Pravat K Rout. “The implementation framework of a microgrid: A review”. In: *International Journal of Energy Research* 45.3 (2021), pp. 3523–3547.
- [10] Qiang Fu, Adel Nasiri, Ashishkumar Solanki, Abedalsalam Bani-Ahmed, Luke Weber, and Vijay Bhavaraju. “Microgrids: architectures, controls, protection, and demonstration”. In: *Electric Power Components and Systems* 43.12 (2015), pp. 1453–1465.
- [11] Sheetal Chandak, Pritam Bhowmik, Manohar Mishra, and Pravat Kumar Rout. “Autonomous microgrid operation subsequent to an anti-islanding scheme”. In: *Sustainable cities and society* 39 (2018), pp. 430–448.
- [12] Abir Muhtadi, Dilip Pandit, Nga Nguyen, and Joydeep Mitra. “Distributed energy resources based microgrid: Review of architecture, control, and reliability”. In: *IEEE Transactions on Industry Applications* (2021).
- [13] Salman Hajiaghasi, Ahmad Salemnia, and Mohsen Hamzeh. “Hybrid energy storage system for microgrids applications: A review”. In: *Journal of Energy Storage* 21 (2019), pp. 543–570.
- [14] Adam Hirsch, Yael Parag, and Josep Guerrero. “Microgrids: A review of technologies, key drivers, and outstanding issues”. In: *Renewable and sustainable Energy reviews* 90 (2018), pp. 402–411.

- 
- [15] Riaz Khan, Naimul Islam, Sajal K Das, SM Muyeen, Sumaya I Moyeen, Md Firoz Ali, Zinat Tasneem, Md Robiul Islam, Dip K Saha, Md Faisal R Badal, et al. “Energy Sustainability–Survey on Technology and Control of Microgrid, Smart Grid and Virtual Power Plant”. In: *IEEE Access* 9 (2021), pp. 104663–104694.
- [16] Sergio F Contreras, Camilo A Cortes, and Johanna MA Myrzik. “Optimal microgrid planning for enhancing ancillary service provision”. In: *Journal of Modern Power Systems and Clean Energy* 7.4 (2019), pp. 862–875.
- [17] Rima Kasia Oueid. “Microgrid finance, revenue, and regulation considerations”. In: *The Electricity Journal* 32.5 (2019), pp. 2–9.
- [18] Haifeng Qiu, Wei Gu, Yinliang Xu, Wenwu Yu, Guangsheng Pan, and Pengxiang Liu. “Tri-level mixed-integer optimization for two-stage microgrid dispatch with multi-uncertainties”. In: *IEEE Transactions on Power Systems* 35.5 (2020), pp. 3636–3647.
- [19] Haifeng Qiu, Wei Gu, Xiaochun Xu, Guangsheng Pan, Pengxiang Liu, Zhi Wu, and Lu Wang. “A historical-correlation-driven robust optimization approach for microgrid dispatch”. In: *IEEE Transactions on Smart Grid* 12.2 (2020), pp. 1135–1148.
- [20] John J Grainger. *Power system analysis*. McGraw-Hill, 1999.
- [21] Hao Wang and Jianwei Huang. “Cooperative planning of renewable generations for interconnected microgrids”. In: *IEEE Transactions on Smart Grid* 7.5 (2016), pp. 2486–2496.
- [22] Junior Alexis Villanueva-Rosario, Félix Santos-García, Miguel Euclides Aybar-Mejía, Patricio Mendoza-Araya, and Angel Molina-García. “Coordinated ancillary services, market participation and communication of multi-microgrids: A review”. In: *Applied Energy* 308 (2022), p. 118332.

- 
- [23] Najmeh Bazmohammadi, Ahmadreza Tahsiri, Amjad Anvari-Moghaddam, and Josep M Guerrero. “A hierarchical energy management strategy for interconnected microgrids considering uncertainty”. In: *International Journal of Electrical Power & Energy Systems* 109 (2019), pp. 597–608.
- [24] Hao Wang and Jianwei Huang. “Incentivizing energy trading for interconnected microgrids”. In: *IEEE Transactions on Smart Grid* 9.4 (2016), pp. 2647–2657.
- [25] Wayes Tushar, Tapan Kumar Saha, Chau Yuen, David Smith, and H Vincent Poor. “Peer-to-peer trading in electricity networks: An overview”. In: *IEEE Transactions on Smart Grid* 11.4 (2020), pp. 3185–3200.
- [26] Muhammad Fahad Zia, Elhoussin Elbouchikhi, and Mohamed Benbouzid. “Microgrids energy management systems: A critical review on methods, solutions, and prospects”. In: *Applied energy* 222 (2018), pp. 1033–1055.
- [27] Zhejing Bao, Qin Zhou, Zhihui Yang, Qiang Yang, Lizhong Xu, and Ting Wu. “A multi time-scale and multi energy-type coordinated microgrid scheduling solution—Part I: Model and methodology”. In: *IEEE Transactions on Power Systems* 30.5 (2014), pp. 2257–2266.
- [28] Xiaolong Jin, Jianzhong Wu, Yunfei Mu, Mingshen Wang, Xiandong Xu, and Hongjie Jia. “Hierarchical microgrid energy management in an office building”. In: *Applied Energy* 208 (2017), pp. 480–494.
- [29] Seyed Ali Arefifar, Martin Ordonez, and Yasser Abdel-Rady I Mohamed. “Energy management in multi-microgrid systems—Development and assessment”. In: *IEEE Transactions on Power Systems* 32.2 (2016), pp. 910–922.

- 
- [30] Elizaveta Kuznetsova, Yan-Fu Li, Carlos Ruiz, and Enrico Zio. “An integrated framework of agent-based modelling and robust optimization for microgrid energy management”. In: *Applied Energy* 129 (2014), pp. 70–88.
- [31] Eneko Unamuno and Jon Andoni Barrena. “Hybrid ac/dc microgrids—Part I: Review and classification of topologies”. In: *Renewable and Sustainable Energy Reviews* 52 (2015), pp. 1251–1259.
- [32] Eneko Unamuno and Jon Andoni Barrena. “Hybrid ac/dc microgrids—Part II: Review and classification of control strategies”. In: *Renewable and Sustainable Energy Reviews* 52 (2015), pp. 1123–1134.
- [33] Quanyuan Jiang, Meidong Xue, and Guangchao Geng. “Energy management of microgrid in grid-connected and stand-alone modes”. In: *IEEE transactions on power systems* 28.3 (2013), pp. 3380–3389.
- [34] Saeid Esmaili, Amjad Anvari-Moghaddam, and Shahram Jadid. “Optimal operation scheduling of a microgrid incorporating battery swapping stations”. In: *IEEE Transactions on Power Systems* 34.6 (2019), pp. 5063–5072.
- [35] Dimitrios Papadaskalopoulos, Danny Pudjianto, and Goran Strbac. “Decentralized coordination of microgrids with flexible demand and energy storage”. In: *IEEE Transactions on Sustainable Energy* 5.4 (2014), pp. 1406–1414.
- [36] Zhengmao Li, Yan Xu, Xue Feng, and Qiuwei Wu. “Optimal stochastic deployment of heterogeneous energy storage in a residential multienergy microgrid with demand-side management”. In: *IEEE Transactions on Industrial Informatics* 17.2 (2020), pp. 991–1004.
- [37] Alexander Shapiro, Darinka Dentcheva, and Andrzej Ruszczyński. *Lectures on stochastic programming: modeling and theory*. SIAM, 2021.

- 
- [38] ILR Gomes, Rui Melicio, and VMF Mendes. “A novel microgrid support management system based on stochastic mixed-integer linear programming”. In: *Energy* 223 (2021), p. 120030.
- [39] Zhaohao Ding, Yujie Cao, Liye Xie, Ying Lu, and Peng Wang. “Integrated stochastic energy management for data center microgrid considering waste heat recovery”. In: *IEEE Transactions on Industry Applications* 55.3 (2019), pp. 2198–2207.
- [40] Per Aaslid, Magnus Korpas, Michael Martin Belsnes, and Olav Fosso. “Stochastic Optimization of Microgrid Operation With Renewable Generation and Energy Storages”. In: *IEEE Transactions on Sustainable Energy* (2022), pp. 1–11.
- [41] Dimitris Bertsimas, David B Brown, and Constantine Caramanis. “Theory and applications of robust optimization”. In: *SIAM review* 53.3 (2011), pp. 464–501.
- [42] Aharon Ben-Tal and Arkadi Nemirovski. “Robust convex optimization”. In: *Mathematics of operations research* 23.4 (1998), pp. 769–805.
- [43] Jun Yang and Changqi Su. “Robust optimization of microgrid based on renewable distributed power generation and load demand uncertainty”. In: *Energy* 223 (2021), p. 120043.
- [44] Juan S Giraldo, Jhon A Castrillon, Juan Camilo Lopez, Marcos J Rider, and Carlos A Castro. “Microgrids energy management using robust convex programming”. In: *IEEE Transactions on Smart Grid* 10.4 (2018), pp. 4520–4530.

- 
- [45] Tengpeng Chen, Yuhao Cao, Xinlin Qing, Jingrui Zhang, Yuhao Sun, and Gehan AJ Amaratunga. “Multi-energy microgrid robust energy management with a novel decision-making strategy”. In: *Energy* 239 (2022), p. 121840.
- [46] Mohsen Mohammadi, Faraz Talebpour, Esmaeil Safaee, Noradin Ghadimi, and Oveis Abedinia. “Small-scale building load forecast based on hybrid forecast engine”. In: *Neural Processing Letters* 48.1 (2018), pp. 329–351.
- [47] Yahong Chen, Changhong Deng, Weiwei Yao, Ning Liang, Pei Xia, Peng Cao, Yiwang Dong, Yuan-ao Zhang, Zhichao Liu, Dinglin Li, et al. “Impacts of stochastic forecast errors of renewable energy generation and load demands on microgrid operation”. In: *Renewable Energy* 133 (2019), pp. 442–461.
- [48] Pawel Malysz, Shahin Sirouspour, and Ali Emadi. “An optimal energy storage control strategy for grid-connected microgrids”. In: *IEEE Transactions on Smart Grid* 5.4 (2014), pp. 1785–1796.
- [49] Avijit Das and Zhen Ni. “A novel fitted rolling horizon control approach for real-time policy making in microgrid”. In: *IEEE Transactions on Smart Grid* 11.4 (2020), pp. 3535–3544.
- [50] Bolun Xu, Alexandre Oudalov, Andreas Ulbig, Göran Andersson, and Daniel S Kirschen. “Modeling of lithium-ion battery degradation for cell life assessment”. In: *IEEE Transactions on Smart Grid* 9.2 (2016), pp. 1131–1140.
- [51] Bolun Xu, Jinye Zhao, Tongxin Zheng, Eugene Litvinov, and Daniel S Kirschen. “Factoring the cycle aging cost of batteries participating in electricity markets”. In: *IEEE Transactions on Power Systems* 33.2 (2017), pp. 2248–2259.

- 
- [52] Wenbo Shi, Na Li, Chi-Cheng Chu, and Rajit Gadh. “Real-time energy management in microgrids”. In: *IEEE Transactions on Smart Grid* 8.1 (2015), pp. 228–238.
- [53] Adriana C Luna, Lexuan Meng, Nelson L Diaz, Moises Graells, Juan Carlos Vasquez, and Josep M Guerrero. “Online energy management systems for microgrids: Experimental validation and assessment framework”. In: *IEEE transactions on power electronics* 33.3 (2017), pp. 2201–2215.
- [54] Youwei Jia, Xue Lyu, Peng Xie, Zhao Xu, and Minghua Chen. “A novel retrospect-inspired regime for microgrid real-time energy scheduling with heterogeneous sources”. In: *IEEE Transactions on Smart Grid* 11.6 (2020), pp. 4614–4625.
- [55] Youwei Jia, Xue Lyu, Chun Sing Lai, Zhao Xu, and Minghua Chen. “A retroactive approach to microgrid real-time scheduling in quest of perfect dispatch solution”. In: *Journal of Modern Power Systems and Clean Energy* 7.6 (2019), pp. 1608–1618.
- [56] Eduardo F Camacho and Carlos Bordons Alba. *Model predictive control*. Springer science & business media, 2013.
- [57] Radu Godina, Eduardo MG Rodrigues, Edris Pouresmaeil, and João PS Catalão. “Optimal residential model predictive control energy management performance with PV microgeneration”. In: *Computers & Operations Research* 96 (2018), pp. 143–156.
- [58] Zhuoli Zhao, Juntao Guo, Xi Luo, Chun Sing Lai, Ping Yang, Loi Lei Lai, Peng Li, Josep M Guerrero, and Mohammad Shahidehpour. “Distributed Robust Model Predictive Control-Based Energy Management Strategy for Islanded Multi-Microgrids Considering Uncertainty”. In: *IEEE Transactions on Smart Grid* (2022).

- 
- [59] Frank Allgöwer and Alex Zheng. *Nonlinear model predictive control*. Vol. 26. Birkhäuser, 2012.
- [60] Javier Tobajas, Felix Garcia-Torres, Pedro Roncero-Sánchez, Javier Vázquez, Ladjel Bellatreche, and Emilio Nieto. “Resilience-oriented schedule of microgrids with hybrid energy storage system using model predictive control”. In: *Applied Energy* 306 (2022), p. 118092.
- [61] Hongwen He, Yunlong Wang, Ruoyan Han, Mo Han, Yunfei Bai, and Qingwu Liu. “An improved MPC-based energy management strategy for hybrid vehicles using V2V and V2I communications”. In: *Energy* 225 (2021), p. 120273.
- [62] D Mariano-Hernández, L Hernández-Callejo, A Zorita-Lamadrid, O Duque-Pérez, and F Santos García. “A review of strategies for building energy management system: Model predictive control, demand side management, optimization, and fault detect & diagnosis”. In: *Journal of Building Engineering* 33 (2021), p. 101692.
- [63] Yuxin Wu, Aleksi Mäki, Juha Jokisalo, Risto Kosonen, Simo Kilpeläinen, Sonja Salo, Hong Liu, and Baizhan Li. “Demand response of district heating using model predictive control to prevent the draught risk of cold window in an office building”. In: *Journal of Building Engineering* 33 (2021), p. 101855.
- [64] Jiefeng Hu, Yinghao Shan, Josep M Guerrero, Adrian Ioinovici, Ka Wing Chan, and Jose Rodriguez. “Model predictive control of microgrids—An overview”. In: *Renewable and Sustainable Energy Reviews* 136 (2021), p. 110422.
- [65] Daniela Yassuda Yamashita, Ionel Vechiu, and Jean-Paul Gaubert. “Two-level hierarchical model predictive control with an optimised cost function

- for energy management in building microgrids”. In: *Applied Energy* 285 (2021), p. 116420.
- [66] Hong Wang, Yanjun Huang, Amir Khajepour, and Qiang Song. “Model predictive control-based energy management strategy for a series hybrid electric tracked vehicle”. In: *Applied Energy* 182 (2016), pp. 105–114.
- [67] Ayman Esmat, Martijn de Vos, Yashar Ghiassi-Farrokhfal, Peter Palensky, and Dick Epema. “A novel decentralized platform for peer-to-peer energy trading market with blockchain technology”. In: *Applied Energy* 282 (2021), p. 116123.
- [68] Rüdiger Schollmeier. “A definition of peer-to-peer networking for the classification of peer-to-peer architectures and applications”. In: *Proceedings First International Conference on Peer-to-Peer Computing*. IEEE. 2001, pp. 101–102.
- [69] Chenghua Zhang, Jianzhong Wu, Yue Zhou, Meng Cheng, and Chao Long. “Peer-to-Peer energy trading in a Microgrid”. In: *Applied Energy* 220 (2018), pp. 1–12.
- [70] Cheng Lyu, Youwei Jia, and Zhao Xu. “A Novel Communication-less Approach to Economic Dispatch for Microgrids”. In: *IEEE Transactions on Smart Grid* 12.1 (2020), pp. 901–904.
- [71] Yue Zhou, Jianzhong Wu, and Chao Long. “Evaluation of peer-to-peer energy sharing mechanisms based on a multiagent simulation framework”. In: *Applied Energy* 222 (2018), pp. 993–1022.
- [72] Chao Long, Jianzhong Wu, Yue Zhou, and Nick Jenkins. “Peer-to-peer energy sharing through a two-stage aggregated battery control in a community Microgrid”. In: *Applied energy* 226 (2018), pp. 261–276.

- 
- [73] Muhammad Raisul Alam, Marc St-Hilaire, and Thomas Kunz. “Peer-to-peer energy trading among smart homes”. In: *Applied energy* 238 (2019), pp. 1434–1443.
- [74] Nian Liu, Xinghuo Yu, Cheng Wang, and Jinjian Wang. “Energy sharing management for microgrids with PV prosumers: A Stackelberg game approach”. In: *IEEE Transactions on Industrial Informatics* 13.3 (2017), pp. 1088–1098.
- [75] Amrit Paudel, Mohsen Khorasany, and Hoay Beng Gooi. “Decentralized local energy trading in microgrids with voltage management”. In: *IEEE Transactions on Industrial Informatics* 17.2 (2020), pp. 1111–1121.
- [76] Quan Zhou, Mohammad Shahidehpour, Aleksi Paaso, Shay Bahramirad, Ahmed Alabdulwahab, and Abdullah Abusorrah. “Distributed control and communication strategies in networked microgrids”. In: *IEEE Communications Surveys & Tutorials* 22.4 (2020), pp. 2586–2633.
- [77] Kelvin Anoh, Sabita Maharjan, Augustine Ikpehai, Yan Zhang, and Bamidele Adebisi. “Energy peer-to-peer trading in virtual microgrids in smart grids: A game-theoretic approach”. In: *IEEE Transactions on Smart Grid* 11.2 (2019), pp. 1264–1275.
- [78] Fengji Luo, Zhao Yang Dong, Gaoqi Liang, Junichi Murata, and Zhao Xu. “A distributed electricity trading system in active distribution networks based on multi-agent coalition and blockchain”. In: *IEEE Transactions on Power Systems* 34.5 (2018), pp. 4097–4108.
- [79] Cheng Lyu, Youwei Jia, and Zhao Xu. “Fully decentralized peer-to-peer energy sharing framework for smart buildings with local battery system and aggregated electric vehicles”. In: *Applied Energy* 299 (2021), p. 117243.

- 
- [80] Jiayong Li, Chaorui Zhang, Zhao Xu, Jianhui Wang, Jian Zhao, and Ying-Jun Angela Zhang. “Distributed transactive energy trading framework in distribution networks”. In: *IEEE Transactions on Power Systems* 33.6 (2018), pp. 7215–7227.
- [81] Hongseok Kim, Joohee Lee, Shahab Bahrani, and Vincent WS Wong. “Direct energy trading of microgrids in distribution energy market”. In: *IEEE Transactions on Power Systems* 35.1 (2019), pp. 639–651.
- [82] He Hao, Charles D Corbin, Karanjit Kalsi, and Robert G Pratt. “Transactive control of commercial buildings for demand response”. In: *IEEE Transactions on Power Systems* 32.1 (2016), pp. 774–783.
- [83] Wayes Tushar, Tapan Kumar Saha, Chau Yuen, Thomas Morstyn, H Vincent Poor, Richard Bean, et al. “Grid influenced peer-to-peer energy trading”. In: *IEEE Transactions on Smart Grid* 11.2 (2019), pp. 1407–1418.
- [84] Juan Clavier, Francois Bouffard, Dmitry Rimorov, and Gza Jos. “Generation dispatch techniques for remote communities with flexible demand”. In: *IEEE Transactions on Sustainable Energy* 6.3 (2015), pp. 720–728.
- [85] Yingzhong Gu and Le Xie. “Stochastic look-ahead economic dispatch with variable generation resources”. In: *IEEE Transactions on Power Systems* 32.1 (2016), pp. 17–29.
- [86] Wencong Su, Jianhui Wang, and Jaehyung Roh. “Stochastic energy scheduling in microgrids with intermittent renewable energy resources”. In: *IEEE Transactions on Smart grid* 5.4 (2013), pp. 1876–1883.
- [87] Peikai Li, Yun Liu, Huanhai Xin, and Xichen Jiang. “A robust distributed economic dispatch strategy of virtual power plant under cyber-attacks”. In: *IEEE Transactions on Industrial Informatics* 14.10 (2018), pp. 4343–4352.

- 
- [88] Lian Lu, Jinlong Tu, Chi-Kin Chau, Minghua Chen, and Xiaojun Lin. “Online energy generation scheduling for microgrids with intermittent energy sources and co-generation”. In: *ACM SIGMETRICS Performance Evaluation Review* 41.1 (2013), pp. 53–66.
- [89] Youwei Jia, Yufei He, Xue Lyu, Songjian Chai, Zhao Xu, and Minghua Chen. “Hardware-in-the-loop implementation of residential intelligent microgrid”. In: *2018 IEEE Power & Energy Society General Meeting (PESGM)*. IEEE. 2018, pp. 1–5.
- [90] Zhengshuo Li, Qinglai Guo, Hongbin Sun, and Jianhui Wang. “Sufficient conditions for exact relaxation of complementarity constraints for storage-concerned economic dispatch”. In: *IEEE Transactions on Power Systems* 31.2 (2015), pp. 1653–1654.
- [91] Yuanyuan Shi, Bolun Xu, Yushi Tan, Daniel Kirschen, and Baosen Zhang. “Optimal battery control under cycle aging mechanisms in pay for performance settings”. In: *IEEE Transactions on Automatic Control* 64.6 (2018), pp. 2324–2339.
- [92] Xiaoxi Zhang, Zhiyi Huang, Chuan Wu, Zongpeng Li, and Francis CM Lau. “Online auctions in IaaS clouds: Welfare and profit maximization with server costs”. In: *Proceedings of the 2015 ACM SIGMETRICS International Conference on Measurement and Modeling of Computer Systems*. 2015, pp. 3–15.
- [93] Alessandra Parisio, Evangelos Rikos, and Luigi Glielmo. “A model predictive control approach to microgrid operation optimization”. In: *IEEE Transactions on Control Systems Technology* 22.5 (2014), pp. 1813–1827.

- 
- [94] Xiangyu Zhang, Manisa Pipattanasomporn, Tao Chen, and Saifur Rahman. “An IoT-based thermal model learning framework for smart buildings”. In: *IEEE Internet of Things Journal* 7.1 (2019), pp. 518–527.
- [95] Tariq Samad, Edward Koch, and Petr Stluka. “Automated demand response for smart buildings and microgrids: The state of the practice and research challenges”. In: *Proceedings of the IEEE* 104.4 (2016), pp. 726–744.
- [96] Syed Aftab Rashid, Zeeshan Haider, SM Chapal Hossain, Kashan Memon, Fazil Panhwar, Momoh Karmah Mbogba, Peng Hu, and Gang Zhao. “Retrofitting low-cost heating ventilation and air-conditioning systems for energy management in buildings”. In: *Applied Energy* 236 (2019), pp. 648–661.
- [97] Abdul Afram and Farrokh Janabi-Sharifi. “Theory and applications of HVAC control systems—A review of model predictive control (MPC)”. In: *Building and Environment* 72 (2014), pp. 343–355.
- [98] Jide Niu, Zhe Tian, Yakai Lu, and Hongfang Zhao. “Flexible dispatch of a building energy system using building thermal storage and battery energy storage”. In: *Applied Energy* 243 (2019), pp. 274–287.
- [99] Esteban A Soto, Lisa B Bosman, Ebisa Wollega, and Walter D Leon-Salas. “Peer-to-peer energy trading: A review of the literature”. In: *Applied Energy* (2020), p. 116268.
- [100] Yue Zhou, Jianzhong Wu, and Chao Long. “Evaluation of peer-to-peer energy sharing mechanisms based on a multiagent simulation framework”. In: *Applied Energy* 222 (2018), pp. 993–1022.
- [101] Muhammad Raisul Alam, Marc St-Hilaire, and Thomas Kunz. “Peer-to-peer energy trading among smart homes”. In: *Applied energy* 238 (2019), pp. 1434–1443.

- 
- [102] Weijia Liu, Donglian Qi, and Fushuan Wen. “Intraday residential demand response scheme based on peer-to-peer energy trading”. In: *IEEE Transactions on Industrial Informatics* 16.3 (2019), pp. 1823–1835.
- [103] Thomas Morstyn and Malcolm D McCulloch. “Multiclass energy management for peer-to-peer energy trading driven by prosumer preferences”. In: *IEEE Transactions on Power Systems* 34.5 (2018), pp. 4005–4014.
- [104] Jianming Lian, Huiying Ren, Yannan Sun, and Donald J Hammerstrom. “Performance evaluation for transactive energy systems using double-auction market”. In: *IEEE Transactions on Power Systems* 34.5 (2018), pp. 4128–4137.
- [105] Wayes Tushar, Bo Chai, Chau Yuen, Shisheng Huang, David B Smith, H Vincent Poor, and Zaiyue Yang. “Energy storage sharing in smart grid: A modified auction-based approach”. In: *IEEE Transactions on Smart Grid* 7.3 (2016), pp. 1462–1475.
- [106] Su Nguyen, Wei Peng, Peter Sokolowski, Daminda Alahakoon, and Xinghuo Yu. “Optimizing rooftop photovoltaic distributed generation with battery storage for peer-to-peer energy trading”. In: *Applied Energy* 228 (2018), pp. 2567–2580.
- [107] Wayes Tushar, Tapan Kumar Saha, Chau Yuen, Thomas Morstyn, Malcolm D McCulloch, H Vincent Poor, and Kristin L Wood. “A motivational game-theoretic approach for peer-to-peer energy trading in the smart grid”. In: *Applied energy* 243 (2019), pp. 10–20.
- [108] Amrit Paudel, Kalpesh Chaudhari, Chao Long, and Hoay Beng Gooi. “Peer-to-peer energy trading in a prosumer-based community microgrid: A game-theoretic model”. In: *IEEE Transactions on Industrial Electronics* 66.8 (2018), pp. 6087–6097.

- 
- [109] Shichang Cui, Yan-Wu Wang, and Jiang-Wen Xiao. “Peer-to-peer energy sharing among smart energy buildings by distributed transaction”. In: *IEEE Transactions on Smart Grid* 10.6 (2019), pp. 6491–6501.
- [110] Shichang Cui, Yan-Wu Wang, Yang Shi, and Jiang-Wen Xiao. “A new and fair peer-to-peer energy sharing framework for energy buildings”. In: *IEEE Transactions on Smart Grid* 11.5 (2020), pp. 3817–3826.
- [111] Fakeha Sehar, Manisa Pipattanasomporn, and Saifur Rahman. “Coordinated control of building loads, PVs and ice storage to absorb PEV penetrations”. In: *International Journal of Electrical Power & Energy Systems* 95 (2018), pp. 394–404.
- [112] Tao Jiang, Zening Li, Xiaolong Jin, Houhe Chen, Xue Li, and Yunfei Mu. “Flexible operation of active distribution network using integrated smart buildings with heating, ventilation and air-conditioning systems”. In: *Applied energy* 226 (2018), pp. 181–196.
- [113] Wanrong Tang and Ying Jun Zhang. “A model predictive control approach for low-complexity electric vehicle charging scheduling: Optimality and scalability”. In: *IEEE transactions on power systems* 32.2 (2016), pp. 1050–1063.
- [114] Zhanbo Xu, Guoqiang Hu, and Costas J Spanos. “Coordinated optimization of multiple buildings with a fair price mechanism for energy exchange”. In: *Energy and Buildings* 151 (2017), pp. 132–145.
- [115] Tsung-Hui Chang. “A proximal dual consensus ADMM method for multi-agent constrained optimization”. In: *IEEE Transactions on Signal Processing* 64.14 (2016), pp. 3719–3734.
- [116] Hui Hou, Mengya Xue, Yan Xu, Zhenfeng Xiao, Xiangtian Deng, Tao Xu, Peng Liu, and Rongjian Cui. “Multi-objective economic dispatch of

- a microgrid considering electric vehicle and transferable load”. In: *Applied Energy* 262 (2020), p. 114489.
- [117] TF Ishugah, Y Li, RZ Wang, and JK Kiplagat. “Advances in wind energy resource exploitation in urban environment: A review”. In: *Renewable and sustainable energy reviews* 37 (2014), pp. 613–626.
- [118] Yu Yang, Qing-Shan Jia, Geert Deconinck, Xiaohong Guan, Zhifeng Qiu, and Zechun Hu. “Distributed coordination of EV charging with renewable energy in a microgrid of buildings”. In: *IEEE Transactions on Smart Grid* 9.6 (2017), pp. 6253–6264.
- [119] Thomas Baroche, Pierre Pinson, Roman Le Goff Latimier, and Hamid Ben Ahmed. “Exogenous cost allocation in peer-to-peer electricity markets”. In: *IEEE Transactions on Power Systems* 34.4 (2019), pp. 2553–2564.
- [120] Yigao Du, Jing Wu, Shaoyuan Li, Chengnian Long, and Ioannis Ch Paschalidis. “Distributed MPC for coordinated energy efficiency utilization in microgrid systems”. In: *IEEE Transactions on Smart Grid* 10.2 (2017), pp. 1781–1790.
- [121] Jose Luis Crespo-Vazquez, Tarek AlSkaif, Ángel Manuel González-Rueda, and Madeleine Gibescu. “A community-based energy market design using decentralized decision-making under uncertainty”. In: *IEEE Transactions on Smart Grid* 12.2 (2020), pp. 1782–1793.
- [122] Thomas Morstyn, Alexander Teytelboym, Cameron Hepburn, and Malcolm D McCulloch. “Integrating P2P energy trading with probabilistic distribution locational marginal pricing”. In: *IEEE Transactions on Smart Grid* 11.4 (2019), pp. 3095–3106.

- 
- [123] Mikael Amelin. “An evaluation of intraday trading and demand response for a predominantly hydro-wind system under nordic market rules”. In: *IEEE Transactions on Power Systems* 30.1 (2014), pp. 3–12.
- [124] Felix Garcia-Torres, Carlos Bordons, Javier Tobajas, Juan José Márquez, Joaquin Garrido-Zafra, and Antonio Moreno-Muñoz. “Optimal schedule for networked microgrids under deregulated power market environment using model predictive control”. In: *IEEE Transactions on Smart Grid* 12.1 (2020), pp. 182–191.
- [125] Esteban A Soto, Lisa B Bosman, Ebisa Wollega, and Walter D Leon-Salas. “Peer-to-peer energy trading: A review of the literature”. In: *Applied Energy* 283 (2021), p. 116268.
- [126] Georgios Tsaousoglou, Juan S Giraldo, Pierre Pinson, and Nikolaos G Paterakis. “Mechanism design for fair and efficient dso flexibility markets”. In: *IEEE transactions on smart grid* 12.3 (2021), pp. 2249–2260.
- [127] Mingyu Yan, Mohammad Shahidehpour, Aleksi Paaso, Liuxi Zhang, Ahmed Alabdulwahab, and Abdullah Abusorrah. “Distribution network-constrained optimization of peer-to-peer transactive energy trading among multi-microgrids”. In: *IEEE Transactions on Smart Grid* 12.2 (2020), pp. 1033–1047.
- [128] Xiong Hu, Zhi-Wei Liu, Guanghui Wen, Xinghuo Yu, and Chen Liu. “Voltage control for distribution networks via coordinated regulation of active and reactive power of DGs”. In: *IEEE Transactions on Smart Grid* 11.5 (2020), pp. 4017–4031.
- [129] Wen-Yi Zhang, Boshen Zheng, Wei Wei, Laijun Chen, and Shengwei Mei. “Peer-to-peer transactive mechanism for residential shared energy storage”. In: *Energy* (2022), p. 123204.

- 
- [130] Amrit Paudel, LPMI Sampath, Jiawei Yang, and Hoay Beng Gooi. “Peer-to-peer energy trading in smart grid considering power losses and network fees”. In: *IEEE Transactions on Smart Grid* 11.6 (2020), pp. 4727–4737.
- [131] Jiayong Li, Chengying Liu, Mohammad E Khodayar, Ming-Hao Wang, Zhao Xu, Bin Zhou, and Canbing Li. “Distributed online VAR control for unbalanced distribution networks with photovoltaic generation”. In: *IEEE Transactions on Smart Grid* 11.6 (2020), pp. 4760–4772.
- [132] Hao Zhu and Hao Jan Liu. “Fast local voltage control under limited reactive power: Optimality and stability analysis”. In: *IEEE Transactions on Power Systems* 31.5 (2016), pp. 3794–3803.